A Radio Frequency Interference Survey of Alston Observatory for Small Radio Telescopes

MSc Astrophysics
Thesis Submitted for Partial Fulfilment

Christopher Paul John Everest

Jeremiah Horrocks Institute
University of Central Lancashire

September 2021

Declaration

Type of Award: Master of Science in Astrophysics

School: Natural Sciences

I declare that while registered as a candidate for the research degree, I have not been a registered candidate or enrolled student for another award of the University or other academic or professional institution.

I declare that no material contained in this thesis has been used in any other submission for an academic award and is solely my own work

No proof-reading service was used in the compilation of this thesis

Christopher Paul John Everest

September 2021

Abstract

Alston Observatory currently only has optical telescopes, however there is a potential for a Small Radio Telescope (SRT) for the site as a teaching aid. An investigation into the Radio Environment of the site found that around the bandwidth a telescope would observe at (1420 MHz) the noise floor is acceptable for a radio telescope being observed at -195 dBW/m^2/Hz, which should be able to view objects around the same brightness as M31 in the 21cm line with a minimum 2.4m dish on the site. A few peaks of potential interference were found at 1419.649 MHz, 1420.609 MHz, and 1421.569 MHz that were consistent across the site and also in a comparison reading done in Preston, the nearby city. Although no confirmed source was found, the fact that the peaks did not change over the site and were also present in Preston indicate they may be from the survey setup, which requires further investigation. There was also interference near the main building on the site, the Planetarium, as expected, leading to a suggestion of the placement of the telescope to be on top of the Planetarium building, where RFI from the building would not be able to enter the dish, and where shielding can be placed below the telescope to minimise any interference regardless. It was also found that the current Moses Holden Telescope would not cause interference in the 1420 MHz band, meaning that both telescopes could be used concurrently if needed. A potential issue going forward however is that these results may over the next few years, with the increasing amount of satellite constellations, which could make the site unusable for radio observations at certain bands.

List of Figures

1 A diagram showing which frequencies can pass through the atmosphere and which cannot [van Driel, 2009] . . . 1
2 A map of neutral hydrogen in the Milky Way, taken using a small radio telescope with a 3.1m dish, giving it a beam width of 4.7 degrees [Saje and Vidmar, 2017] . . . 2
3 A diagram showing how different sources of RFI can enter a radio telescope [van Driel, 2009] . . . 3
7 A diagram of a basic dipole antenna . . . 10
8 The gain diagram for a typical directional antenna, such as an aperture or reflector antenna, with a stronger gain in one direction [Minoli, 2009] . . . 11
9 A diagram of the processing flow of an SDR transceiver [Jondral, 2005] . 13
10 Different Signals and their Fourier transforms [Burke et al., 2019] 14
11 Illustration of the 21cm line from hydrogen [Santo and Uddin, 2013] . . . 16
13 Global Profile of M31, with the red/blue shift converted to velocity and the strength of the signal being the Antenna Temperature [Cram et al., 1980] . . . 18
14 Global Profile of UGC 11707, a galaxy, taken with a 140 ft, or 42m telescope [Condon and Ransom, 2016] . . . 19
15 Image showing a spectrum at 1420 MHz (Left), with the 21cm line and continuum labelled (Right), with the continuum showing a decrease as frequency increases [Phuong et al., 2014] . . . 20
16 Spectra of various different radio sources [Wilson et al., 2013] . . . 21
17 How a FM and AM signal is modulated from a carrier signal [Frost, 2010] 22
18 How an AM or FM signal looks when frequency is plotted along the x axis and signal power along the y axis [Johnson, 2013] . . . 23
19 How Harmonics are related to the source signal, with (a) showing the first harmonic which is equivalent to half a wavelength, (b) showing a full wavelength and (c) showing a wavelength and a half. [Halliday et al., 2014] 25
20 Example of a mesh dish provided by RF HAMDESIGN . . . 28
21 Example of a antenna and feedhorn provided by Radio Astronomy Supplies 29
44
35 A Map of the Alston Site with points of interest noted . . . 45
36 A Map of the Alston Site with a grid overlaid, each point is 6.5m apart from each other . . . 46
37 A Map of the Alston Site with the grid overlaid, and each point either green or red, to show which points can be surveyed (green) or are inaccessible (red) . . . 47
38 How the RFI of the laptop will be measured as a comparison . . . 49
39 The setup for the recordings done for the grid observations . . . 49
40 A map of the site with the grid overlaid, with the points surveyed in blue 52
41 The average mode narrow band comparison reading . . . 54
42 The peak mode narrow band comparison reading . . . 54
43 The average mode wide band comparison reading . . . 55
44 The peak mode wide band comparison reading . . . 55
45 The average mode wide band comparison reading with potential sources of features listed . . . 56

46 Spectrum with the receiver placed on top of the Laptop, as shown in Figure 38 . . . 57
47 Comparison Peak measurement from Preston overlaid on top of the Laptop Peak measurement . . . 57
48 Averaged Spectrum inside Planetarium . . . 59
49 Peak Spectrum inside Planetarium . . . 60
50 Peak Spectrum taken while the MHT was put through the full range of motion . . . 61
51 Peak Spectrum from the MHT overlaid onto the comparison reading . . . 62
52 Averaged Spectra of H11 . . . 63
53 Peak Spectra of H11 . . . 63
54 The H11 spectrum overlaid with the average comparison spectrum . . . 64
55 Averaged Spectra of F5 . . . 65
56 Peak Spectra of F5 . . . 65
57 Averaged Spectrum of J5 . . . 67
58 Peak Spectrum of J5 . . . 67
59 Averaged Spectra of F1 . . . 68
60 Peak Spectrum of F1 . . . 68
61 The Wide spectrum taken at G2, spanning from 1170 to 1670 MHz overlaid with the comparison wide spectrum, both taken in average mode . . . 69
62 The Wide spectrum taken at G2, spanning from 1170 to 1670 MHz overlaid with the comparison wide spectrum, both taken in peak mode . . . 70
63 The Wide spectrum taken at F9, spanning from 1170 to 1670 MHz overlaid with the comparison wide spectrum, both taken in average mode . . . 70
64 The Wide spectrum taken at F9, spanning from 1170 to 1670 MHz overlaid with the comparison wide spectrum, both taken in peak mode . . . 71
65 The results taken and graphed to see if there is any change in features over the site, with the respective colours corresponding to the colours on the following graphs . . . 72
66 The power level of the tallest peak in average mode across the site . . . 73
67 The power level of the tallest peak in peak mode across the site . . . 73
68 The power level of the noise in average mode across the site . . . 74
69 The power level of the noise in peak mode across the site . . . 75
70 A peak spectrum captured when doing the initial testing on site (22/06/2021) 75

Contents

1 Introduction **1**

2 Theory **9**
2.1 An Overview of the basic parts of a Radio Telescope 9
2.2 Software Defined Radio 13
2.3 The Hydrogen Line 16
2.4 Spectral Index 20
2.5 FM and AM modes, Carrier Signals 22
2.5.1 Broad and Narrow Band Signals 24
2.6 Harmonics 25

3 Telescope Plan **27**
3.1 Dish 27
3.2 Antenna and Filters 28
3.3 Receiver and Software 29

4 Previous Examples of Surveys **31**
4.1 Thai Radio Telescope 31
4.2 Square Kilometre Array (Australia) 32
4.3 Square Kilometre Array (South Africa) 36

5 Survey System **41**

6 Survey Plan **44**

7 Results and Analysis **51**
7.1 Comparison Measurements 53
7.1.1 Preston 53
7.1.2 Laptop 57
7.1.3 Inside Planetarium 59
7.1.4 MHT In Use 61
7.2 Grid Readings 63
7.2.1 Furthest Point (H11) 63
7.2.2 Moses Holden Telescope (F5) 65
7.2.3 Wilfred Hall Observatory (J5) 67
7.2.4 Planetarium (F1) 68
7.3 Wide Band Readings 69
7.3.1 Wide Band Survey at G2 69
7.3.2 Wide Band Survey at F9 70
7.4 Discussion 72
7.4.1 Tallest Peak-Potential Source 72
7.4.2 Noise Floor 74
7.4.3 Comparison to other Surveys 76
7.4.4 Noise floor Compared to Observational Signals 76
7.4.5 Future Survey Plan 77
7.4.6 Placement of the Telescope 77

8 Conclusion **79**

1 Introduction

Owned by the University of Central Lancashire, operated by the Jeremiah Horrocks Institute, and located in Preston, England, Alston observatory currently has a CDK700 optical telescope with various optical filters. This is fine for most observational projects and undergraduate labs, but a radio telescope would greatly increase the observational capabilities of the site and provide a new source of both undergraduate labs and postgraduate projects. Therefore this project has investigated the suitability of the site for a radio telescope.

Radio telescopes view frequencies outside of the optical wavelengths, and can view from 0.3mm to 30m [van Driel, 2009]. This allows them to observe processes that do not occur within the narrow optical range, such as emissions from neutral hydrogen in gas clouds, allowing the estimation of their velocity (see Section 2.3) or by measuring the variation in flux over a range of frequencies, which can tell the mechanism that is causing emission from a particular object (See Section 2.4). The radio spectrum is also one of the few parts of the EM spectrum that the atmosphere does not block, as shown in Figure 1 [van Driel, 2009]. This allows for radio telescopes to be ground based, with large singular dishes such as the Lovell telescope at Jodrell bank, which has a diameter of 76 metres[1], or large arrays of smaller dishes, such as the in progress Square Kilometre Array (SKA), which will consist of thousands of 15m dishes[2].

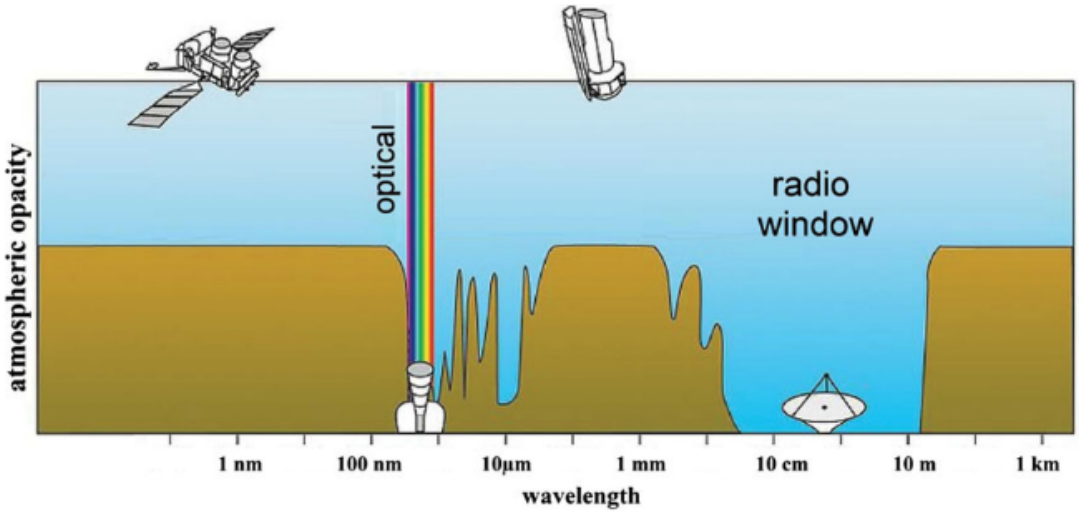

Figure 1: A diagram showing which frequencies can pass through the atmosphere and which cannot [van Driel, 2009]

Large telescopes are not necessary however for some observations, as shown by the various installations of Small Radio Telescopes (SRTs). These are often designed as teaching telescopes, allowing for undergraduates to learn how radio telescopes work with a few experiments such as observations of the Hydrogen Line and Continuum spectrum as stated above. A few examples of these telescopes include the Such A Lovely Small Antenna (SALSA) in Sweden [Horellou et al., 2015], the VATLY telescope in Hanoi

[1]https://www.jodrellbank.net/explore/science/telescopes/
[2]https://www.skatelescope.org/dishes/

[Phuong et al., 2014], and the Haystack Observatory telescope [Ballard et al., 2008], which will be used as points of comparison for the planned telescope on the Alston site. These telescopes are between 2.3-3.1m in diameter, and observe at and around the 21cm wavelength. Although these telescopes have a far lower resolution than the professional telescopes, they are still able to to do observations such as shown in Figure 2.

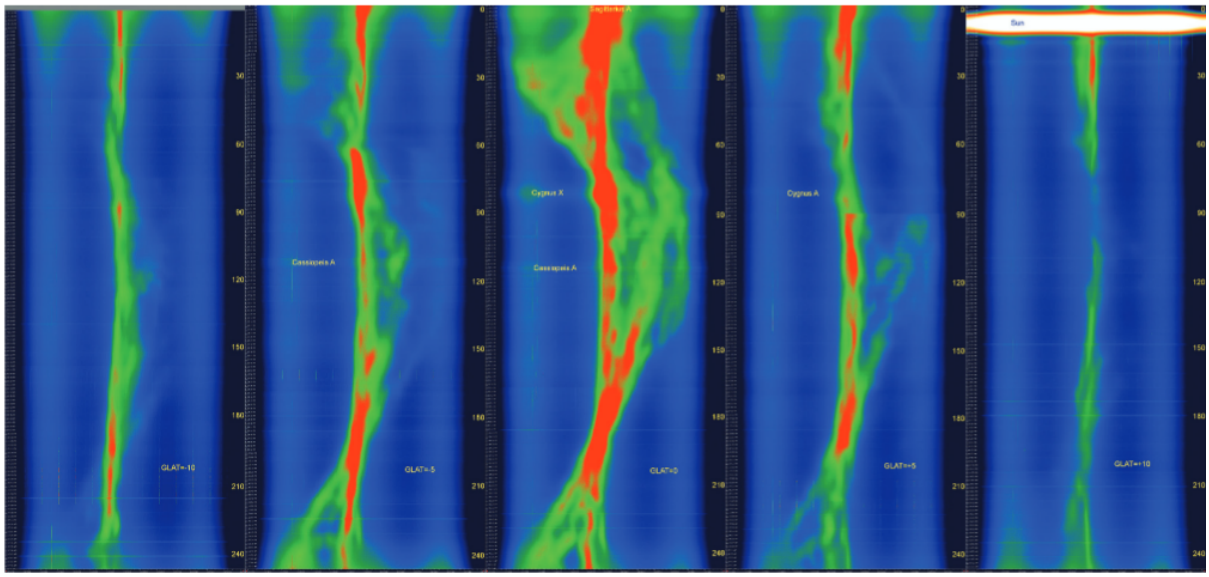

Figure 2: A map of neutral hydrogen in the Milky Way, taken using a small radio telescope with a 3.1m dish, giving it a beam width of 4.7 degrees [Saje and Vidmar, 2017]

In Figure 2, we can see waterfall plots going across the Milky Way, taken at galactic latitudes -10°, -5°, 0°, +5° and +10 going left to right with a 5 degree span. The different colours represent the intensity of the signal in the 21cm line, and therefore the density of the clouds, with blue being the weaker signals from thinner clouds, and red being the strongest, from the denser clouds, with green/yellow being and intermediary. This shows that even with smaller telescopes, detailed maps of the Milky Way can still be created, and could be a potential undergraduate teaching product for the telescope. Projects such as these will also provide a greater understanding of how Radio Telescopes work and how their observing methods differ from optical telescopes.

Due to the difference in how radio telescopes operate compared to optical telescopes, different units are used for measurements, and some of these units will be used for the survey as well. First is decibels, or dB. dB is the comparison between two voltages, current or power on a logarithmic scale, and so is dimensionless. dBm and dBi are variations, with dBm being a comparison between a unit of power, and 1 milliwatt. dBi is the difference in gain compared to a theoretically fully isotropic antenna, an antenna that radiates/receives power equally in all directions [Minoli, 2009]. A unit that will also be used is Spectral Irradiance. This is the amount of power received over an area at a specific frequency, which is useful in the field of radio astronomy, where the flux will vary over frequency. The Janksy is a non-SI variant of Spectral Irradiance, which is used in radio astronomy, and is equivalent to 10^{-26} W/m^2/Hz. This is more often used as the majority of readings are very low power, so having a smaller unit allows for easier comparison.

Much like optical telescopes, Radio telescopes have interference to contend with, commonly known as Radio Frequency Interference (RFI). It is an issue that can occur when taking an observation in the radio band, when unwanted signals get captured as well as the desired signals from space. The desirable limit for RFI is under a 10% increase in the noise level, or in other words a 10% increase in the uncertainty of a reading, as outlined by the International Telecommunications Union [ITU-Radiocommunication-Assembly-RA.769-2, 2004]. These unwanted signals can come from a variety of prevalent sources:

- Electronic devices such as computers, phones, TV, Wifi
- Devices that are designed to transmit over long distances, such as Aeroplane Communications, Radar etc.
- Cars, due to parts such as the ignition switches, parking sensors and on board computers
- Satellite Communications, especially down link signals from the satellites to ground based receivers
- Radio Broadcasts, such as AM and FM Radio signals from broadcasting towers

The majority of these sources however do not cause major issues to radio telescopes, due to the fact that most of these sources come from ground level, or from the horizon in cases such as broadcasting towers. This means they enter the telescope at an angle, meaning they enter the antenna at the less sensitive side-lobes as opposed to the main beam (see section 2.1) as seen in Figure 3. This means that most signals will not increase the uncertainty of the noise by the limit of 10%, and as most RFI comes from far away from the site, and outside the spectrum being observed. [van Driel, 2009].

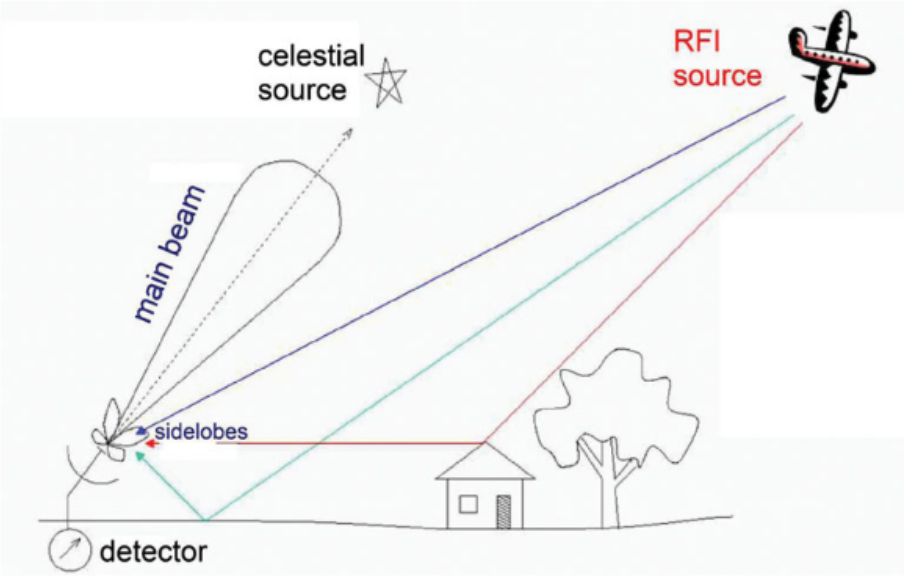

Figure 3: A diagram showing how different sources of RFI can enter a radio telescope [van Driel, 2009]

However, some of these sources, such as satellite down link signals and signals from ground based sources reflected into the dish from passing planes could potentially enter the main beam. This could cause any signals from a celestial source to be masked by the comparatively much stronger sources. Although we would not expect many satellites to be broadcasting directly at the site that is being surveyed, Alston Observatory, side lobes from broadcasting antennas could be pointing towards the site, and may be strong enough to cause issues with observations due to the sensitivity of the equipment used in radio astronomy [Dai et al., 2019]. This is a problem due to the spectrum allocation for radio communications being near the protected band for radio astronomy, as shown in Figure 4[3].

Furthermore, a site survey is needed to see what the current radio environment of the site is like, to see if there are any potential interference sources in the band that may be observed by the telescope, from devices on the site. For most telescope sites, these surveys are done over a wide bandwidth, such as the test observations for the SKA candidate sites, where the radio environment was surveyed from 150 MHz to 2.2GHz [Peng et al., 2004]. This is done as modern radio telescopes can observe over a wide range of frequencies, as so the characteristics of the radio environment over a wide band is useful to see sections of the bandwidth that may cause issues, especially for observations that require wider bandwidth, such as those for measuring the spectral index of objects (see Section 2.4).

[3]https://www.ofcom.org.uk/___data/assets/pdf_file/0010/103303/space-science-meteorology.pdf

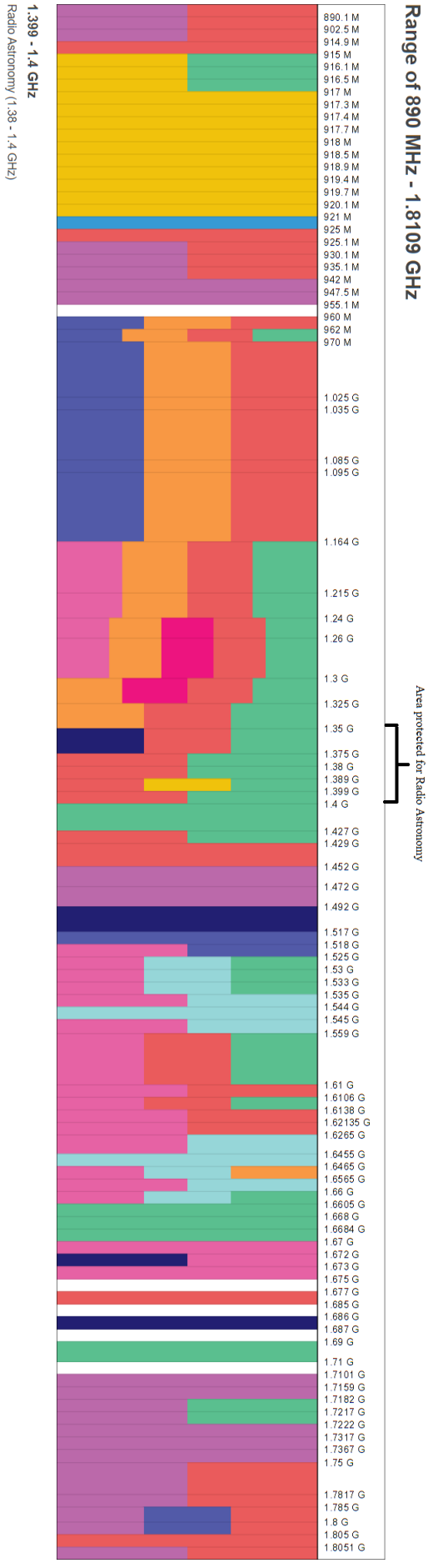
Range of 890 MHz - 1.8109 GHz
890.1 M
902.5 M
914.9 M
915 M
916.1 M
916.5 M
917 M
917.3 M
917.4 M
917.7 M
918 M
918.5 M
918.9 M
919.4 M
919.7 M
920.1 M
921 M
925 M
925.1 M
930.1 M
935.1 M
942 M
947.5 M
955.1 M
960 M
962 M
970 M
1.025 G
1.035 G
1.085 G
1.095 G
1.164 G
1.215 G
1.24 G
1.26 G
1.3 G
1.325 G
1.35 G
1.375 G
1.38 G
1.389 G
1.399 G
1.4 G
1.427 G
1.429 G
1.452 G
1.472 G
1.492 G
1.517 G
1.518 G
1.525 G
1.53 G
1.533 G
1.535 G
1.544 G
1.545 G
1.559 G
1.61 G
1.6106 G
1.6138 G
1.62135 G
1.6265 G
1.6455 G
1.6465 G
1.6565 G
1.66 G
1.6605 G
1.668 G
1.6684 G
1.67 G
1.672 G
1.673 G
1.675 G
1.677 G
1.685 G
1.686 G
1.687 G
1.69 G
1.71 G
1.7101 G
1.7159 G
1.7182 G
1.7217 G
1.7222 G
1.7317 G
1.7367 G
1.75 G
1.7817 G
1.785 G
1.8 G
1.805 G
1.8051 G
Area protected for Radio Astronomy
1.399 - 1.4 GHz
Radio Astronomy (1.38 - 1.4 GHz)

Figure 4: Part of the Ofcom spectrum allocation table[4]

As for ground based interference, the site is expected to have some interference from a few notable sources, first is the Planetarium, the main building on the site that houses server racks, computers, WiFi and other devices, which could cause interference, although as any interference from these sources should be relatively weak, due to the inverse square law, the power of these signals should drop significantly over the site. If there is a signal that persists over the site, then the source is most likely due to an external source, such as the Winter Hill transmitter[5], which can be seen from the site, and transmits AM and FM signals.

The topography of the surround area will also affect the radio environment, as hills can help block out radio waves. Figure 5 shows the map of the area around the observatory, with the contour maps showing the site is on a slight slope going south east.[6]

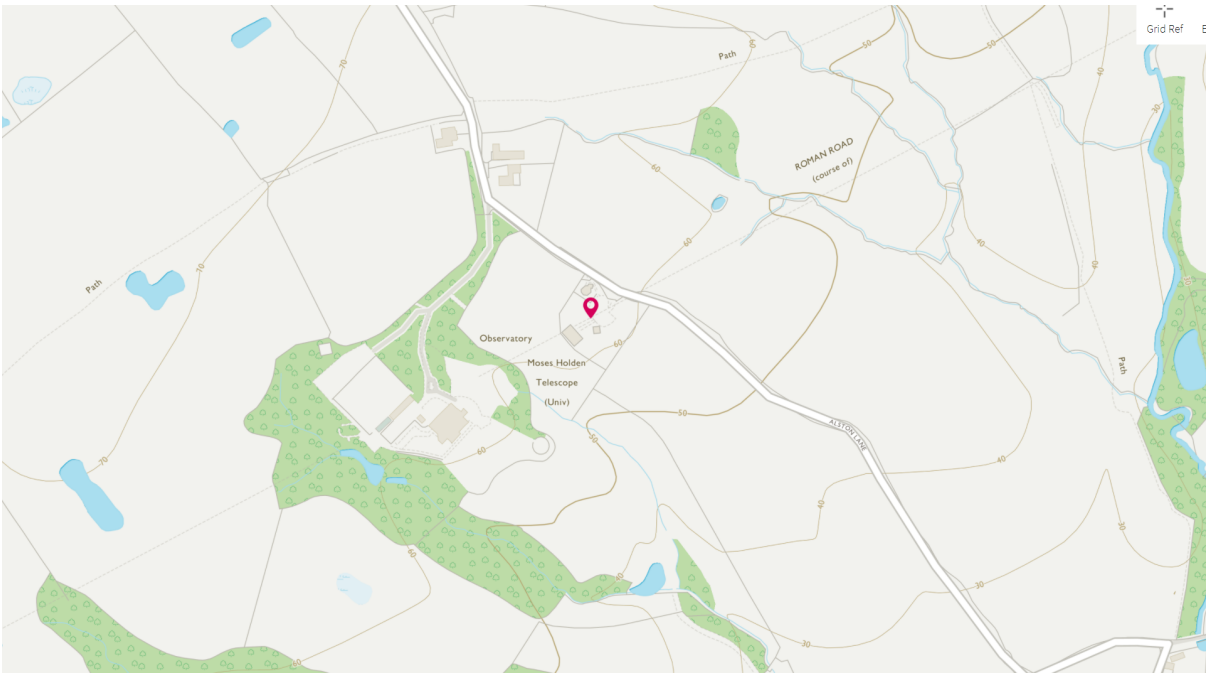

Figure 5: Topgraphy of the area surrounding Alston, courtesy of Ordnance Survey Maps

This slope should help shield the site, as Fulwood and Preston is to the west, and Longridge to the north, as shown in Figure 6

[4]http://static.ofcom.org.uk/static/spectrum/map.html
[5]https://en.wikipedia.org/wiki/Winter_Hill_transmitting_station
[6]https://osmaps.ordnancesurvey.co.uk/53.80106,-2.59368,11/pin

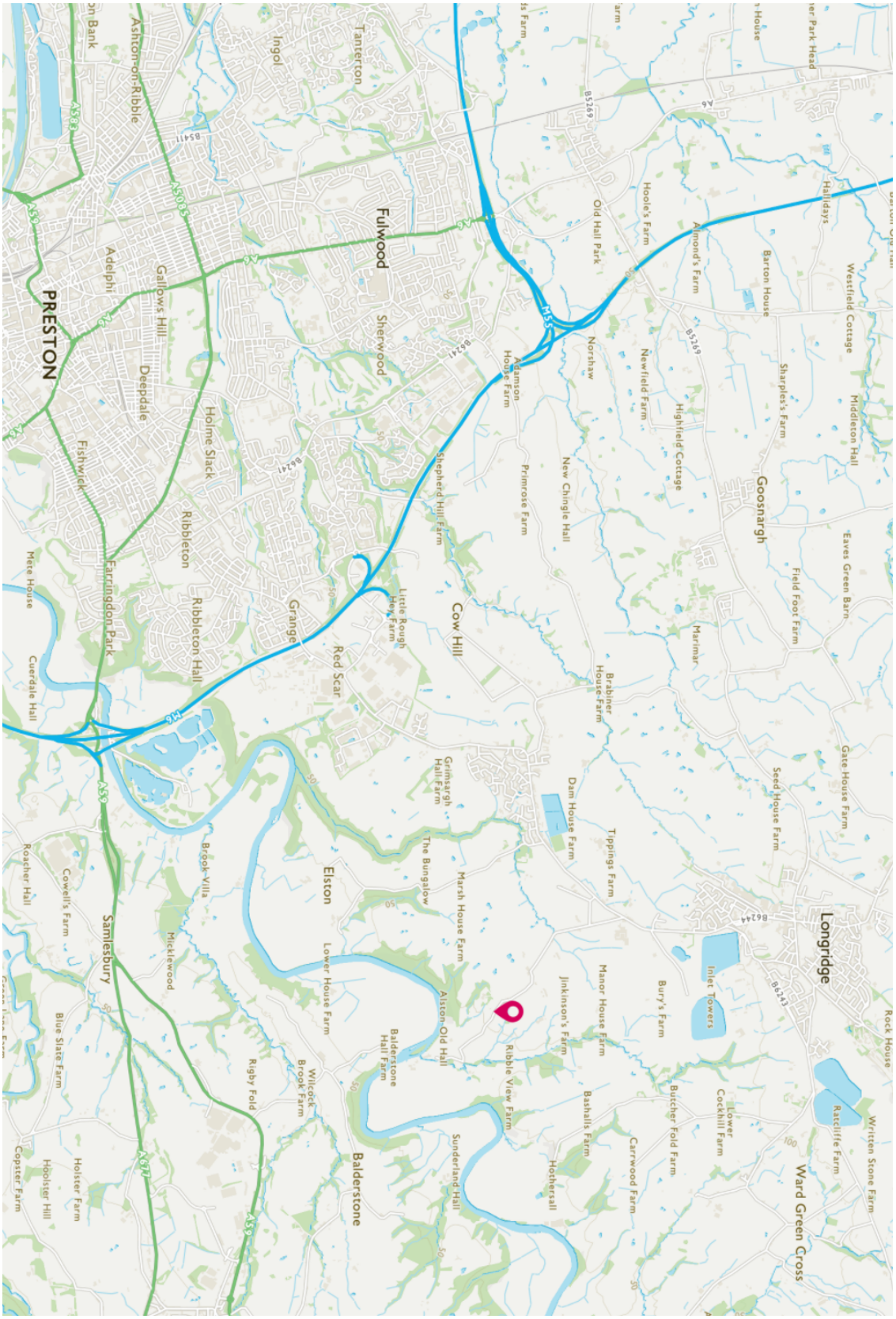

Figure 6: Topgraphy of a wider area surrounding Alston, courtesy of Ordnance Survey Maps

A potential plan to help mitigate the effect of any interference is for the installation of an RFI monitoring station on the site. This would consist of an antenna, software

defined radio receiver, either wired back to a PC on the site, or a raspberry Pi that can be remotely operated, and store surveys. This would be useful as it can either be run 24/7, to have a continuous profile of the radio environment of the site, or run alongside observations with the radio telescope. This would allow signals to be cross-referenced, to confirm whether they are from an astronomical source or not.

2 Theory

This Section will start with an overview of the units used in this thesis, then go over the basics of the parts of a radio telescope, including the antenna, dish, and how these parts dictate what sort of objects can be viewed with the telescope. This is followed with an explanation of the 21cm line, which is the wavelength that the telescope is planned to observe at. This will lead into an explanation of Spectral Index, which the potential telescope could observe if it is fitted with a wide band antenna. There is then an explanation on potential sources of interference can come from, primarily being FM and AM broadcasts, but also an explanation on broad and narrow band signals, how they can cause interference, as well as how harmonics from various devices can emit in bands that the devices are not designed to emit intentionally, which could cause interference for the telescope.

2.1 An Overview of the basic parts of a Radio Telescope

As radio telescopes cannot use CCDs, or technologies equivalent due to the larger wavelengths they operate at, a different sort of photon collection is needed to measure the waves. For radio waves an antenna is used, most of which are based of the simple half-dipole antenna for narrow band uses, however wider bands can be achieved with more complex systems, and are used in larger radio telescopes than the potential one for use on the Alston site.

A basic half-wave dipole antenna is built with two metal wires placed end to end, with the inner of each end connected to the receiver, with each half being electrically insulated from each other. This complete assembly should measure half the wavelength you want to receive. As the wave passes through the wires, it will induce a current and voltage in the wire, the current will be in the form of a standing wave across the two wires [Grant and Phillips, 1990] (see Figure 7). The current and voltage sent down the transmission line can then be processed, by first amplifying, as the signal will be weak, then filtering and digitizing the data where it can then be used.

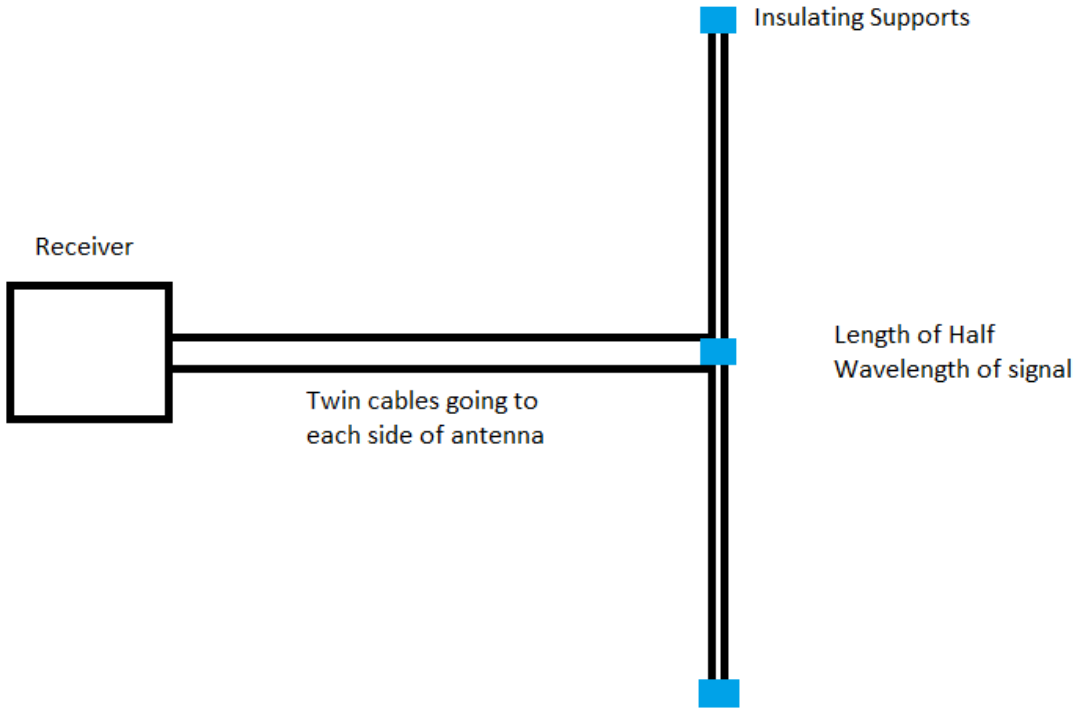

Figure 7: A diagram of a basic dipole antenna

The other key component to a Radio Telescope is the dish. This will define key parameters of the telescope, such as the Gain and Half-Power Beam width.

The Gain of an antenna is the ability of the antenna to receive/transmit power in a certain direction, when compared to a isotropic antenna, which is an antenna which radiates/receives power uniformly in all directions. A typical antenna has a gain with relation to direction as shown in Figure 8 [Minoli, 2009].

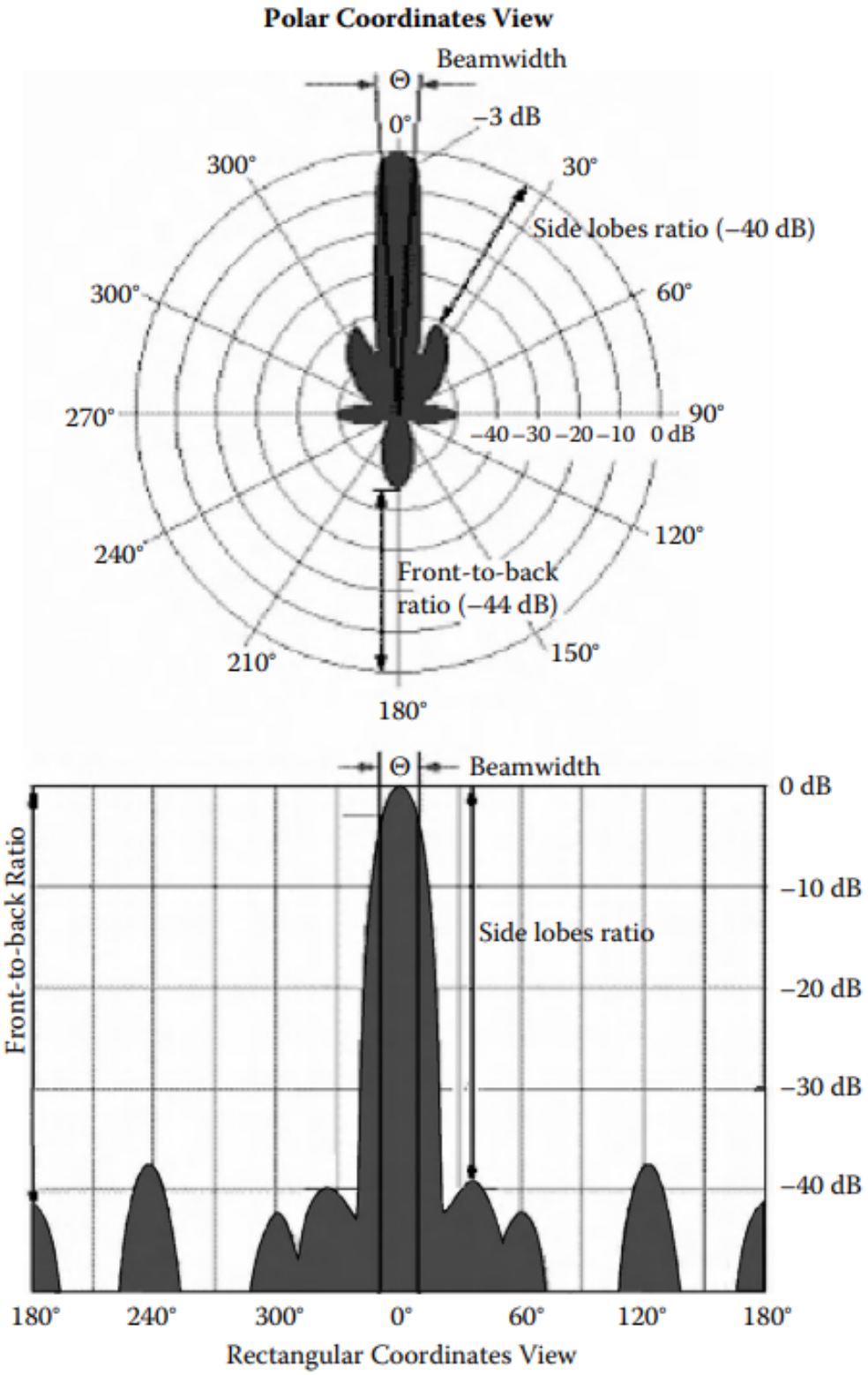

Figure 8: The gain diagram for a typical directional antenna, such as an aperture or reflector antenna, with a stronger gain in one direction [Minoli, 2009]

The gain of a telescope is dependant on its dish characteristics, as shown via the relation below:

$$G = \left(\frac{\pi d}{\lambda}\right)^2 e_a \tag{1}$$

Where G is the Gain, d is the diameter of the dish (m), λ is the wavelength (m) and e_a is a dimensionless parameter called aperture efficiency, and is between 0 and 1, for most parabolic dishes it is between 0.55 to 0.70 [Anderson, 2003]

The Half Power Beam Width is the angular separation between the half power points on the main radiation beam of the telescope [Minoli, 2009] as shown in Figure 8. This angle is what is considered the "resolution" of the telescope, as it is effectively the size of a single "pixel" on the sky when compared to a CCD. It is calculated via the relation below:

$$\theta = \frac{k\lambda}{d} \tag{2}$$

Where θ is the angle size of the beam in degrees, k is a factor that depends on the shape of the reflector, but for a typical parabolic dish is 70 (1.22 if the beam width is in radians). λ is the wavelength (m) and d is the diameter of the dish [Minoli, 2009].

For a small radio telescope that is similar to the one planned at the site, such as the SALSA Telescope , which has a diameter of 2.3m, and assuming it has a k value of 70, this gives a beam width of 6.4 degrees at the 1420 MHz that is it is designed to observe at [Horellou et al., 2015].

2.2 Software Defined Radio

Software Defined Radio is a type of radio system that uses software instead of hardware to dictate the parameters which it can receive at, such as being able to change its bandwidth, frequency, decoding method, gain etc. as opposed to a more traditional system that used hardware components to set these, which makes changing these parameters much more difficult, usually requiring specialised tools [Collins et al., 2018]. This allows for far more flexibility compared to non software based receivers, which would have some of these variables be hard wired into the system, and either not be able to be changed or require manual switches/dials. This not only makes them far less versatile, as the variables are fixed in hardware as opposed to software which can be altered and updated to a certain extent, but also far bulkier, as the more modes and additions added onto a hardware receiver requires additional parts to accommodate them, making them far larger than some of the SDRs today, which are quite small and portable.

SDRs work by taking in a signal via an antenna, then converting that signal from the analog signal to a digital signal. This then allows this new digital signal to be processed and used, as shown in Figure 9

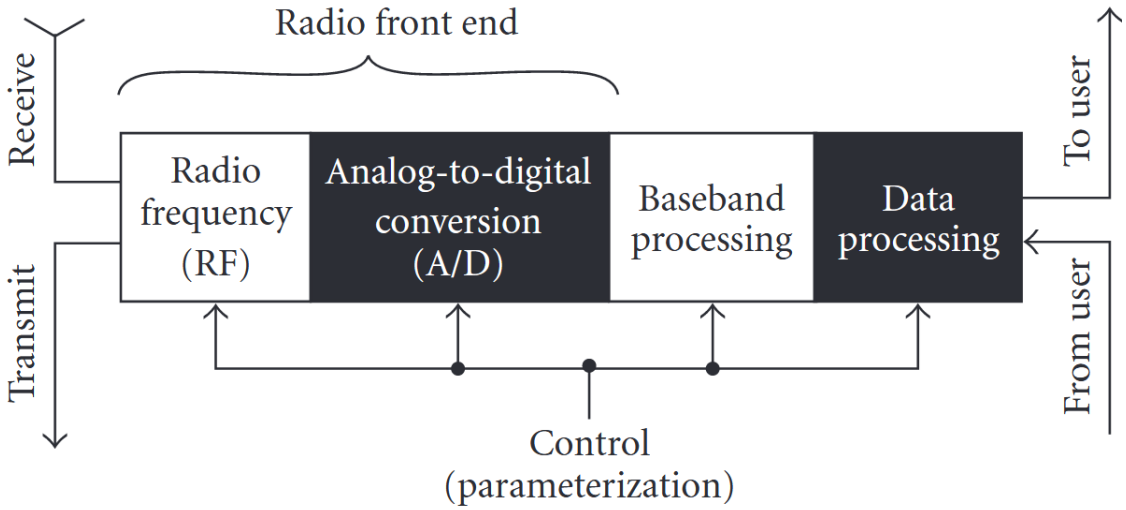

Figure 9: A diagram of the processing flow of an SDR transceiver [Jondral, 2005]

Fourier transforms are a key point in this process, being used in SDRs in the conversion and processing stage, and are used with antennas, receivers and spectrometers for single dish telescopes. This process starts with the antenna receiving a signal, which will generate a varying voltage in the system over time. A Fourier transform can be used to convert that variance over time into frequency, which can then be output. Fourier transforms also have further use in processes such as aperture synthesis and interferometry which is used in multi-telescope arrays such as the SKA. It can also used to look for periodic patterns in the data that cannot be seen by eye alone [Condon and Ransom, 2016].

This is because any signal, no matter how complicated, can be explained as an addition

of sine and cosine waves, Fourier transforms take a signal and can extract each of those individual waves, for example, in Figure 10 , it shows 3 different modulated waves and their Fourier transforms.

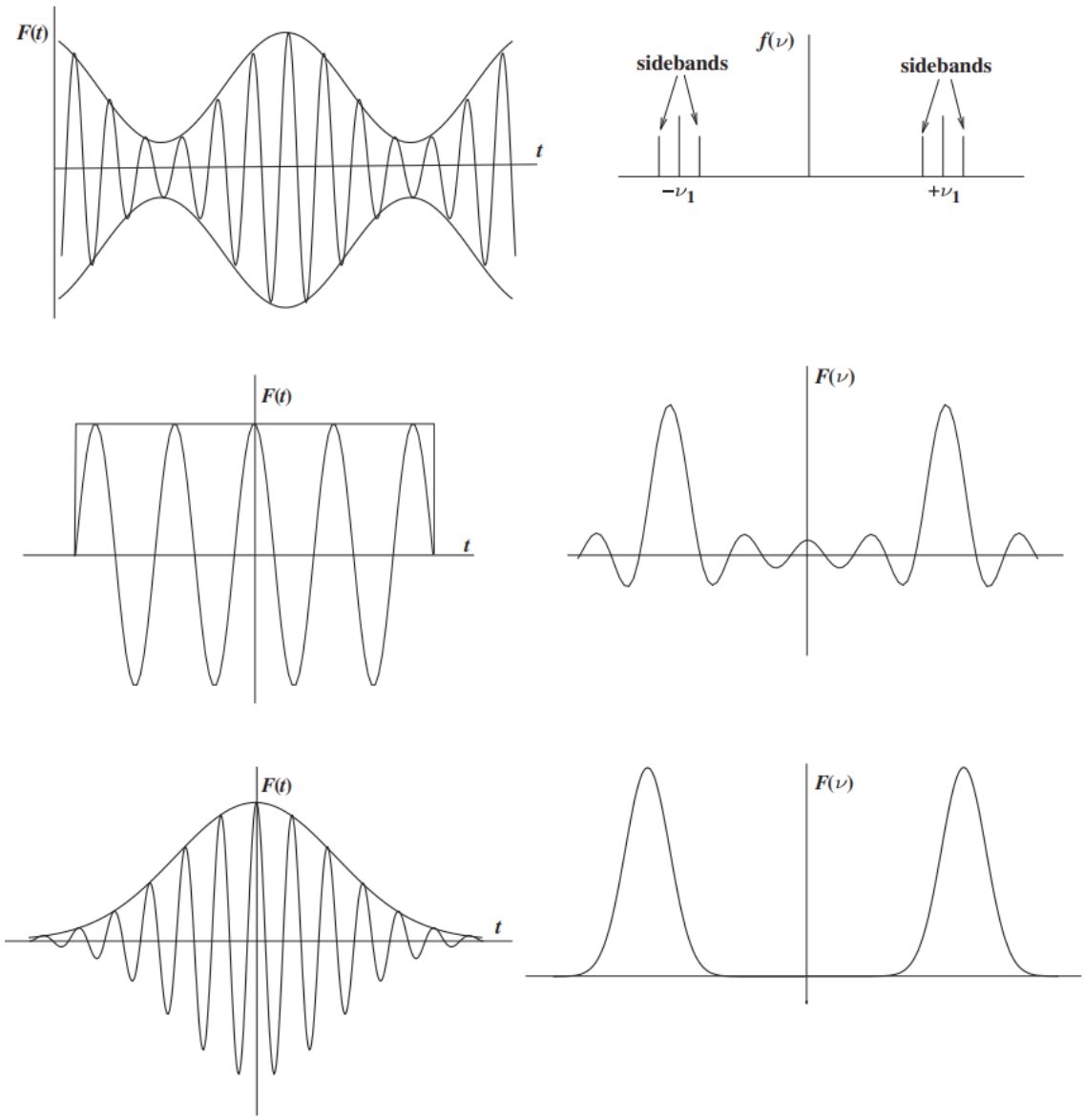

Figure 10: Different Signals and their Fourier transforms [Burke et al., 2019]

This allows any particular periodicity to be taken out of a particular observation, and so can be used as a basis for spectrometers for use with radio telescopes, such as the APEX telescope's Fast Fourier Transform Spectrometer (AFFTS) [Klein et al., 2006], and the later the eXtended bandwidth FFTS (XFFTS) that was used on the telescope [Klein et al., 2012]. These spectrometers and further development of the Fourier transform allow for observations of objects like Pulsars [Kumar and Western, 2021], which could be a potential future project for undergraduates assuming the telescope is upgraded beyond its basic configuration.

2.3 The Hydrogen Line

One of the main wavelengths used in radio astronomy is the 21cm line. This wavelength is important, as it signifies a specific element, hydrogen, which makes up the overwhelming majority of baryonic matter of the universe [Ward-Thompson and Whitworth, 2011]. It is also important as it does not need to be excited via a photon like other elements to emit this wavelength. This means it can be used to detect the colder hydrogen gas in galaxies that is invisible to optical telescopes. This wavelength emission comes from the spin of the proton and electron.

Both particles have a total spin (s) of 1/2 and a spin in the z-direction (m) of 1/2 or $-1/2$. This results in Spin-Spin Coupling. This gives the ground state what is called hyperfine-splitting, or in other words 2 different energy levels very close to each other, where the higher, excited state comes from the state $m_e = 1/2$ and $m_p = 1/2$, where the spins are parallel, and the lower energy level comes from the state where $m_e = 1/2$ and $m_p = -1/2$, where the spins are anti-parallel. (see Figure 11).

Due to this second state being lower energy, when it de-excites, a photon is emitted with a 21cm wavelength or 1420.405 MHz frequency. This process has an average occurrence every 10 million years for a given atom however, which would suggest that the radiation would be rather weak, however the large amount of neutral hydrogen in the Interstellar Medium compensates for this, meaning it can be detected, even by smaller telescopes. [Ward-Thompson and Whitworth, 2011].

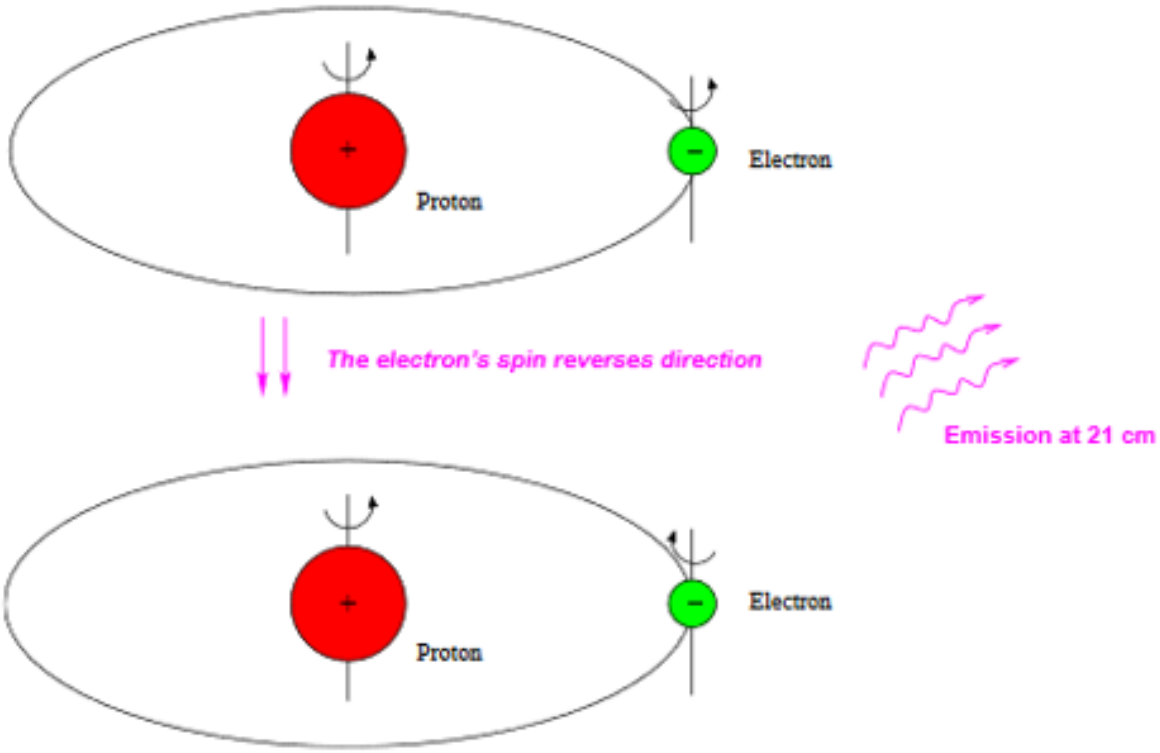

Figure 11: Illustration of the 21cm line from hydrogen [Santo and Uddin, 2013]

The fact that hydrogen emits consistently at the 21cm wavelength does mean that observations can tell us a few properties about the cloud, such as the movement of the cloud relative to the observer via the Doppler shift of the line, causing shift of the line away from 1420 MHz. This effect is seen in observations of the Milky Way, showing the rotation of the spiral arms, as seen in Figure 12. You can also tell properties such as the temperature and density of the clouds, as even if a cloud is stationary relative to an observer, due to Brownian motion, at any given time, some particles will be moving towards the observer, and some away. This will cause a slight broadening to the line around 1420 MHz (assuming the cloud is stationary relative to the observer), so instead of a point line at 1420 MHz, there will be a slight spread to the line, creating a peak around 1420 MHz (in a theoretical cloud that is stationary compared to the observer. If this broadening can be isolated from the Doppler effect of the movement of the cloud, it can be used to determine the velocity of the particles in the cloud, and therefore can be used to infer properties of the cloud [Sobel'man et al., 1995].

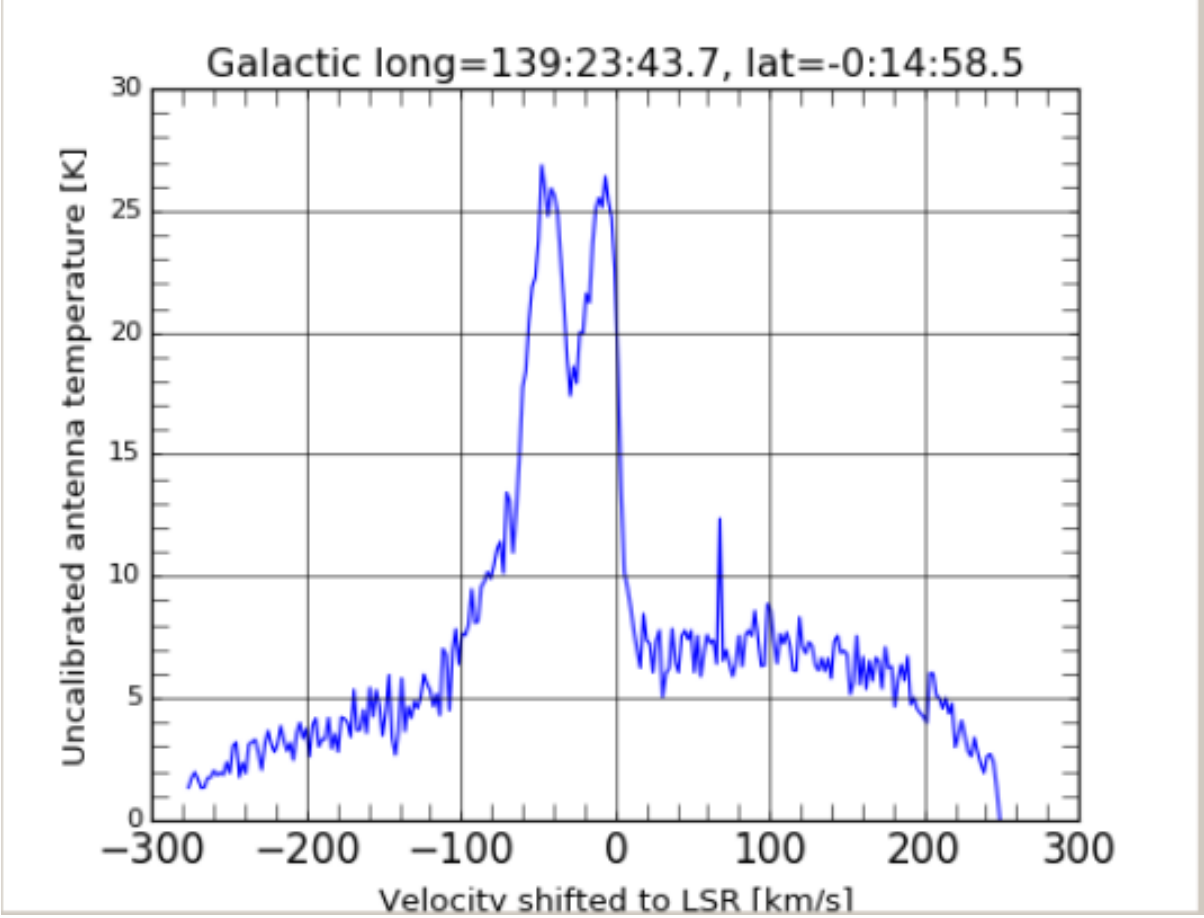

Figure 12: Observation showing the broadening of the hydrogen line due to the rotation of the Milky Way via the SALSA Telescope [Varenius, 2018]. The velocity is calculated to a Local-Standard-of-Rest (LSR), which takes into account the movement of the Sun and Earth in relation to the observed target.

This can also be seen in observations of M31, shifted to shorter wavelengths due to the overall velocity of M31 coming towards us. For telescopes where the beam width, or the angular diameter that the telescope can observe at once, is wider than M31, and so collects photons from the entire profile of the galaxy in one observation, the integrated

observation will show the broadened line shifted up to a higher frequency. This shift can be seen with telescopes that have much narrower beam widths than Andromeda, that need multiple observations to capture the full galaxy (see Figure 13). The line is broadened due to the rotation, where each extreme of the line profile shows the rotation at the edge of the galaxy, whether that be towards or away from us. This broad line is shifted however to the higher frequency due to the galaxy itself coming towards us, blue shifting the radio waves to a higher frequency. [Ward-Thompson and Whitworth, 2011].

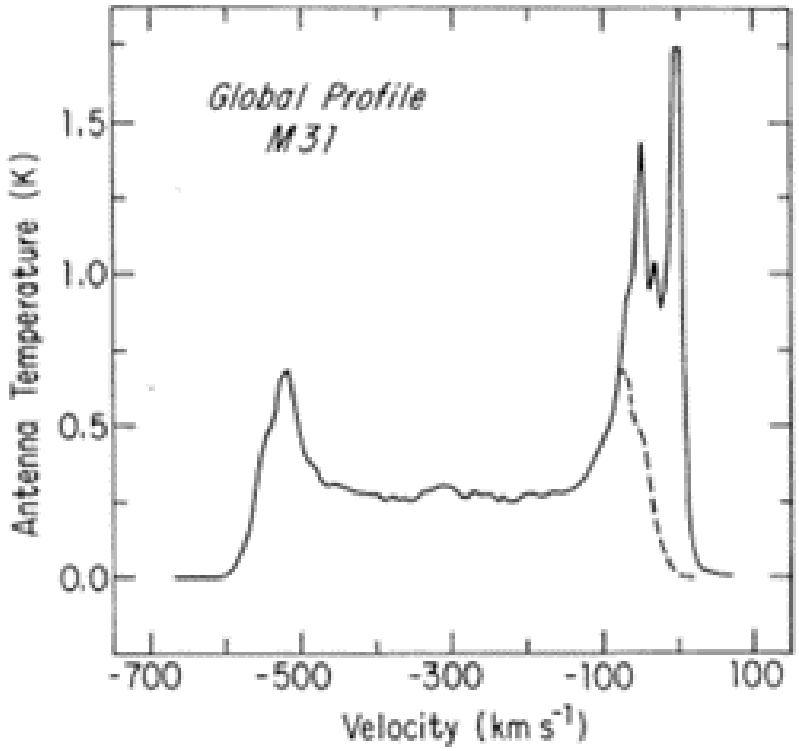

Figure 13: Global Profile of M31, with the red/blue shift converted to velocity and the strength of the signal being the Antenna Temperature [Cram et al., 1980]

These properties of the Hydrogen Line make it a good undergraduate study, as it means a simple setup can take useful measurements, such as the SALSA, Haystack and VATLY [Phuong et al., 2014] telescopes (See Section 1), which are small telescopes that the planned telescope will be modelled after.

Even with their limited resolution compared to larger telescopes, they can still take global profiles of objects such as M31 as shown in Figure 13, which is still a technique used today, with much larger telescopes observing much smaller, further away objects, such as shown in Figure 14

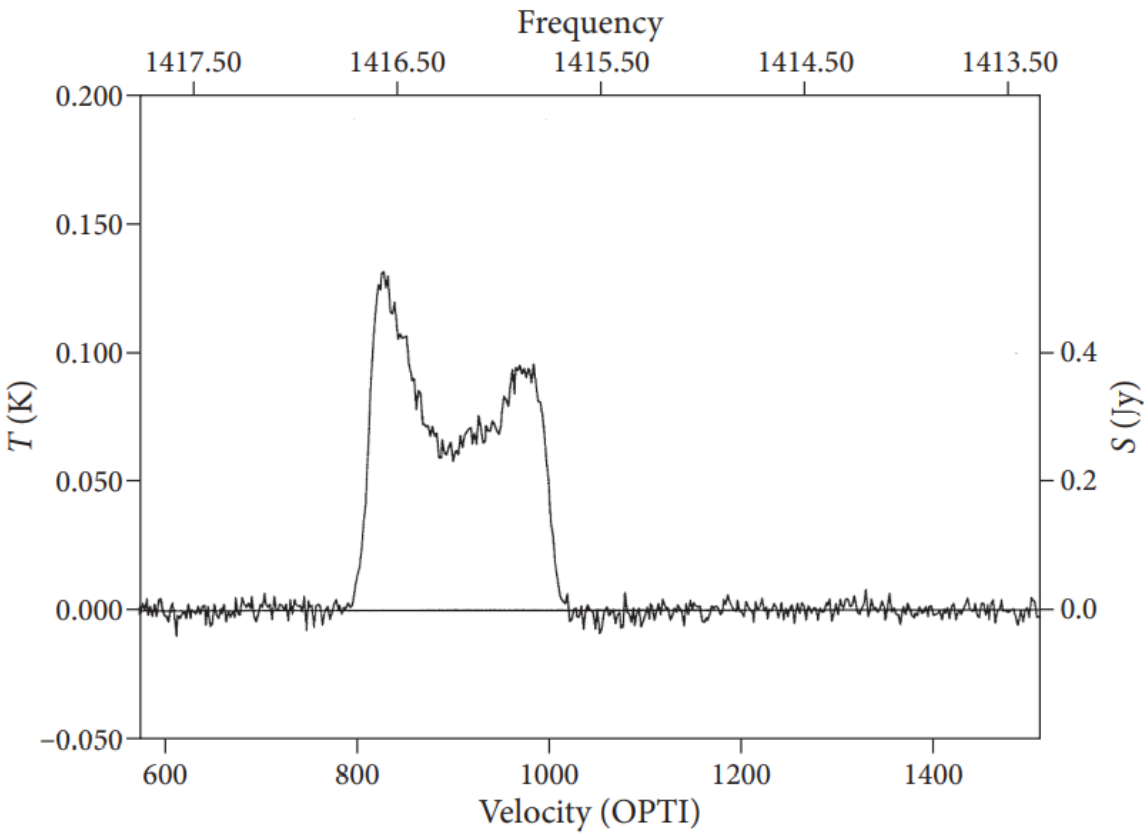

Figure 14: Global Profile of UGC 11707, a galaxy, taken with a 140 ft, or 42m telescope [Condon and Ransom, 2016]

2.4 Spectral Index

Although the telescope is planned to observe at and around 1420 MHz, there is more of the spectrum that could be covered, if the telescope is fitted with a wideband receiver, either initially or via an upgrade, thus allowing it to cover more of the 30HZ-300GHz radio spectrum [Halliday et al., 2014]. This would allow the telescope to take continuum measurements. Continuum measurements are measurements taken over a wide range of frequencies, and allow the measurement of how the flux density can change over the frequency band. This can be seen in Figure 15, where the flux density of the base reading decreases going right, as you increase in frequency.

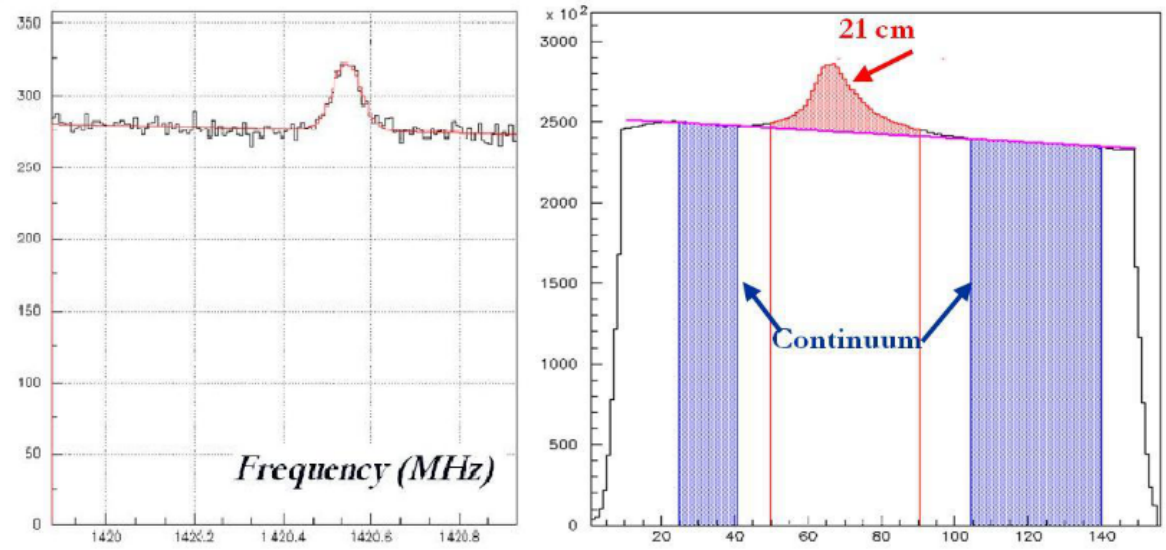

Figure 15: Image showing a spectrum at 1420 MHz (Left), with the 21cm line and continuum labelled (Right), with the continuum showing a decrease as frequency increases [Phuong et al., 2014]

Spectral Index is the factor of how the continuum of objects, changes in flux density over a range of frequency values, as shown by the relation below:

$$\epsilon \propto \nu^{\alpha} \tag{3}$$

where ϵ is the radiative flux density W/m^2, ν is the frequency (Hz) and α is the spectral index [Wilson et al., 2013].

This means if a telescope can get at least two data points they can work out the spectral index of the object. This is useful as it can tell us something about the source of the emission. For example, an index of -0.1 to 2 is usually thermal emission, while a highly negative index indicates synchrotron emission [Wilson et al., 2013]. It can also tell the opacity of certain structures, for example, a negative gradient indicates a transparent source, while a positive index suggests a more compact, opaque source [Verschuur et al., 2012]. The Spectral Index can also be used in reverse, as you can use it to predict what strength of signal you should expect at particular

wavelengths, if you know the index beforehand. Figure 16 shows how different sources vary in flux density as frequency changes.

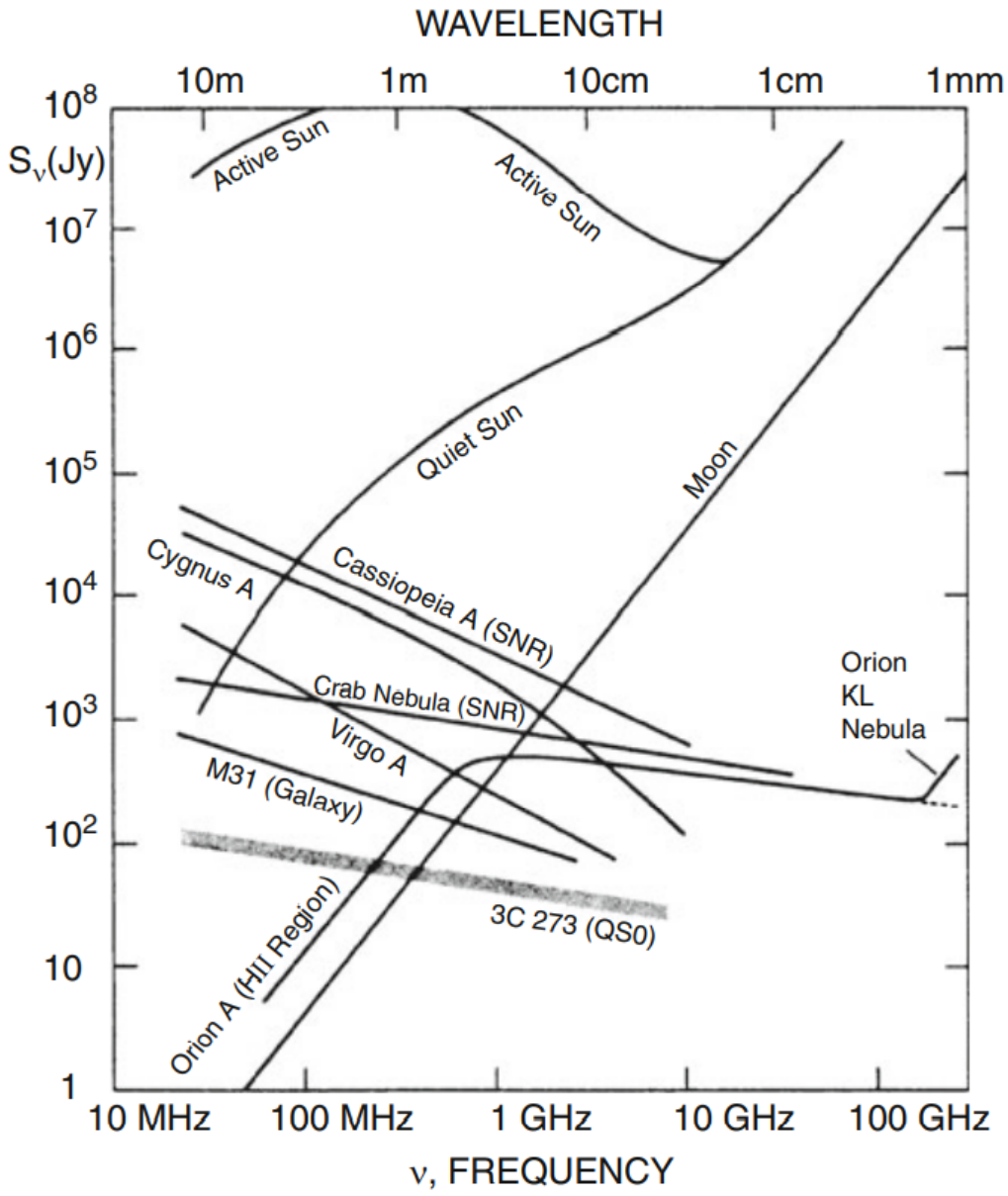

Figure 16: Spectra of various different radio sources [Wilson et al., 2013]

Here we can see the spectral ditribution of various sources. A positive gradient shows thermal sources, such as the moon and the quiet sun, whereas the negative gradients show non-thermal sources, such as Cassiopeia A (3C461), the radio galaxies Cygnus A (3C405), Virgo A (Messier 87, 3C274) and the Quasi Stellar radio source (QSO) 3C273, which suggests synchrotron emission [Wilson et al., 2013].

2.5 FM and AM modes, Carrier Signals

A major source of interference that may be present at Alston are AM and FM radio signals, especially from the Winter Hill broadcasting antenna, so being able to recognise these signals will be important, as we can then tell whether a source of interference is a constant source, like from Winter Hill, or something in the nearby area that may be producing RFI, like an unshielded Wi-Fi camera for example.

The difference between AM and FM signals are how they are modulated, so how information is encoded, and then decoded. For both methods, a base wave, called a carrier wave is used, which is then altered to encode information. For AM, or Amplitude Modulation, the Amplitude (or power of the signal) is changed to add in information, whereas FM, or Frequency Modulation, has the Frequency changing instead. This causes the carrier wave to change as shown in Figure 17 :

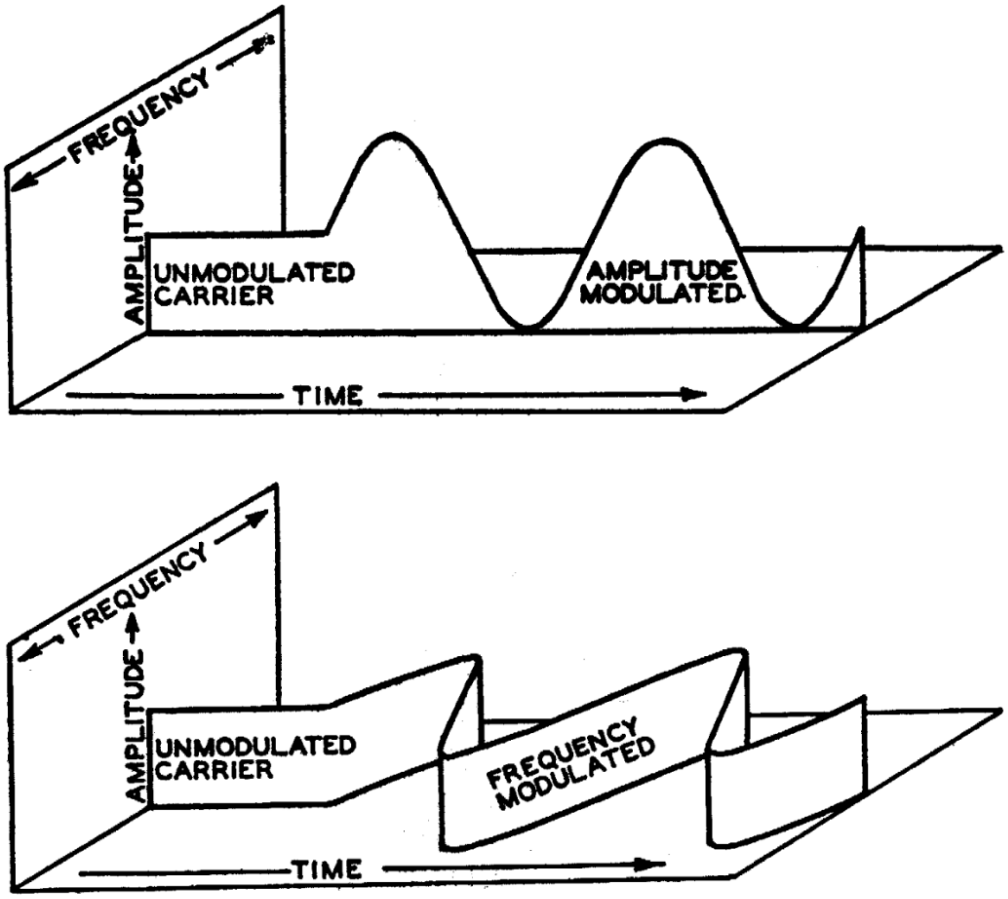

Figure 17: How a FM and AM signal is modulated from a carrier signal [Frost, 2010]

However, as the signal is a modulated wave, the carrier wave is still detectable in most forms of modulation, as shown in Figure 18. In some forms of modulation, the carrier signal is removed, as well as one of the side bands. This does result in a lower bandwidth and quality of signal however.

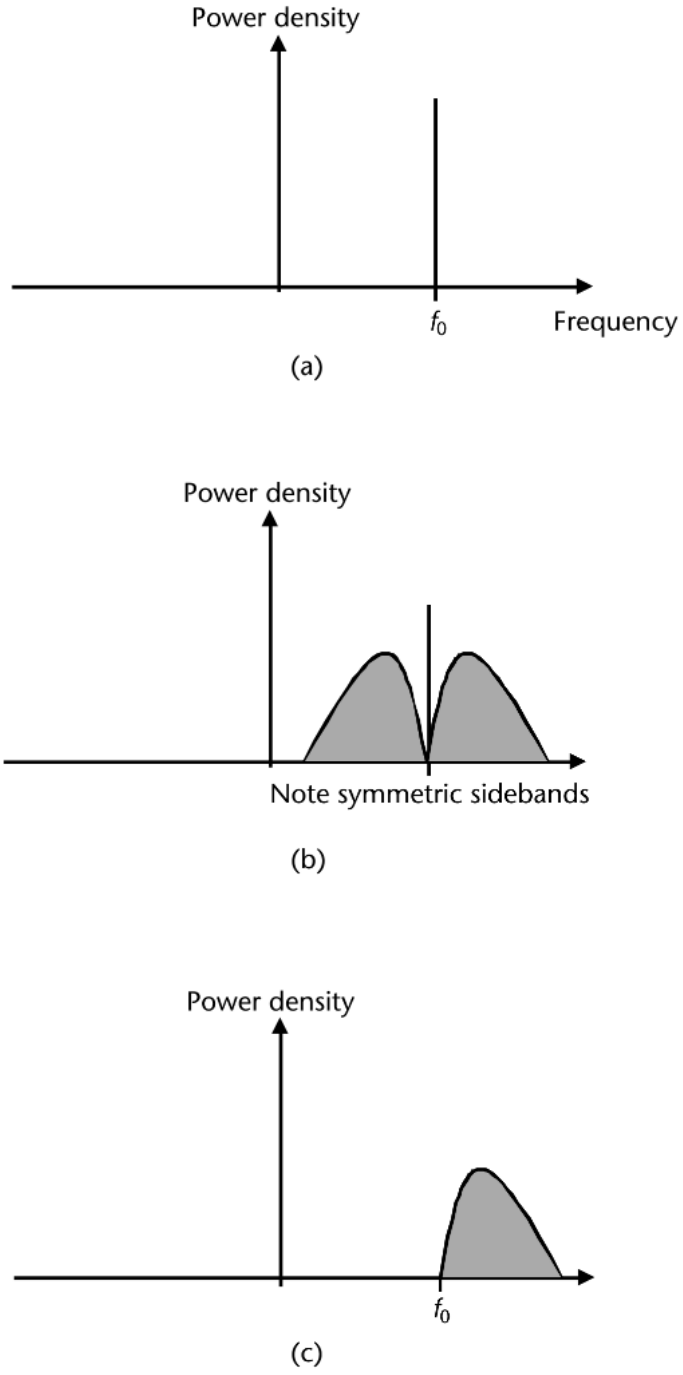

Figure 18: How an AM or FM signal looks when frequency is plotted along the x axis and signal power along the y axis [Johnson, 2013]

In Figure 18 (a), only the carrier wave is present, in (b), both sidebands are present and symmetrical, while in (c), only one sideband is present.

AM modulation also has sidebands, however this is not due to the frequency changing, as only the amplitude is changed, but because the modulated wave shown can be expressed as a combination of three separate uniform waves, when the signal is decoded, AM signals also have an upper and lower band, but with a much lower bandwidth, meaning they take up a lot less of the spectrum than FM signals.

2.5.1 Broad and Narrow Band Signals

FM and AM signals may therefore interfere in two different ways, a narrow FM or AM signal will show up as a spike on a recording, which if its frequency is the same as the signal we are trying to observe (in this project, being around 1420 MHz) then the signals we are trying to observe will undetectable. Broad band FM signals however will have a spike, but due to their wide bandwidth, may raise the floor of the background noise around the carrier frequency, which can obscure any weak signals that we may want to observe, this means any surveys done will need to cover a wider area than just a few MHz either side of 1420, to make sure there are no broad band signals around the frequency. Although we would not necessarily expect a commercial AM or FM broadcast, there is an amateur radio band, as seen in Figure 4, between 1240 MHz and 1325 MHz, which could have broadcasts that may raise the noise floor, as well as other allocations, such as satellite, public sector, and aeronautical uses that could cause issues if any broad band signals are being used in those allocations.

As an example, for the sorts of power received from a standard FM transmitter and a neutral hydrogen in a galaxy, using Alston as a point of reference, the Winter Hill Mast as the FM transmitter and M31 as the galaxy, Winter Hill transmits at a maximum of 100kW, and the power from M31 as 0.24 Janskys. Taking the distance from Alston to the transmitter as 20km, this gives the surface of a sphere with a radius of 20km as 50.2×10^9 m^2. Dividing the power of the transmitter by the surface of the sphere gives the intensity of the transmitter at Alston from the Winter Hill Mast as 2×10^{-5} W/m^2. As Janskys are 10^{-26} W/m^2/Hz, this gives a power value of 2.4×10^{-27} W/m^2/Hz. This shows the vast difference in power between the sources and means that the signal from observations can be easily masked by strong signals around 1420 MHz that may raise the noise floor[7] [Gray and Mooley, 2017].

[7]https://www.aerialsandtv.com/knowledge/transmitters/winter-hill-transmitter

2.6 Harmonics

Harmonics are signals that can arise from another, source signal, where multiple signals arise that have frequencies that are multiples of the original frequency, such as 50Hz having as second harmonic of 100Hz, and a third harmonic of 150Hz, or wavelengths that can fit inside of the original wavelength, as shown in Figure 19.

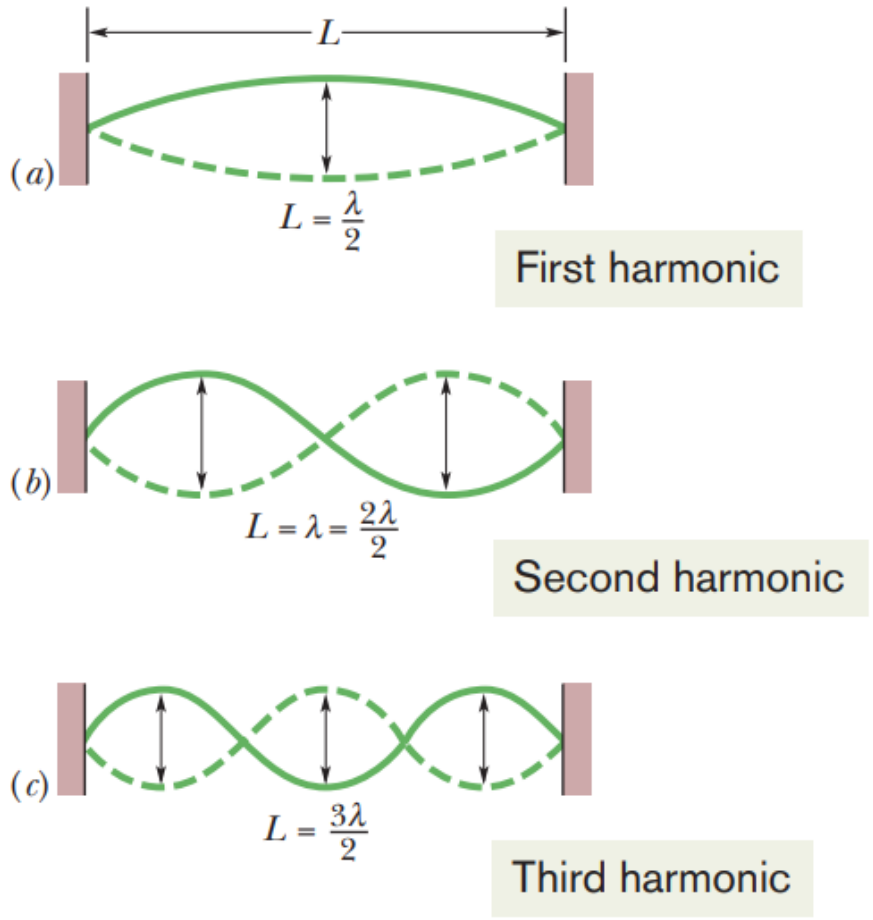

Figure 19: How Harmonics are related to the source signal, with (a) showing the first harmonic which is equivalent to half a wavelength, (b) showing a full wavelength and (c) showing a wavelength and a half. [Halliday et al., 2014]

These are usually not present in most devices, as work is done to reduce this effect, however they can still be present as power system harmonics, and are present in devices such as adjustable speed drives, capacitors, circuit breakers, fuses, conductors, electronic equipment, lighting, metering, protective relays, rotating machines, telephones, and transformers [Wagner et al., 1993].

This can cause a potential issue, as although at and around 1420 MHz is legally protected from broadcasts, harmonics may come from devices that operate at lower frequencies, such as the Winter Hill Mast. This is because the mast operates at and below 700 MHz, so although it does not transmit at the frequencies we are looking at, it could cause interference, and potentially raise the noise floor, as explored above. Most

devices are built to be compliant with EMC standards[8] as well as ITU recommendations which manage unwanted emissions from devices [ITU-Radiocommunication-Assembly-SM.329-10, 2003]. These standards are used to stop devices from interfering with each other in their bandwidths, however as radio astronomy has developed, going outside of the protected 1420 MHz band with continuum observations, it is possible there may be interference from harmonics that could cause issues on the site from devices that emit unwanted signals via harmonics. This means a wide band survey would be needed to see if it has any effects on the radio environment around the 1420 MHz band we are looking at for the planned telescope.

[8]https://www.emcstandards.co.uk/emc-standards-compliance-testing1

3 Telescope Plan

Before the survey can tell whether the site is suitable or not, the general parameters of the planned telescope need to be laid out, as these can factor in to whether the site is suitable or not. The telescope will be modelled after other Small Radio Telescopes (SRTs), most notably the Such A Lovely Small Antenna (SALSA)[9] and the Haystack Observatory SRT[10]. These projects both outline the sort of capabilities expected from a telescope of this size, and also provide information on the parts needed.

The SALSA telescope has a dish diameter of 2.3m and designed to operate at 1420 MHz, and is designed to take observations of the milky way, the sun and satellite signals. It has an angular resolution around 6 degrees at 1420 MHz. It also has a maximum bandwidth of 10 MHz with a maximum bin count of 8192, and is able to track in steps of 0.125 degrees around each axis. The software used is the Universal Software Radio Peripheral (USRP). [Varenius, 2018]

The Haystack SRT is designed as a project that can be undertaken by anyone using commercially available equipment, and so there are varying options depending on budget, and a full manual on construction is available [Johnson, 2012]. Some of the dish options suggested are either a 1.8m solid dish, or a larger 2.4m mesh dish, alongside varying amplifiers, foundations, receivers, enclosures etc.[11]. This means it a bit more flexible than the SALSA telescope design, as it can observe at 1420 MHz, but be altered depending on the users need.

3.1 Dish

For a SRT, a dish around 2-3m is needed, as these can be mounted on simple motorised mounts that are relatively cheap. A potential provider for this dish is RF HAMDESIGN[12], which provide a 2.4 metre dish, along with mounts for the antenna along with motorised mounts for moving the telescope. They have two different variants of their dishes, as they are made of mesh. The mesh allows for a lighter construction, and also a lower wind load, meaning that wind will exert less force on the telescope due to the mesh, as opposed to a solid surface, as seen in Figure 20, meaning a weaker mount and foundation is needed to keep the dish in place in high winds, and is also less expensive.

[9] https://vale.oso.chalmers.se/salsa/welcome

[10] https://www.haystack.mit.edu/haystack-public-outreach/srt-the-small-radio-telescope-for-education/

[11] https://www.haystack.mit.edu/wp-content/uploads/2020/07/srt_SRTPartsList.pdf

[12] https://www.rfhamdesign.com/products/parabolicdishkit/index.php

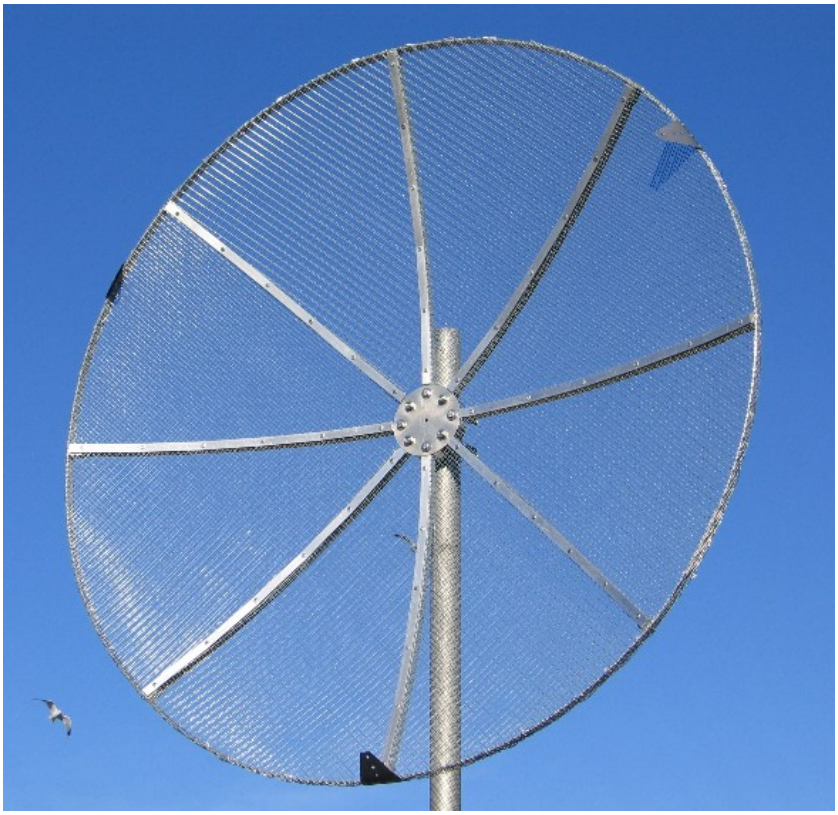

Figure 20: Example of a mesh dish provided by RF HAMDESIGN

This does however limit the frequencies that the telescope can observe at, as wavelengths smaller than 1/10th the mesh may pass through, depending on the magnetic permeability of the material the mesh is made of, and not be detected. One dish type can reflect up to 6GHz, and the other can reflect up to 11GHz. The second option would be the better option as it would allow for a wider range of frequencies to be used in future additions and changes to the telescope without needing a new dish.

If the 2.4m dish is used, this also gives the beam width, or the angle which the telescope will observe at once, as described in Equation 2. This gives the beam width of the potential dish to be approximately 6 degrees at a frequency of 1420 MHz.

The dish size will also effect the gain of the telescope, which is calculated via Equation 1. This gives the potential gain of the telescope on the lower estimate, using an aperture efficiency of 0.55, to be a factor of 709 times, which converted to dBi gives a value of 2.85 dBi.

3.2 Antenna and Filters

The antenna for the initial setup would receive at 1420 Mhz, for example a product similar to those provided by Radio Astronomy Supplies[13] as seen in Figure 21, which provide a antenna at that frequency, as well as supplying filters for the signals captured by it, which would help manage interference around the band that is being looked at. They also provide Low Noise Amplifiers (LNA) that can amplify the weak signals that

[13]https://www.radioastronomysupplies.com/products.html

are captured by the telescopes, that with a good LNA will increase the signal without a large increase to the noise.

Figure 21: Example of a antenna and feedhorn provided by Radio Astronomy Supplies

3.3 Receiver and Software

For the receiver, the one in use for the current survey system would be ideal, the SDRPlay RSPdx, as it can handle signals from 1kHz to 2GHz, which covers the 1420MHz band needed, and it has two separate antenna ports, which would allow both a potential survey station and telescope to be plugged in simultaneously. This would work well with the VIRGO software, which as stated above can do both RFI surveys and telescope observations, so either system could be operated via one computer and software package. In Figure 22 is an example of the sort of observations VIRGO can take [Spanakis-Misirlis et al., 2021].

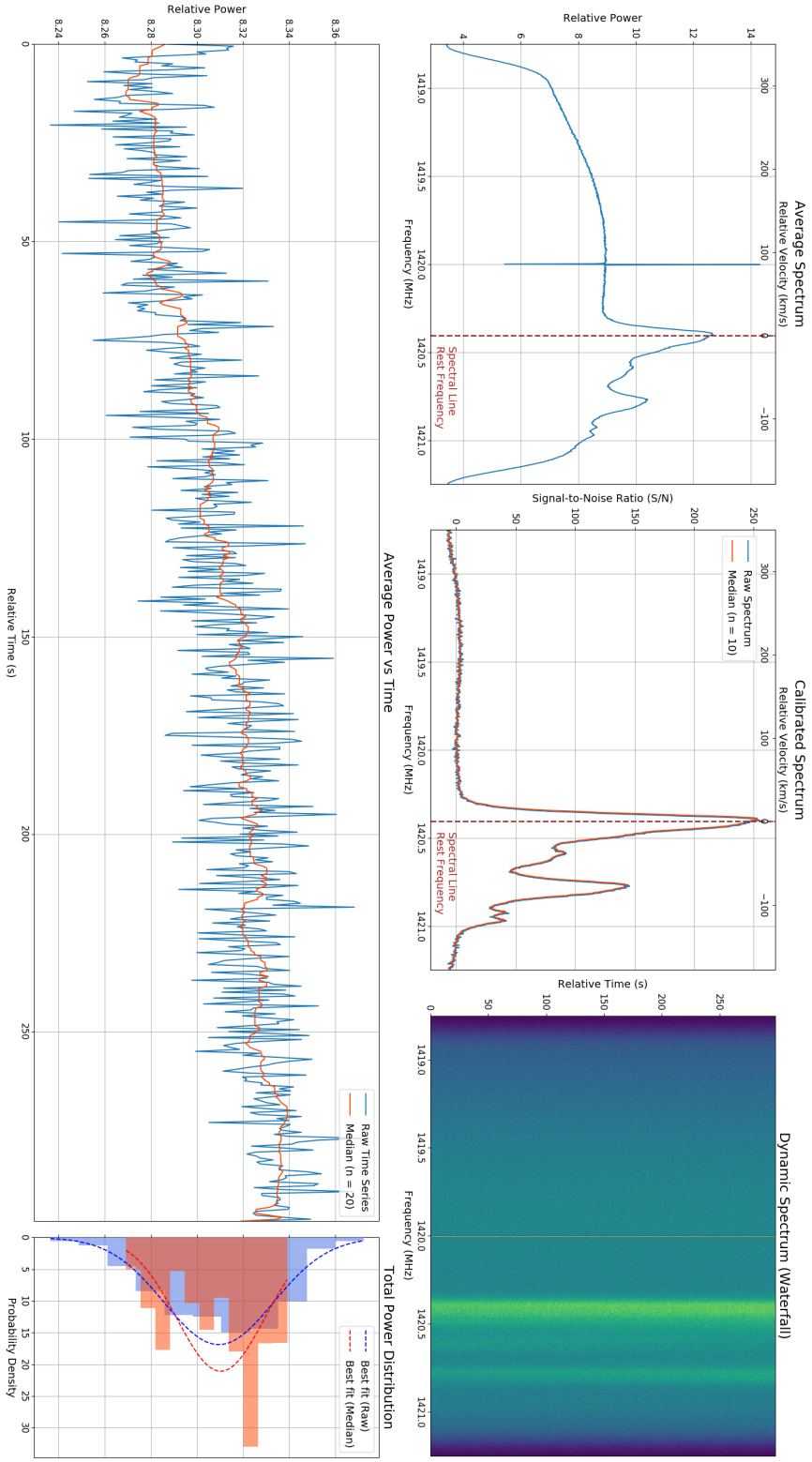

Figure 22: Example observation taken using the VIRGO software of hydrogen gas clouds towards the Cygnus Constellation[14]

This setup of antenna and receiver would be ideal for observing at 1420 MHz, but if any future projects were to look at other bands in the radio spectrum, these would have to be updated.

[14]https://github.com/0xCoto/Virgo

4 Previous Examples of Surveys

4.1 Thai Radio Telescope

For reference, previous surveys for radio telescopes around the world were looked at, to see if any of their methods could be replicated, if suitable, for this survey. One of these papers was Radio Frequency Interference Site Survey for Thai Radio Telescopes [Jaroenjittichai et al., 2017]. Their survey was from 20MHz-6GHz, due to the telescopes being planned to observe within this range. For their survey, they used a directional antenna on a motorised mounting, which took observations at a single point in different directions.

This would not necessarily be ideal for this survey, as the sites being surveyed were more remote locations, so the RFI would not change much over the potential site, whereas Alston has multiple buildings on site that may have potential sources of RFI. This means that one reading is not ideal to get a picture of the radio environment over the entire site, so multiple readings around the site would be better to get a general idea of the environment. A directional antenna would not be good for a first survey, as the time taken to move the antenna may mean signals are lost, so an omnidirectional antenna would be better, however further surveys with a directional antenna would be useful to identify where any signals are coming from.

One point that would be useful to implement from their survey was the setting they took their measurements with, as they took two separate data sets. One was using an average mode, taking the average of all the points at a certain frequency over time. The other was the peak mode, which recorded the highest point at a certain frequency. This allowed them to capture both long term signals (with the average mode) and brief signals (using peak mode) which may be lost using the average mode. As the software being used to do this survey has both modes, recordings of both modes will be used in this survey.

They took measurements of three separate sites, with both the average and peak modes, and found site A was the most polluted, with B and C being less polluted, however the observing window between 1000-1800 MHz was clearer in B than C, making it more ideal for observations of the hydrogen line and pulsars, although site C has a much more convenient location. They also found no major interference from Geo Stationary Satellites in any site, meaning it was not a factor they had to consider, although they did pick up signals from FM, TV, Mobile and Wifi signals in all sites to varying degrees.

Although they did not find signals from satellites however, it is important to note that these surveys were undertaken in 2017, and in the years since, satellite constellations such as Starlink have been launched, and may now cause a measurable level of interference, as the bands used by satellite down link operate near the 1420 MHz band, at 1452-1492 MHz [15]. With an out of spectrum side-lobe [Dai et al., 2019], as discussion in Section 1, this could cause a signal at around 1420 MHz, or potentially cause interference directly with a continuous spectrum observation, as discussed in Section 2.4, which requires a much wider frequency band. This is an increasing worry with

[15] http://static.ofcom.org.uk/static/spectrum/fat.html

radio astronomy, as more of these constellations are planned to be launched, with the goal of worldwide coverage. This could cause far reaching issues for current and future radio telescopes, which rely on radio quiet areas to operate, as those areas may shrink and disappear from even the most remote of locations.

The noise floor they found also will provide a good comparison point to this survey. At around 1420 MHz the noise floor appears to be around -145 dBm for the peak mode, and -160 dBm for the average mode when converted from dBW/m^2/Hz to dBm, reversing the method they used to get their results, as outlined by ITU documentation [ITU-Radiocommunication-Assembly-RA.769-2, 2004], to get a standard unit used in spectrum analyser software, specifically the value $P(f)$, as shown below:

$$\begin{aligned} S(f)[dBW/m^2/Hz] = P(f)[dBm] - G_{ant}(f)[dBi] - G_{LNA}(f)[dB] \\ -10log(\Delta f_0)[kHz] + 10log(f)[MHz] - 95.54 \end{aligned} \quad (4)$$

Where $S(f)$ is the Spectral Flux Density, $P(f)$ is the power measured by the spectral analyser, G_{ant} is the antenna gain, G_{LNA} is the gain of the Low Noise Amplifier (which in the case of the Thai Radio Telescope survey and this survey are both 0), Δf_0 is the resolution bandwith (in kHz), and f is the frequency [ITU-Radiocommunication-Assembly-RA.769-2, 2004]. This will be used later in this thesis to allow for easier comparison between the results found on the site and other surveys, where Spectral Flux Density is used as the standard unit. This noise floor would not necessarily be expected at the Alston site, as although all of the sites are close enough to interference sources such as FM, TV, Mobile and WiFi transmitters that they were picked up in all three sites, all were chosen due to mountains surrounding each site, which Alston does not have the benefit of, as shown in Section 1.

4.2 Square Kilometre Array (Australia)

Another point of comparison would be from the surveys completed for the Square Kilometre Array, as the candidate sites that were chosen were chosen specifically for their remoteness from RFI sources. These therefore provide a good example of what an ideal radio environment would be, and what sort of RFI survey system is used on larger projects.

In total, the SKA site surveys used 5 different measurement modes, Fast Scanning, High Sensitivity, Transient Mode, Rural Hold, and Max Hold Mode. Fast scanning mode was designed to get a rapid overview of the entire spectrum in all directions, integrating for 10 seconds on each pointing axis (as a directional antenna was also used here). High sensitivity uses an integration time of 60 seconds with 120 repetitions, and is more comparable to the peak mode used in the Thai Radio Survey. Transient mode uses an integration time of $1\mu s$ with 5x10^5 repetitions, and a channel bandwidth of 1 MHz (so the entire spectrum is not done at once in an integration). Rural mode has a shorter integration time, 60 seconds, with 10 repetitions for each pointing, this is because the time at the more remote areas was limited, so a more time efficient method was needed for the survey, where the longer High Sensitivity mode could not be done. Max Hold

Mode is the same, and is a more efficient version of the Transient mode. It uses an integration time of 0.1 seconds with 90 repetitions. The Rural and Max Hold Modes do not provide as accurate or sensitive data as the other modes usable in the core sites, but are suitable enough to measure any interference in those areas, as interference is expected to be minimal due to the remoteness of the locations. These however would be more easily implemented in a potential RFI survey station, and could potentially be a base for further surveys on the Alston site if needed, as they take more time, with the Rural mode taking almost 2 days to complete a full spectrum survey, and the Max Hold mode taking just over 1 day [Boonstra and Millenaar, 2011].

Figure 23 shows the spectrum obtained using the High Sensitivity mode in site Y, which is in Australia, looking north. It has known broadcasts annotated in the lower half of the graph, to help identification of any signals found.

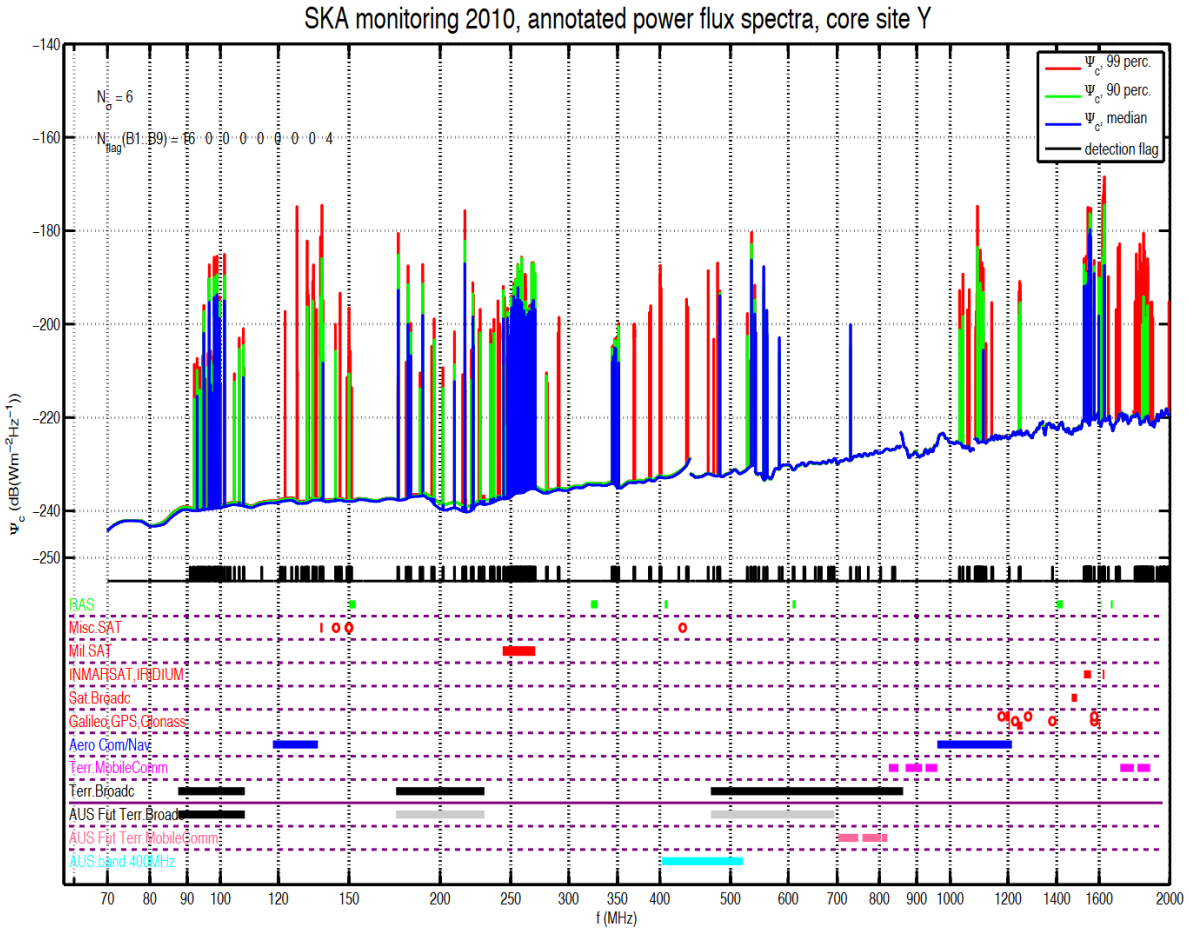

Figure 23: Spectra of site Y in Australia from the SKA RFI Survey, using the High Sensitivity Mode, looking north [Millenaar, 2011]

At 1420 MHz, the spectrum is clear of any identified signals, as expected due to the remote location and bandwidth cleared for radio astronomy. There is however some signals either side. The lower half of the graph suggests the signals to the left are coming from aeronautical communications/navigation, while the signals on the right may come from a mix of GPS satellites and terrestrial mobile communication.

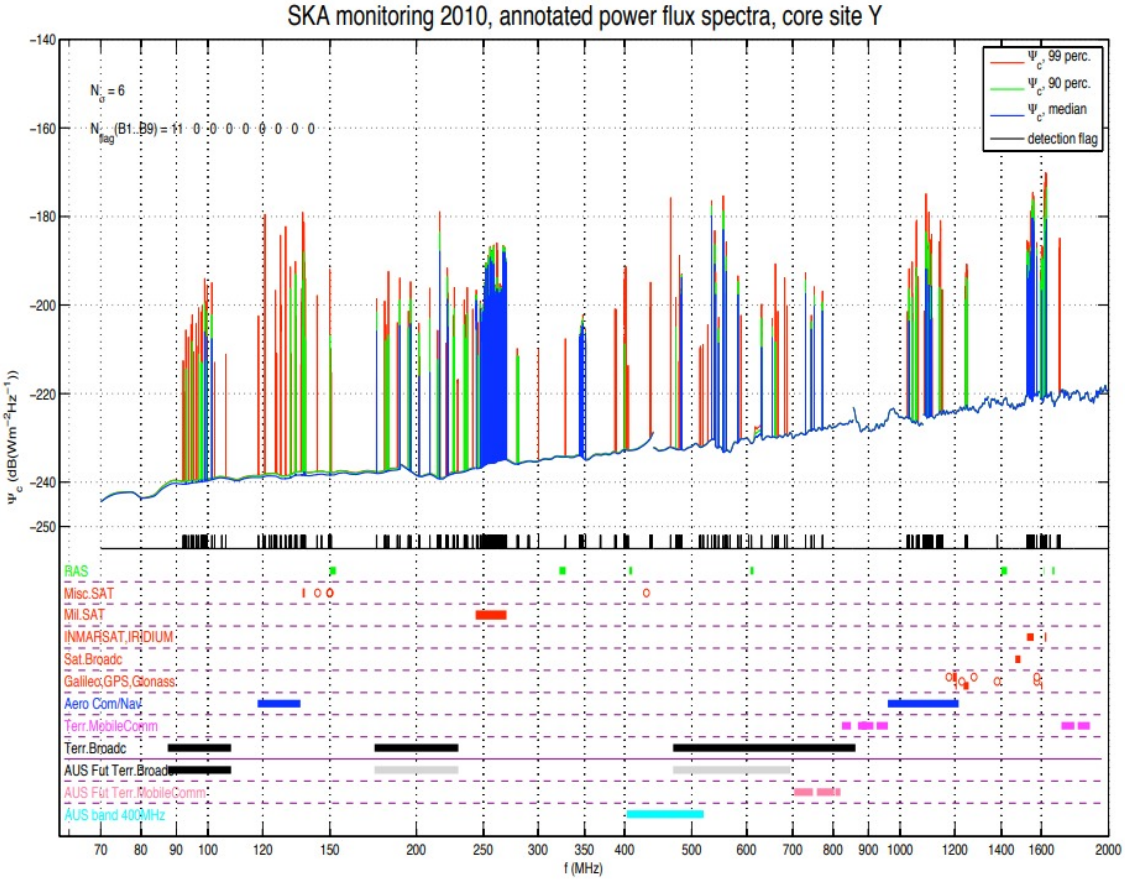

Figure 24: Spectra of site Y in Australia from the SKA RFI Survey, using the High Sensitivity Mode, looking south [Millenaar, 2011]

Looking South, in Figure 24, there is a slight difference in the signals to the right of the 1400 MHz area, as the signals from the terrestrial mobile communications are gone, indicating that that the broadcasting towers are to the north of the site. With the rest of the spectrum, there is a lot more interference between 600 and 800 MHz, most likely coming from terrestrial broadcasts.

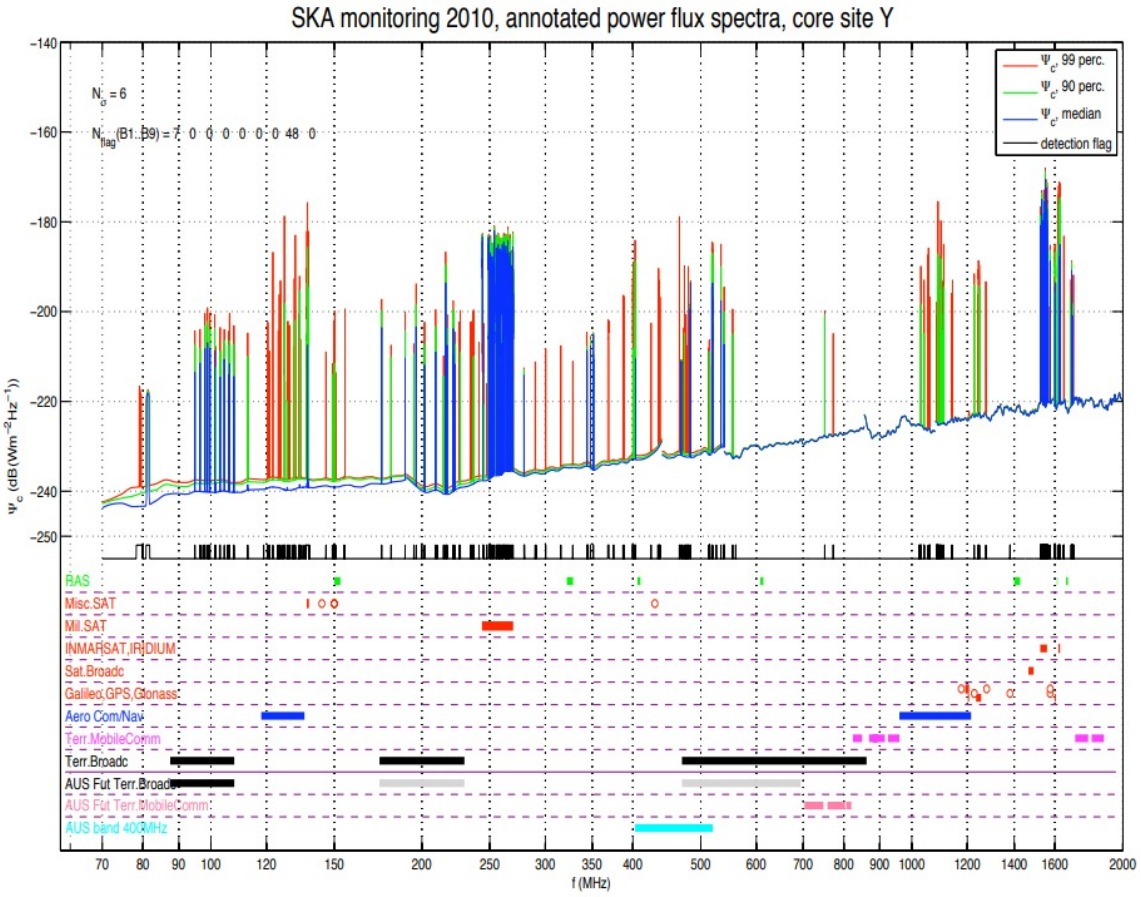

Figure 25: Spectra of site Y in Australia from the SKA RFI Survey, using the High Sensitivity Mode, looking east [Millenaar, 2011]

With Figure 25, towards the east, we again see a band clear of interference between 600 and 800 MHz, and again no interference from the terrestrial mobile communication band, as was shown in Figure 23, the north spectrum. With the final spectrum looking towards the West, in Figure 26, there are a few sources of interference between 600 and 800 MHz, although not as much as some of the other readings. The major difference is a few clear signals at and around 1400 MHz, which may be coming from the Galileo GPS system.

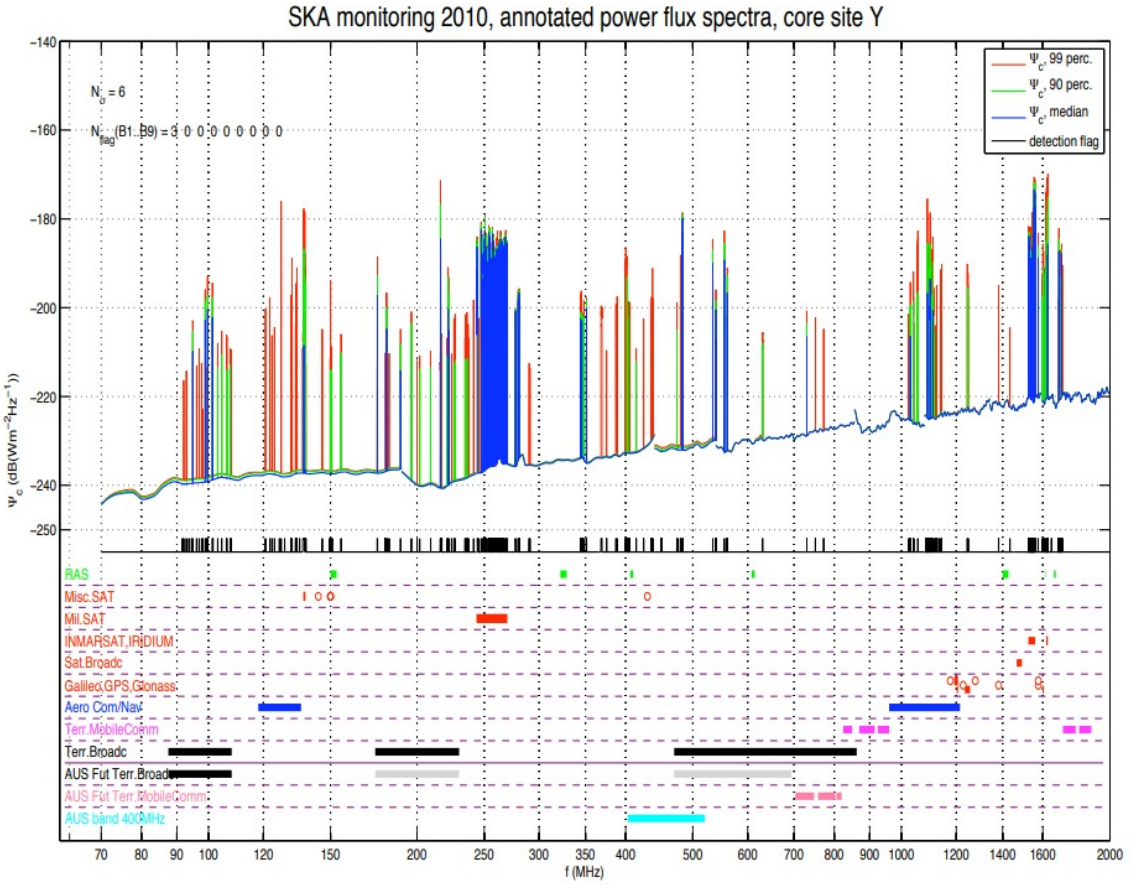

Figure 26: Spectra of site Y in Australia from the SKA RFI Survey, using the High Sensitivity Mode, looking west [Millenaar, 2011]

4.3 Square Kilometre Array (South Africa)

The other sites that was put forwards for the SKA was a site in South Africa. An identical survey to the one in Australia was undertaken, and there are a few differences to note. First is with Figure 27, where around 1400 MHz is similar to the Australia site, except the terrestrial mobile communication signals are not above 1600 MHz like before, but between 900-1000 MHz, suggesting that the broadcasting towers use different frequencies in this area of South Africa. There is also a lot less interference between 300 and 500 Mhz, with a lot fewer peaks, however there does not seem to be one single source to attribute to this, as it seems to be a mix of less interference from terrestrial broadcasting and private/public communication.

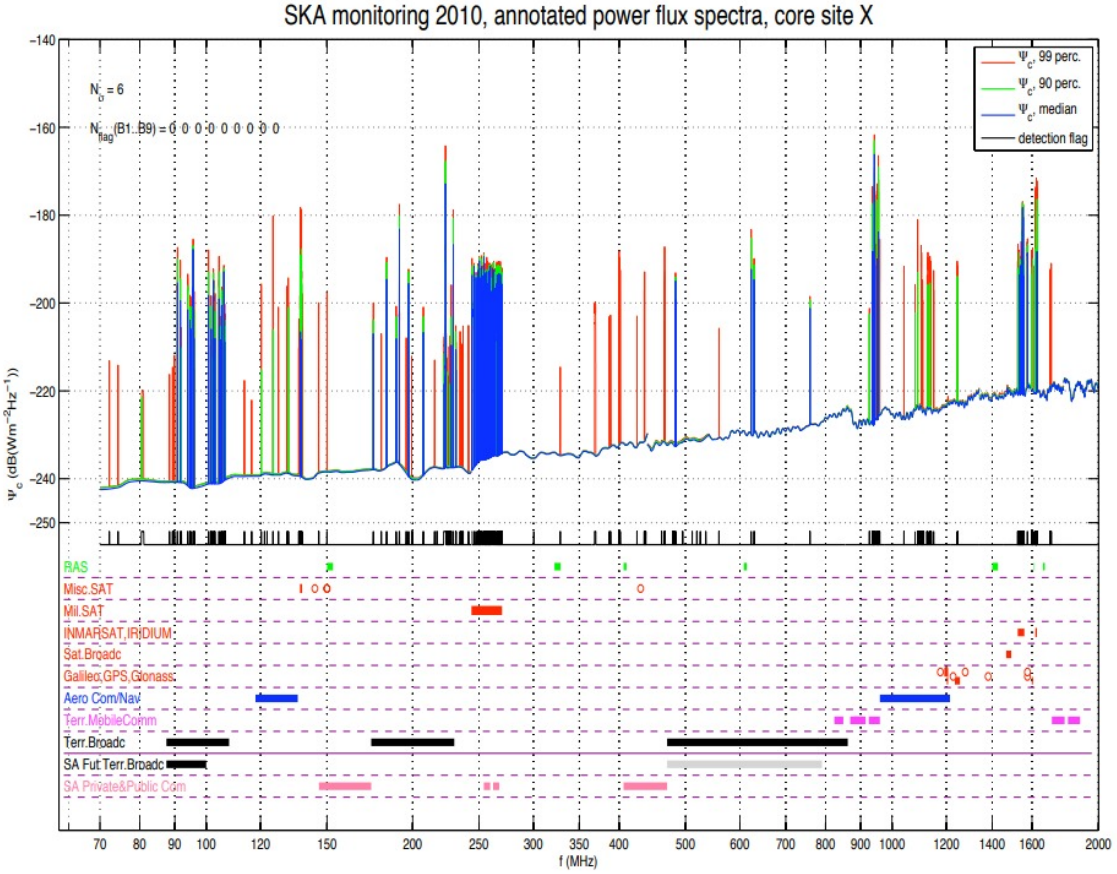

Figure 27: Spectra of site X in South Africa from the SKA RFI Survey, using the High Sensitivity Mode, looking north [Millenaar, 2011]

Looking south in Figure 28, the main difference is from terrestrial broadcasts, with a large patch of interference between 450 to 550 MHz. There does also appear to be slightly less interference around the 1400 MHz band, although the interference from the terrestrial mobile communications is still there.

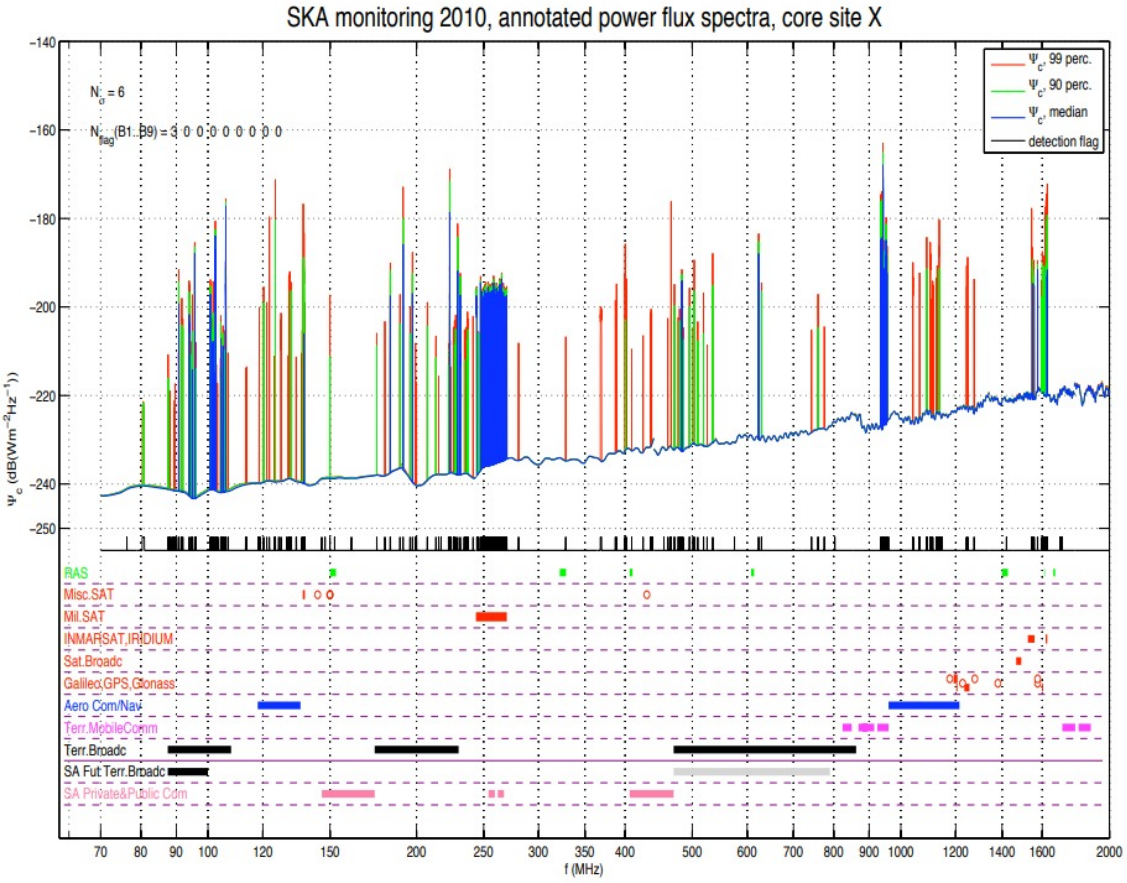

Figure 28: Spectra of site X in South Africa from the SKA RFI Survey, using the High Sensitivity Mode, looking south [Millenaar, 2011]

Figure 29, looking east, shows the most RFI of all of the South Africa readings, with a lot more interference between the 300 to 800 MHz band. A lot of this interference seems to be coming from terrestrial broadcasts.

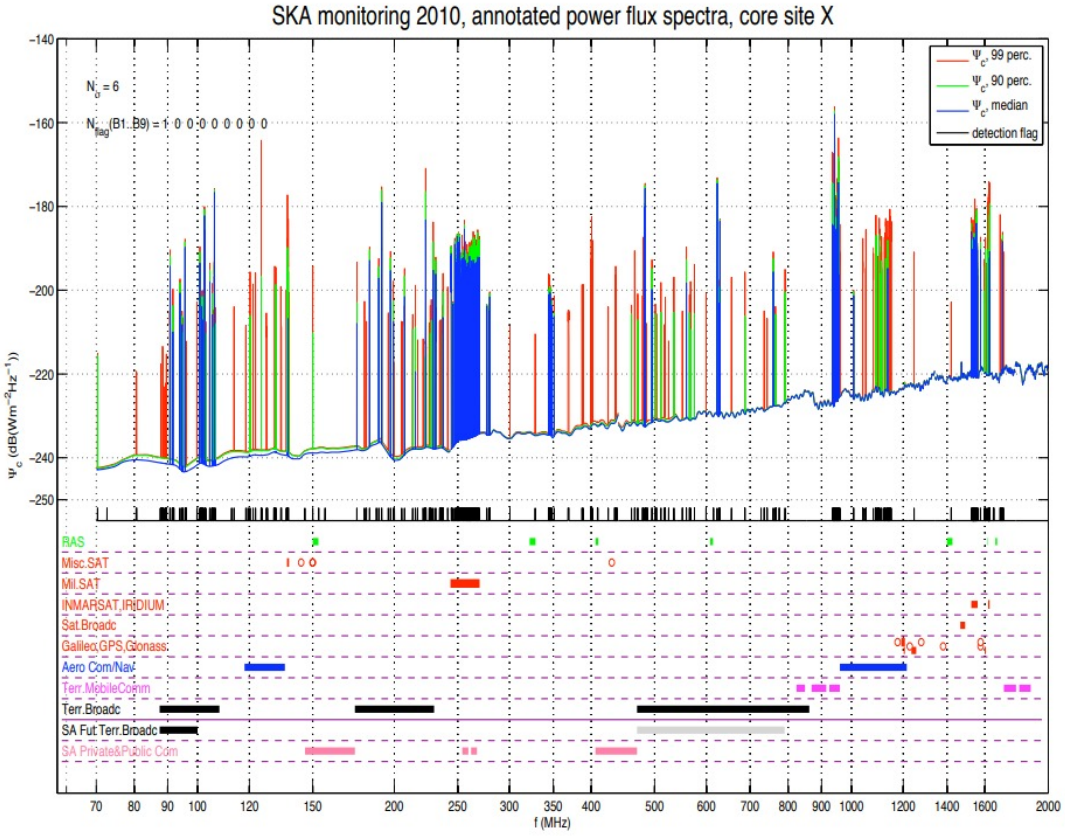

Figure 29: Spectra of site X in South Africa from the SKA RFI Survey, using the High Sensitivity Mode, looking east [Millenaar, 2011]

Towards the west in Figure 30, there is the least interference compared to the rest of the South Africa observations, with a large gap with no interference between 650 to 900 MHz. Overall the South Africa site shows more variation when looking in different directions compared to the Australia site. These observations will be used as a point of comparison with the readings taken in the survey, especially the wide band readings, as due to the remote nature of both the Australia and South Africa sites these are expected to be far better than the results taken in the survey at Alston, specifically with the noise floor and signals at and around 1420 MHz.

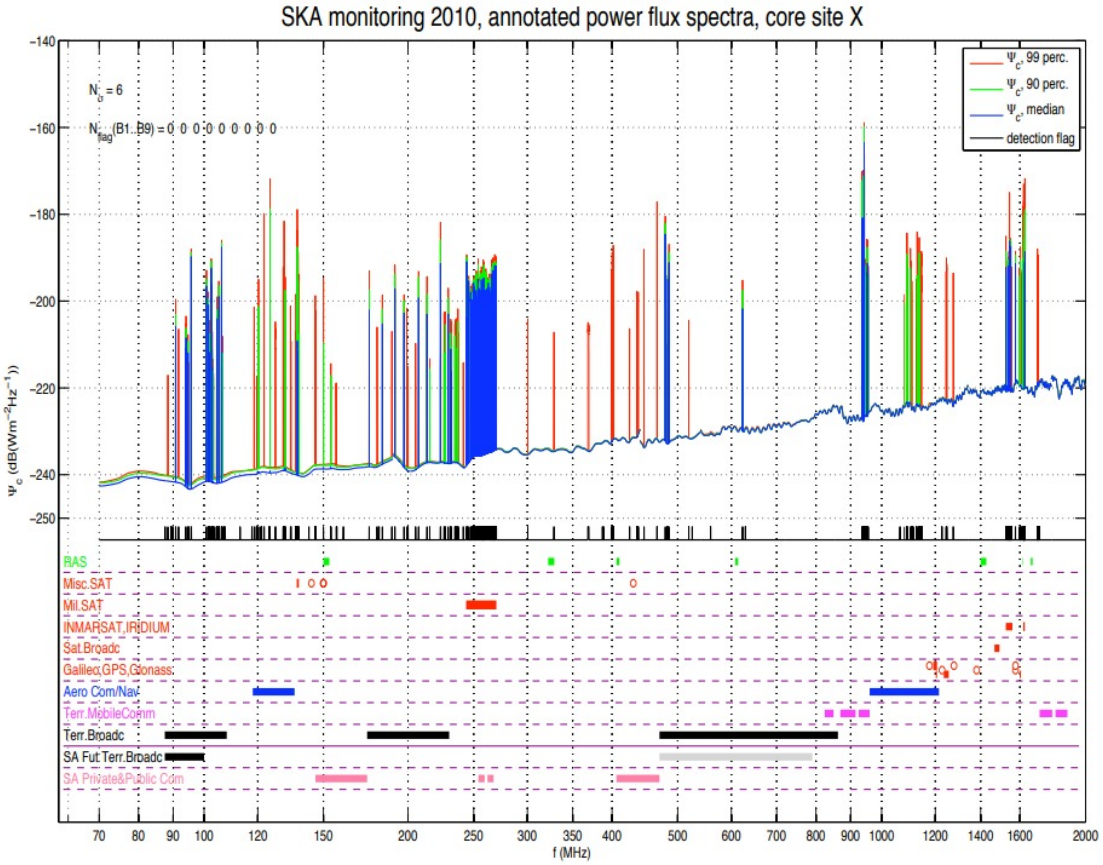

Figure 30: Spectra of site X in South Africa from the SKA RFI Survey, using the High Sensitivity Mode, looking west [Millenaar, 2011]

5 Survey System

The potential 24/7 survey system used will use three separate components, a Software Defined Radio (SDR) receiver, a SDRPlay RSPdx[16], an antenna, an OmniLOG 90200[17], and a Raspberry Pi 4, with the PiSDR image installed onto the SD Card.

The system will run using a raspberry Pi 4, which was chosen as it provides a compact way to interface with the SDR, can run a variety of software, and can run 24/7 if needed. Remote access can also be set up via an ssh, or VnC Viewer, allowing any surveys to be done remotely. A specific image was used instead of the base Raspbian OS, called PiSDR. This was chosen, due to it already having a lot of SDR software pre-installed, including the programs that will be used for the RFI station, however, its wide variety of software would allow the system to accommodate other pieces of hardware, if needed.

The program that will be used to take the RFI surveys is called VIRGO [Spanakis-Misirlis et al., 2021]. VIRGO is a piece of software that has multiple different functions useful for this project. Firstly, it has a RFI plot and RFI monitor function. This allows it to take a snapshot of the current RFI, or monitor it over a period, this would, if the teaching telescope is built, allow the station to monitor over the period of observation, so any anomalies can easily be identified as either an actual signal from space, or interference from nearby.

Its other functions however allow it to also take radio observations and plot them, meaning the same piece of software can be used to monitor RFI and take observations, simultaneously. The SDR being used also facilitates this.

The RSPdx covers the spectrum from 1kHz to 2GHz, which is a wide enough band for any observations being made via a telescope or RFI survey. It also has two separate antenna ports, meaning that both an RFI Survey antenna and cable to a telescope receiver can be connected, or if a wider coverage for the RFI survey is needed, another antenna. This means the system can be initially used to take RFI surveys, but if the site is suitable, then be modified to also run the radio telescope, both at the 1420 MHz band, but also at wider bandwidths if the telescope antenna is improved to be able to take continuous spectra, such as those mentioned in Section 2.4, as the SDR will be able to process the data.

The antenna being used is an Omnilog 90200, as shown in Figure 31. This was chosen primarily due to its uniform receiving pattern, as shown in Figure 32. This means it will be able to pick up signals equally from all directions, meaning that potentially weak signals will not be lost if the antenna is placed facing the wrong direction. It's frequency range is 700MHz-2.5GHz, which covers the 1420 MHz area needed, but can also be used for wider band surveys as well, which will be able to spot any broad-band interference. Due to its size, it also does not need to be mounted to any other surface or bracket. There is a small downside to this antenna however, which is its gain at 1420MHz and around it, which is -14.57dBi, as seen in Figure 33.

[16]https://www.sdrplay.com/rspdx/

[17]https://aaronia.com/antennas/omnilog-series-omnidirectional

Figure 31: A picture of the OMNILog 90200 Antenna[10]

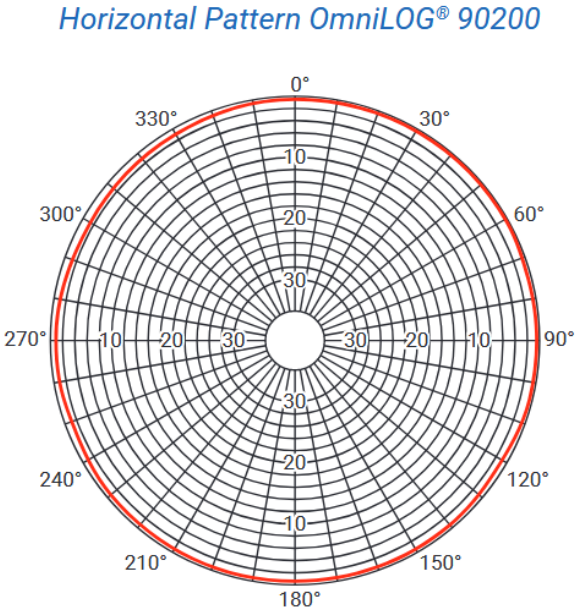

Figure 32: The 360 degree gain profile of the OMNILog 90200 Antenna horizontally[10]

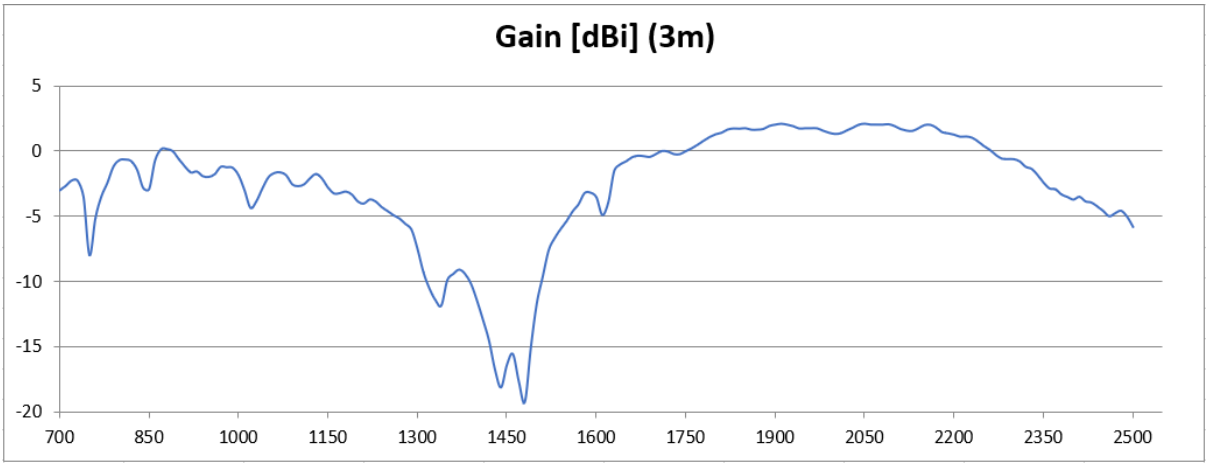

Figure 33: The gain profile of the OMNILog 90200 Antenna[18]

This low gain at 1420 MHz may be an issue, but as any sources that could cause interference would be relatively strong, as stated in Section 2.5.1 , and the RFI survey will be done with a long integration time, so this issue should not cause any problems with the identification of RFI Sources.

For the initial survey of the site itself, a more portable version of the system is needed. Therefore, the SDR receiver and antenna was attached to a laptop and used the spectrum analysis software RSP Spectrum Analyser software[19], to measure the radio environment at different points.

[18]https://aaronia.com/Datasheets/Antennas/Aaronia_Broadband_Antenna OmniLOG_90200_datasheet.pdf

[19]https://www.sdrplay.com/spectrum-analyser/

6 Survey Plan

A drone shot of the site, along with a map of the buildings on the site is show in Figure 34 and Figure 35 respectively.

Figure 34: A drone shot of the site[20]

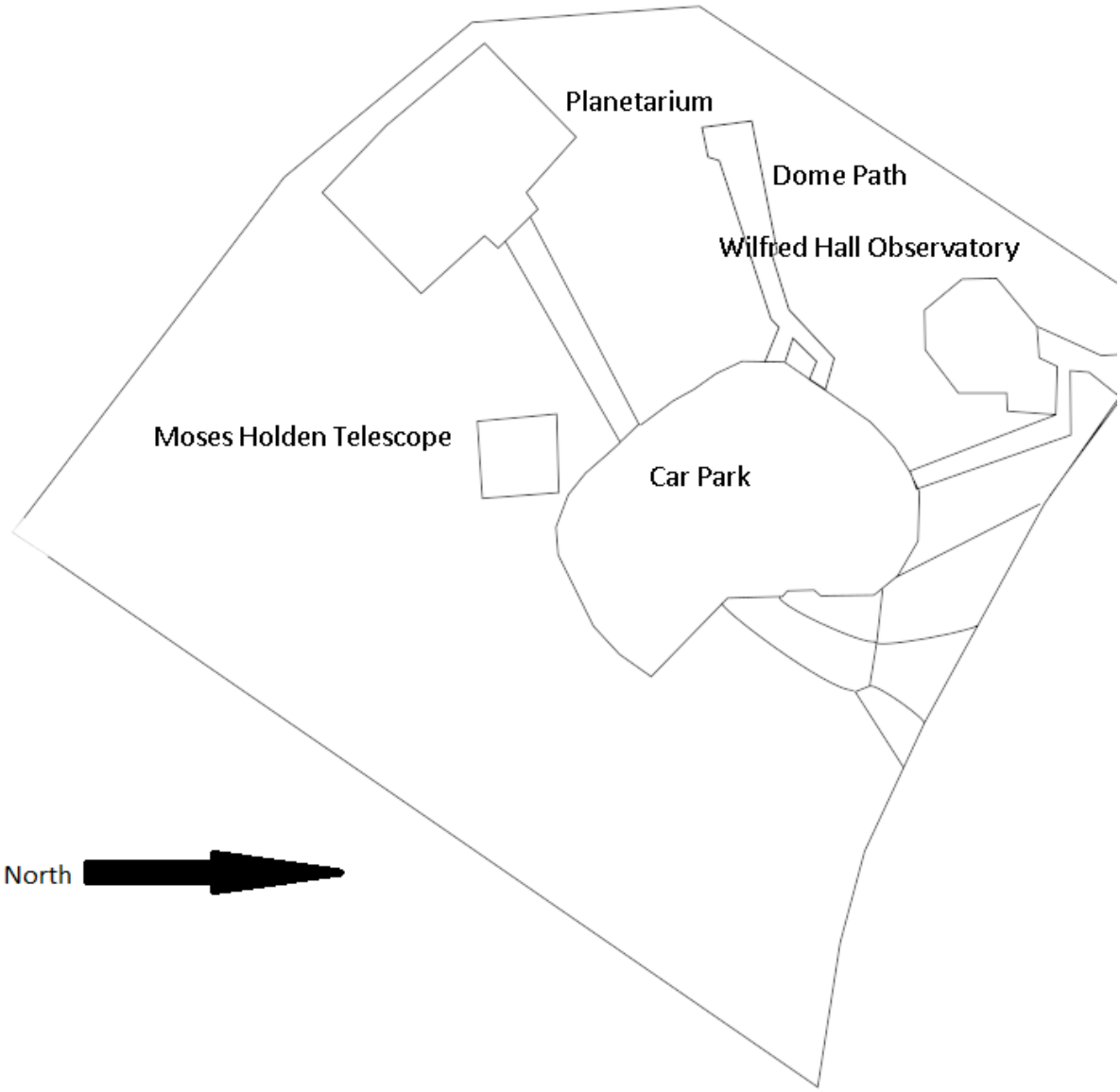

Figure 35: A Map of the Alston Site with points of interest noted

[20]http://www.star.uclan.ac.uk/observatories/alston-observatory/

To do the survey of the site, data was collected at points across the site in a grid format, using the sides of the Moses Holden Telescope as a reference length to the nearest meter, which came out to a grid with a spacing of 6.5m, as shown below in Figure 36

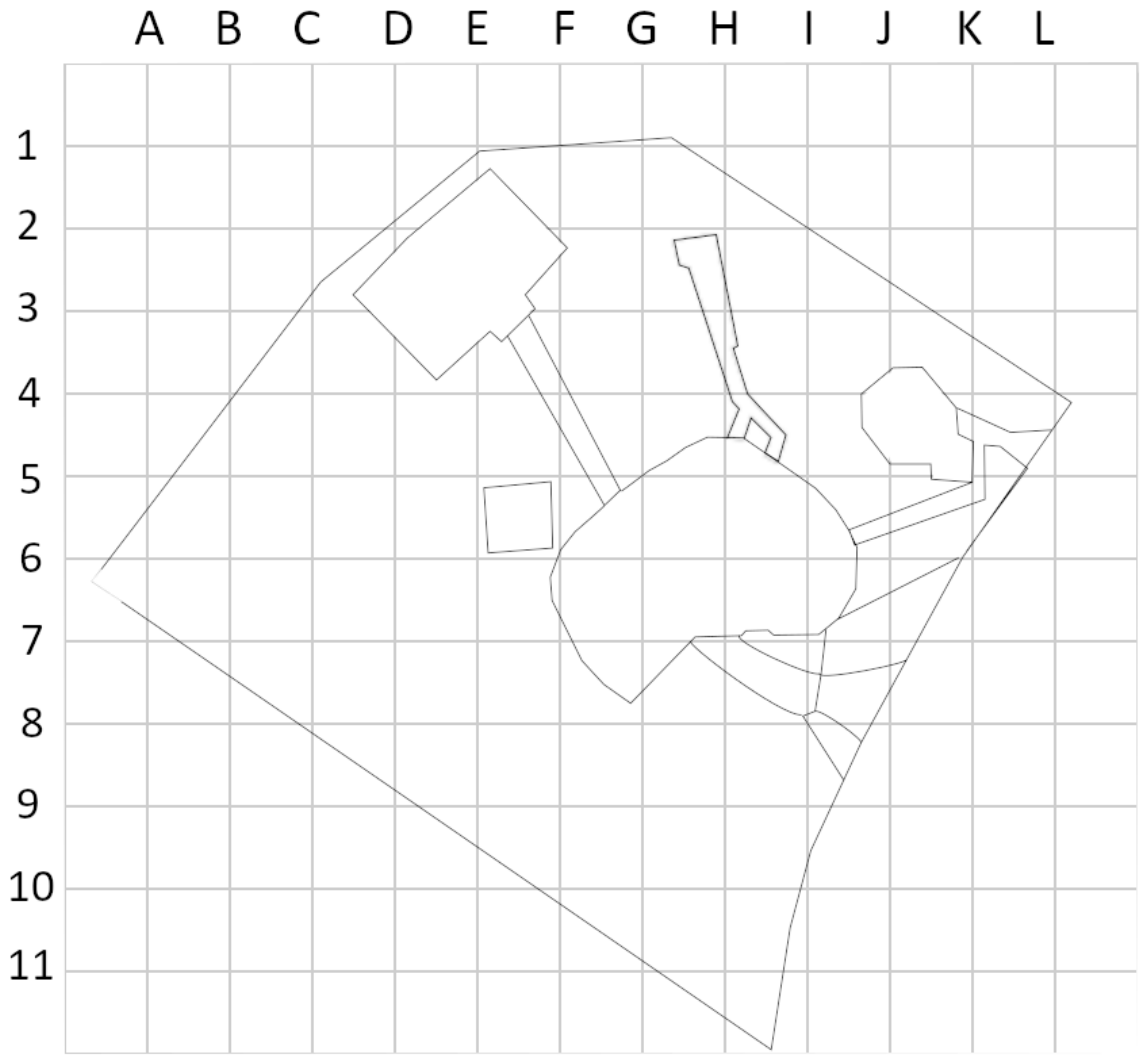

Figure 36: A Map of the Alston Site with a grid overlaid, each point is 6.5m apart from each other

The points are labelled to allow for the data recorded to be easily matched to a site, the buildings are omitted as taking readings there would not be useful for the project, as a potential RFI monitoring station or telescope would not be in the building, and only RFI leaking out of the building is a potential issue. Recordings across the car park were also done even though it is not a suitable place for any installations, as it takes up a large amount of the property and allows the identification of any site wide trends in RFI to be spotted more easily.

After getting to the site, the first task was to see which of the points outlined on the grid were able to be surveyed, as the site has foliage that would make a survey impossible to do, shown in Figure 37

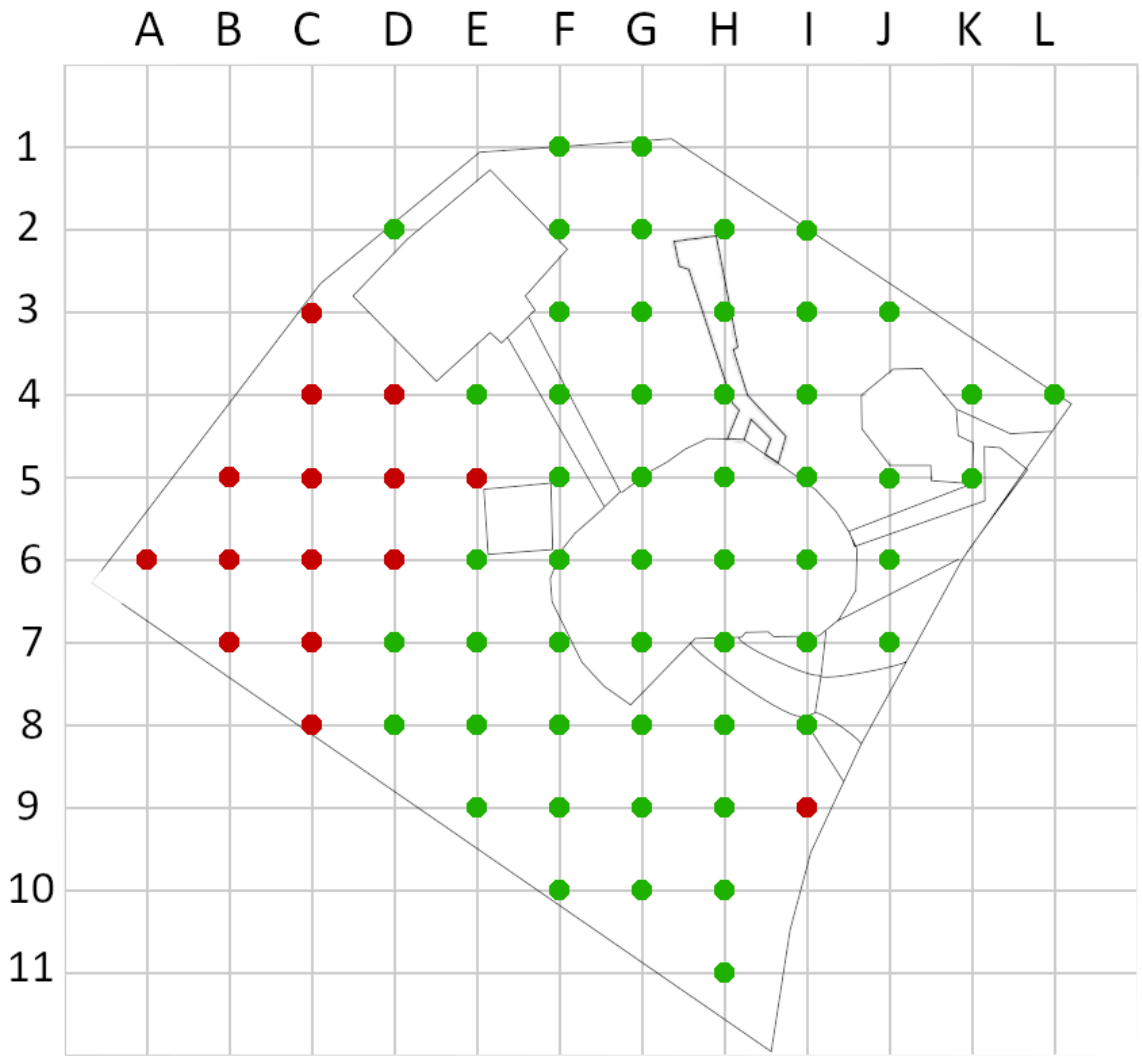

Figure 37: A Map of the Alston Site with the grid overlaid, and each point either green or red, to show which points can be surveyed (green) or are inaccessible (red)

Along with the accessible points, the availability of power was also looked into, and two points, around G2 and F9, both have easy access to power, making them suitable

for the telescope, however to make sure there is not a point on the site that may have significantly lower RFI (and therefore justify potentially burying cables) the entire accessible site was surveyed, with two observations taken at each point: an averaged spectrum and a peak spectrum, as discussed in Section 4, to look at both persistent signals, and more intermittent signals that may be lost in an averaged spectrum. The averaged spectrum was left until the waveform had settled, and then recorded, to make sure the average was taken. For the peak reading, the observation was left for one minute at each point. These grid readings were taken over a 5 MHz bandwidth, starting at 1417.5 MHz and ending at 1422.5 MHz. This narrow band was done to look for any signals that may interfere in the immediate frequency range around 1420 MHz, that could cause issues for the telescope.

Alongside the grid readings at the Alston Observatory, further comparison measurements were taken. Firstly, a comparison measurement in Preston at a house was taken, both in a narrow 5 MHz band and a wider 500 MHz span, these took longer, due to the longer time the software will take to scan and measure the spectrum, so the average and peak measurements were each taken over 5 minutes each to allow the spectrum to settle. These readings will act as comparison points to help determine if any sources may be site specific, or potentially due to the system setup. Secondly, there were measurements taken to take into account various potential sources of interference from the site, such as the MHT or planetarium. These comparison measurements were taken inside the planetarium, to measure any RFI from the building and potentially match it to any RFI found on the site. Measurements in peak mode were also taken while the Moses Holden Telescope was in use, to determine if there is any potential RFI from its use in the 1420 MHz band. Thirdly, to determine any potential interference from the laptop, the receiver was placed on top of the laptop, as shown in Figure 38. This will further help determine if any signals present are from the site or the setup used. To minimise interference from the laptop, the receiver will be placed away from the laptop when recording, as shown in Figure 39.

Figure 38: How the RFI of the laptop will be measured as a comparison

Figure 39: The setup for the recordings done for the grid observations

Furthermore, wider band surveys were also taken at points G2 and F9, the points that have access to power, over a frequency range of 1170 to 1670, a 500 MHz span. This was done to spot any broad or narrow band signals around the 1420 MHz that may be raising the noise floor or otherwise interfering with the range needed for the telescope to operate, as discussed in Section 2.5.1. Wide band readings were also taken in Preston as well, to allow for comparison between the two wide band readings.

7 Results and Analysis

An initial test setup was done on the 22/06/2021, where the system was troubleshooted, and a few initial test spectra were obtained, but were not useful for analysis due to some calibration issues and inconsistencies with how the data was recorded. A second set of data was taken on the 29/07/2021, which included the grid results as well as measurements taken inside the planetarium, the readings with the MHT put through its full range of motion, and the readings with the receiver placed on top of the laptop. Comparison measurements were also taken on this day in Preston, at a typical house in the city, located in the PR1 postcode, one street away from the high street on one side, with the Avenham park on the other side. The room the measurements were taken in had a computer running in the background, with no obstruction between them. There were also other occupants in the house with their own computers and devices running. A second set of readings on the site was also taken in the wide band mode on 06/05/2022, which included the wide band reading at the points G2, F9 and the house in Preston.

Unfortunately, the full planned grid of recordings was not able to be recorded, so every other point on the site was recorded, as shown in Figure 40

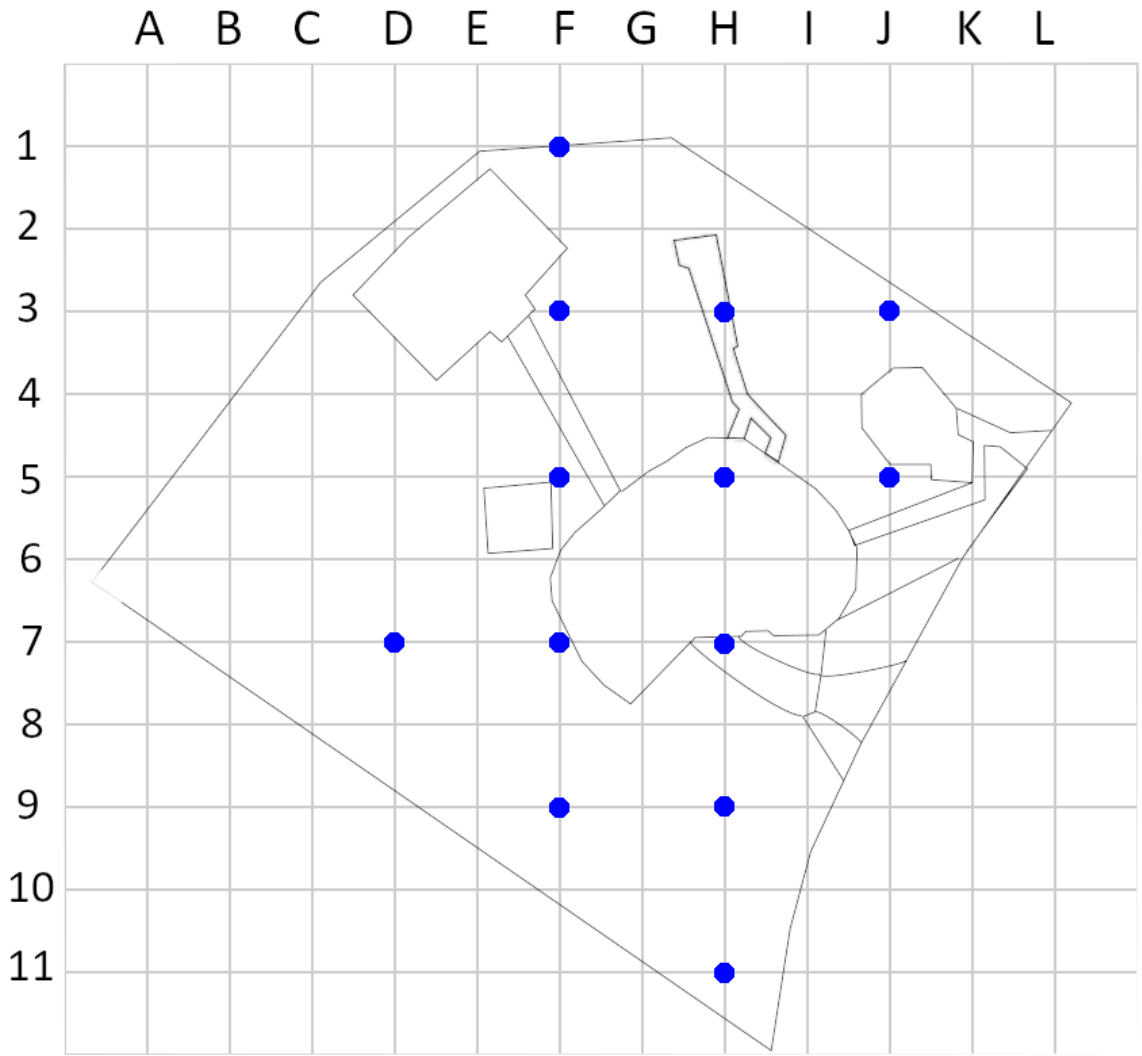

Figure 40: A map of the site with the grid overlaid, with the points surveyed in blue

To help identify what may be noise, and what may be a legitimate signal, an error was calculated for each spectrum. This was done by taking the noise floor (by removing any distinct peaks from the data), and finding the standard deviation of the data. For each spectrum, the value of the noise floor was also found by finding the median of the data set (the same data set that the error was calculated from). These are shown in Table 1, alongside the values for the tallest peak found in each spectrum (which was always at 1420.6 MHz across the site), to see if there was any trend in the peak over the site.

Position	Tallest Peak Value (Average)	Noise Floor (Average)	Tallest Peak Value (Peak)	Noise Floor (Peak)
Preston	-131.0±0.7	-149.0±0.7	-129.4±0.7	-139.1±0.7
F1	-131.3±0.5	-149.9±0.5	-129.0±0.8	-139.6±0.8
F3	-131.6±0.5	-149.6±0.5	-128.7±0.6	-139.4±0.6
F5	-130.9±0.5	-149.4±0.5	-129.6±0.9	-139.8±0.9
F7	-131.3±0.4	-150.0±0.4	-129.4±0.7	-139.5±0.7
F9	-131.4±0.4	-150.1±0.4	-129.4±0.7	-139.9±0.7
D7	-131.3±0.5	-150.14±0.5	-129.4±0.7	-139.8±0.7
H3	-131.17±0.4	-150.3±0.4	-129.6±0.8	-140.3±0.8
H5	-131.4±0.4	-150.2±0.4	-129.7±0.7	-139.8±0.7
H7	-131.4±0.4	-150.0±0.4	-129.1±0.7	-139.5±0.7
H9	-130.9±0.4	-149.9±0.4	-129.2±0.6	-139.5±0.6
H11	-131.13±0.4	-150.1±0.4	-128.5±0.6	-139.8±0.6
J3	-131.17±0.4	-149.8±0.4	-129.2±0.7	-139.6±0.7
J5	-131.3±0.5	-149.7±0.5	-129.5±0.7	-139.5±0.7

Table 1: Table of the results taken from the site, including the value of the tallest peak and noise floor for both the average and peak mode narrow band readings.

For the measurements of both the comparison and grid readings the reference level in the spectrum analyser software was set to be -80 dBm, as recommended in the manual of the RSP Spectrum Analyser Software [21].

7.1 Comparison Measurements

7.1.1 Preston

First, the comparison points taken in Preston included both a peak and average reading, as stated in Section 4, with both a narrow band of 5 MHz and wide band of 500 MHz:

[21] https://www.sdrplay.com/docs/RSP-SpectrumAnalyser-V1.1.pdf

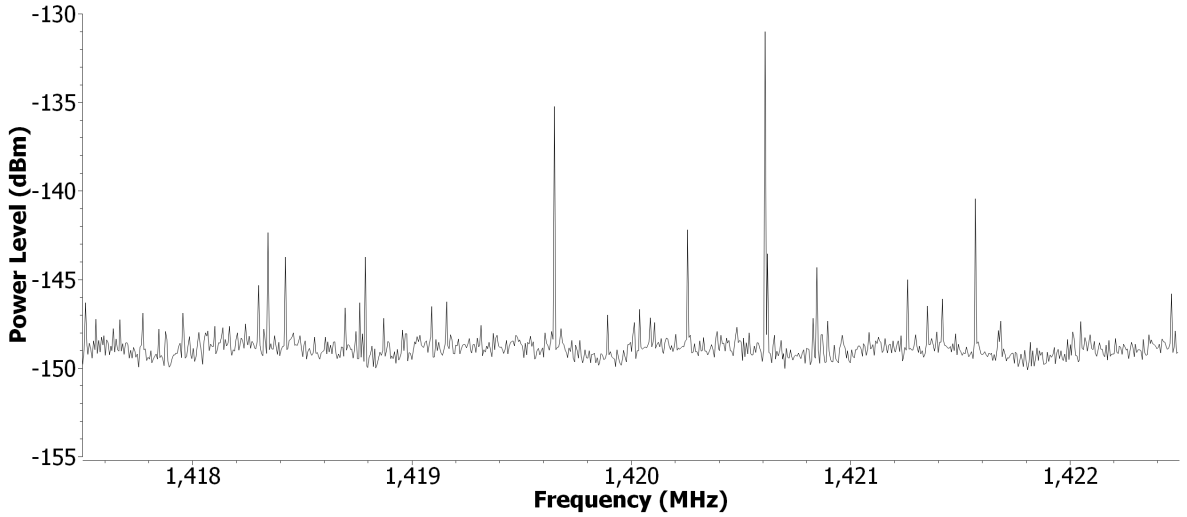

Figure 41: The average mode narrow band comparison reading

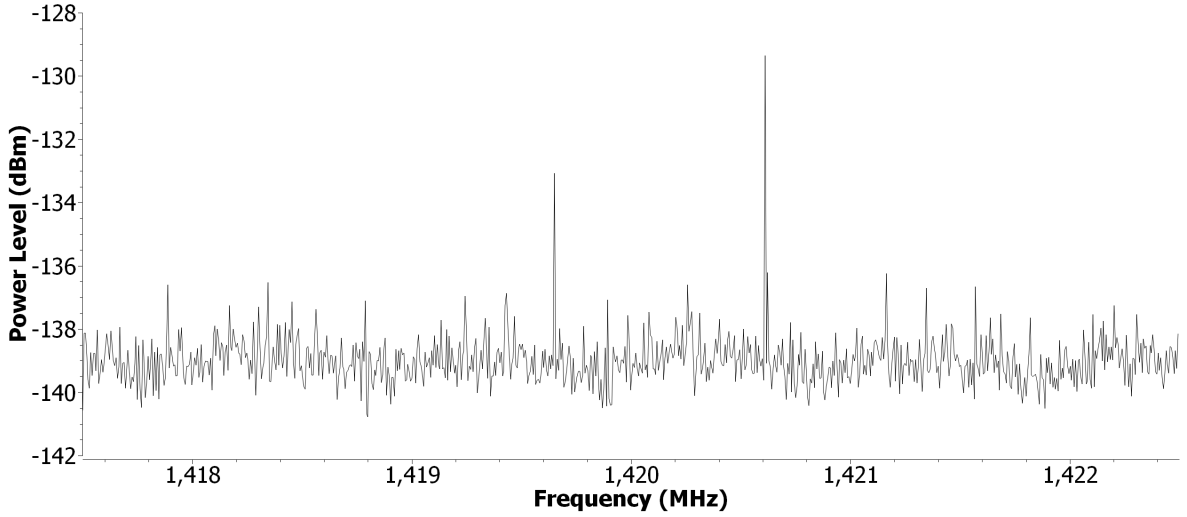

Figure 42: The peak mode narrow band comparison reading

With these narrow readings, we can see a noise floor above -148 dBm, with a multitude of peaks being above the three σ values (or three times the standard deviation, which for this spectrum is 2.1 dBm), indicating that they are actual signals. Most notably however, there are two large peaks at 1419.7 MHz and 1420.6, with dBm values of -135.2 and -131.0 dBm respectively. These are also the only two peaks that rise above the noise floor for the peak readings. With the peak readings, the left peak has a dBm value of -133.1 dBm, while the right peak has a value of -129.4 dBm, which is higher, as we would expect with a peak reading, and gives a baseline for if these peaks come up in readings on the site.

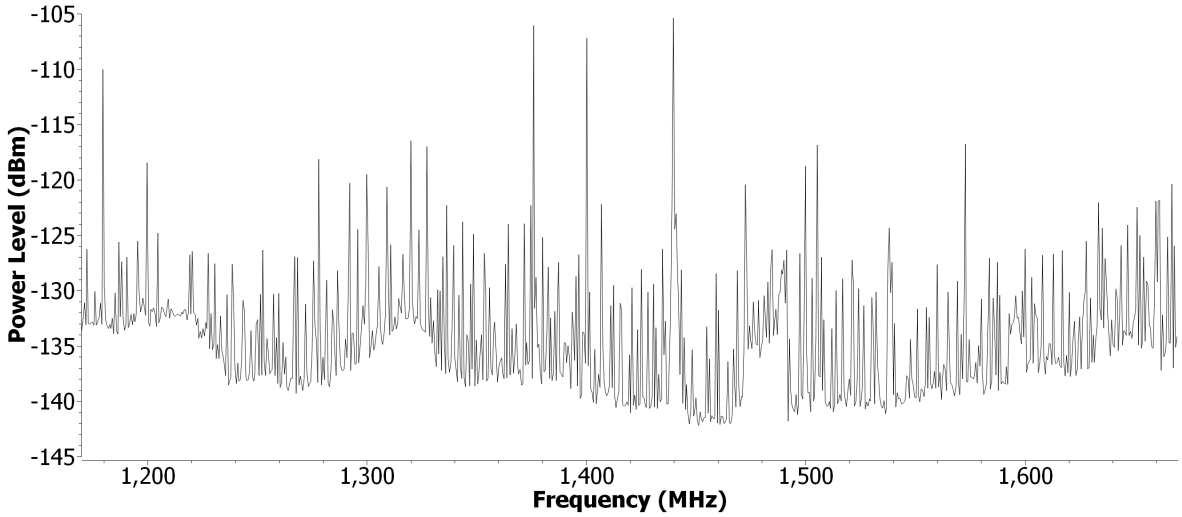

Figure 43: The average mode wide band comparison reading

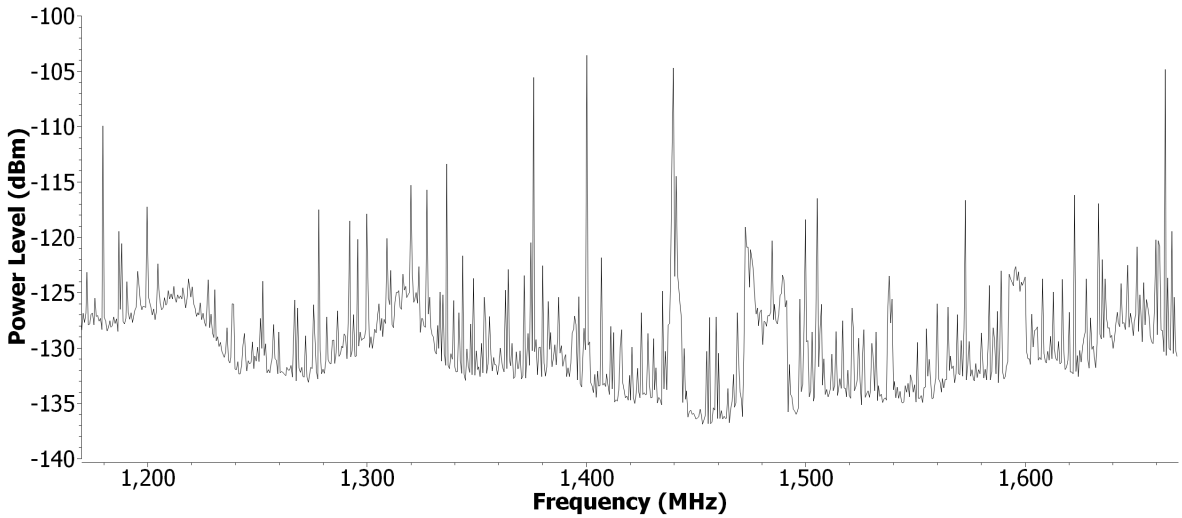

Figure 44: The peak mode wide band comparison reading

The Wide band readings shows a large amount of noise across the entire band width, but also shows distinct patterns in the underlying noise floor, such as the bumps at 1200 MHz and 1320 MHz. There is also a distinct raise in the noise floor between 1460-1500 MHz, where there is a sharp increase then decrease at the start and end of the range. These two spectrum will be overlaid onto the wide band spectrum taken, to allow for easier comparison, and help determine whether the features found in the comparison spectra are potential long range sources, such as those mentioned in Section 1, such as satellite down links, AM/FM broadcasts, etc. The Ofcom frequency table [22] was cross referenced with the wide average result, to see if any features could be identified, and Figure 45 shows an attempt to identify some features.

[22]http://static.ofcom.org.uk/static/spectrum/fat.html

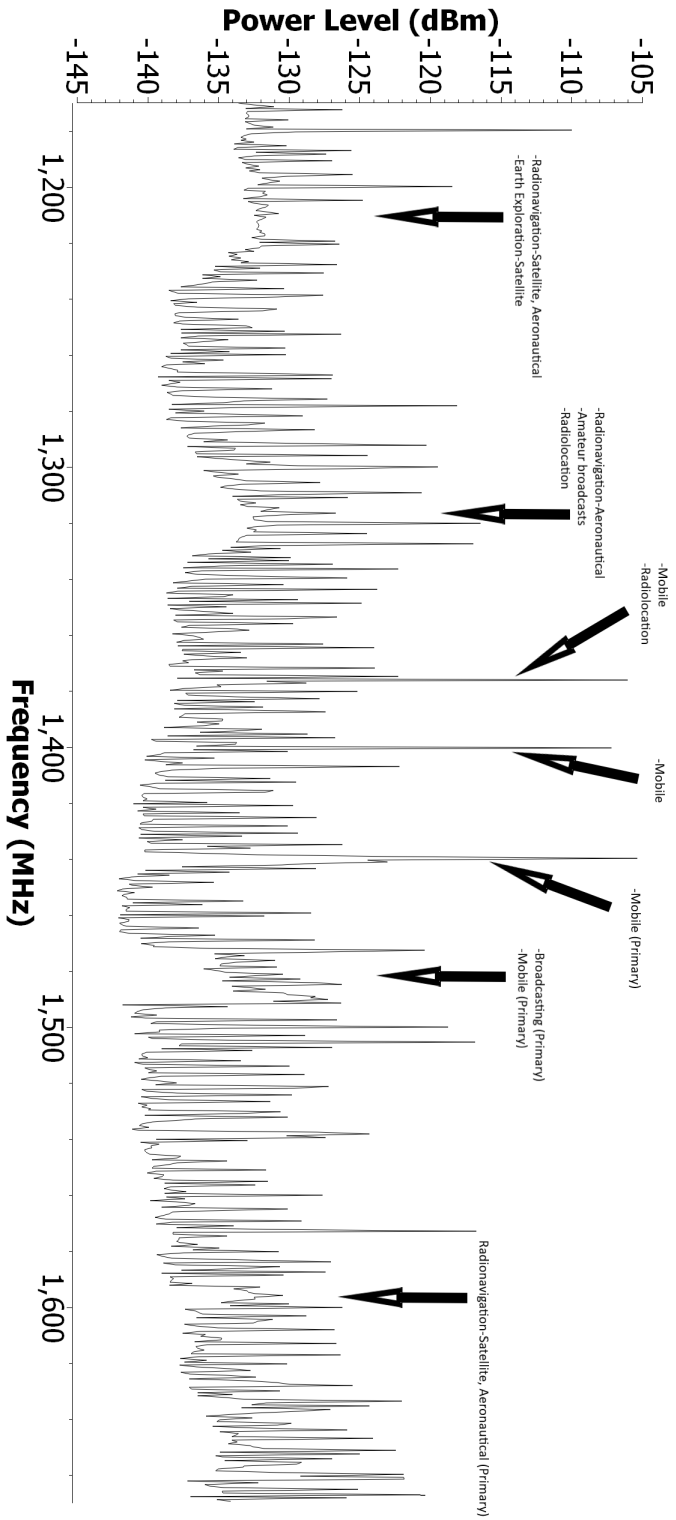

Figure 45: The average mode wide band comparison reading with potential sources of features listed

7.1.2 Laptop

The first comparison measurement taken on the site was with the receiver being placed on top of the laptop, as shown in Section 6, in the Peak mode. Figure 46 shows the spectrum by by itself, and Figure 47 shows the comparison measurement overlaid on top of the laptop measurement.

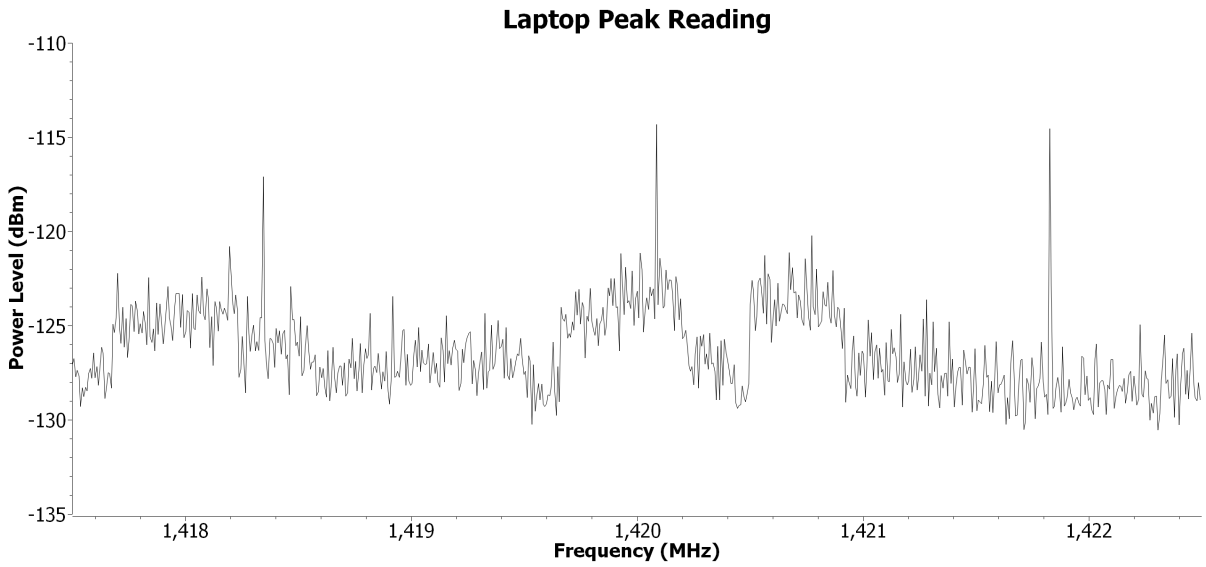

Figure 46: Spectrum with the receiver placed on top of the Laptop, as shown in Figure 38

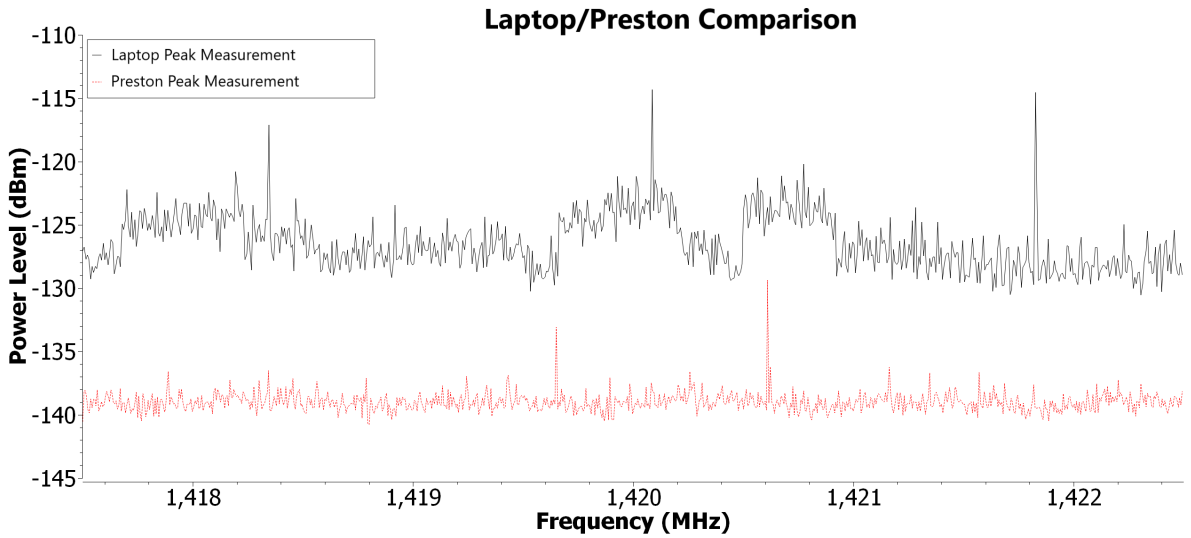

Figure 47: Comparison Peak measurement from Preston overlaid on top of the Laptop Peak measurement

With this comparison, we can see that the laptop is giving off a lot of RFI, which is raising the noise floor, this indicates that laptop has a lot of wide band RFI coming from it, as we would expect, especially at this distance away from the laptop. We can tell however that the peaks that are present in the comparison measurement do not appear to be from the laptop, as if they were from the laptop, we would expect them to get

stronger closer to the laptop due to the inverse square law, suggesting that if the source of these peaks are from the setup, they are from the SDR or other part of the setup.

7.1.3 Inside Planetarium

The second comparison measurement was taken inside the planetarium, with both an average (Figure 48) and peak (Figure 49) reading. With the average reading, we can see the same peaks as shown with the comparison readings, which raises the potential concern that these peaks are from part of the setup other than the laptop, such as the cabling or issue with the SDR itself. There is also the possibility it is a source that would be present in both the centre of Preston and Alston, such as a AM or FM broadcast, or satellite down link, which would be present over a wide area.

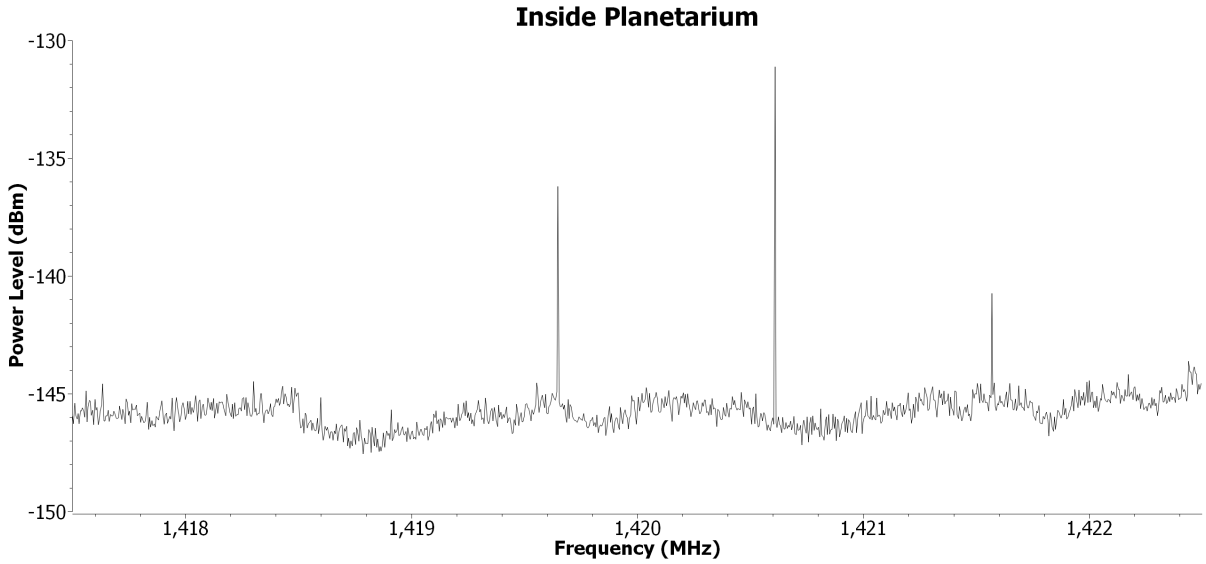

Figure 48: Averaged Spectrum inside Planetarium

With Figure 49, we can clearly see the interference generated by the devices inside the planetarium, as expected. This does also show the potential of the building in causing interference across the site, which will be looked for in the grid readings. This large difference in the peak measurement compared to the average measurement is most likely due to the devices inside the building emitting a lot of short term, strong signals, that would raise the peak spectrum, but be short enough that they would be averaged out over the time the average reading was taken.

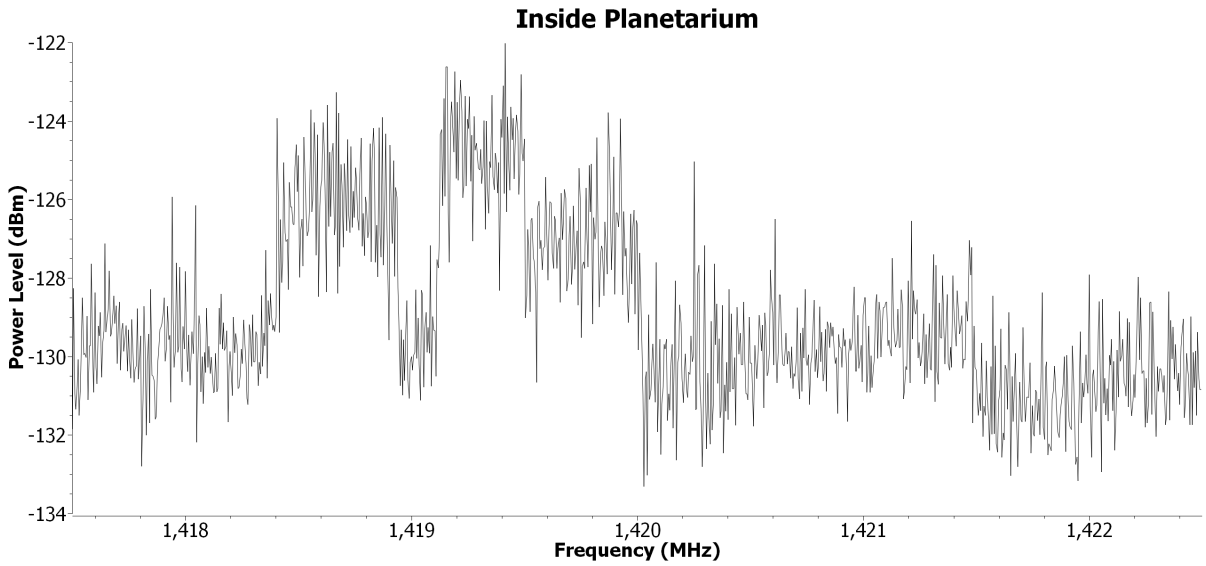

Figure 49: Peak Spectrum inside Planetarium

7.1.4 MHT In Use

To see if the MHT could cause issues if turned on when observations with a radio telescope are being taken, a peak reading was taken while the telescope and dome were taken through a full range of movement, as shown in Figure 50.

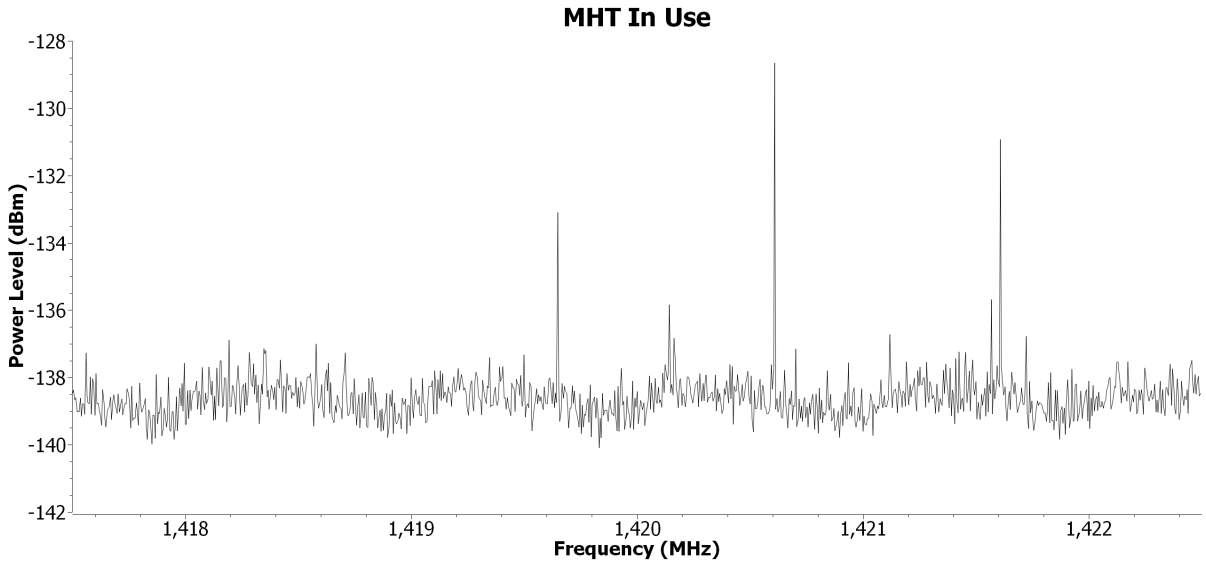

Figure 50: Peak Spectrum taken while the MHT was put through the full range of motion

The spectrum shows a similar reading to the comparison readings, with a few differences. First is an underlying repeating pattern in the noise floor, causing slight 1 MHz wide bumps which is present in the comparison spectrum taken in Preston. This could be potential interference from power cables, however its appearance should not cause any interference with any telescope, so it is not of major concern. Furthermore, overlaying the comparison peak reading, as shown in Figure 51 also shows the appearance of another peak at 1421.61 MHz, which does not appear in any other readings taken, meaning it is most likely from the MHT. Apart from this peak however, the spectrum does not appear to show any particular new features that could cause interference, meaning both telescopes could potentially be operated at the same time.

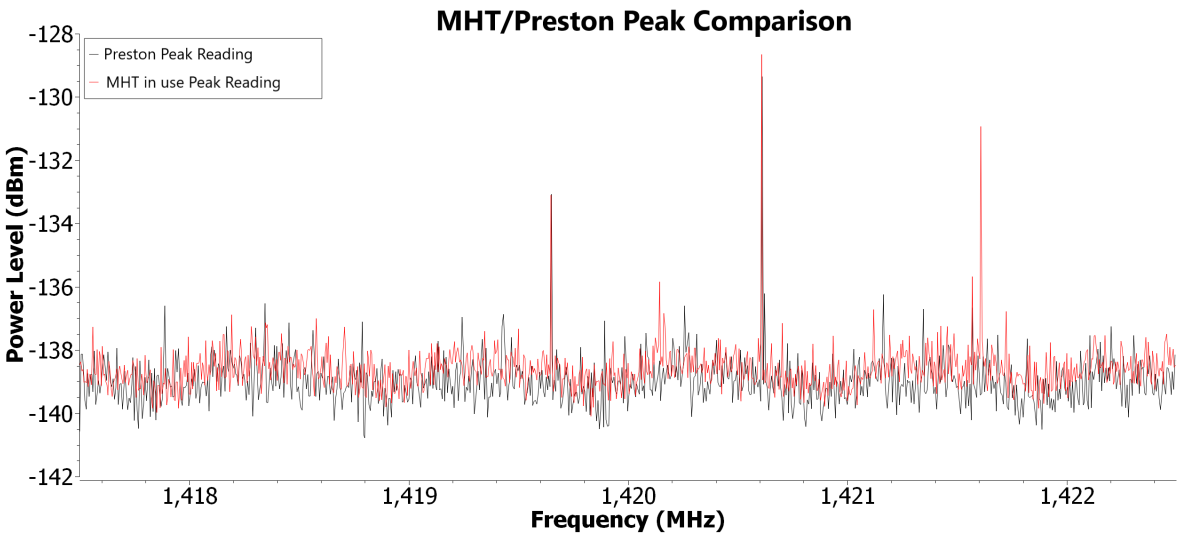

Figure 51: Peak Spectrum from the MHT overlaid onto the comparison reading

7.2 Grid Readings

7.2.1 Furthest Point (H11)

Starting with the lowest point on the map, furthest away from any buildings, H11 has the spectra shown below in Figure 52 and 53.

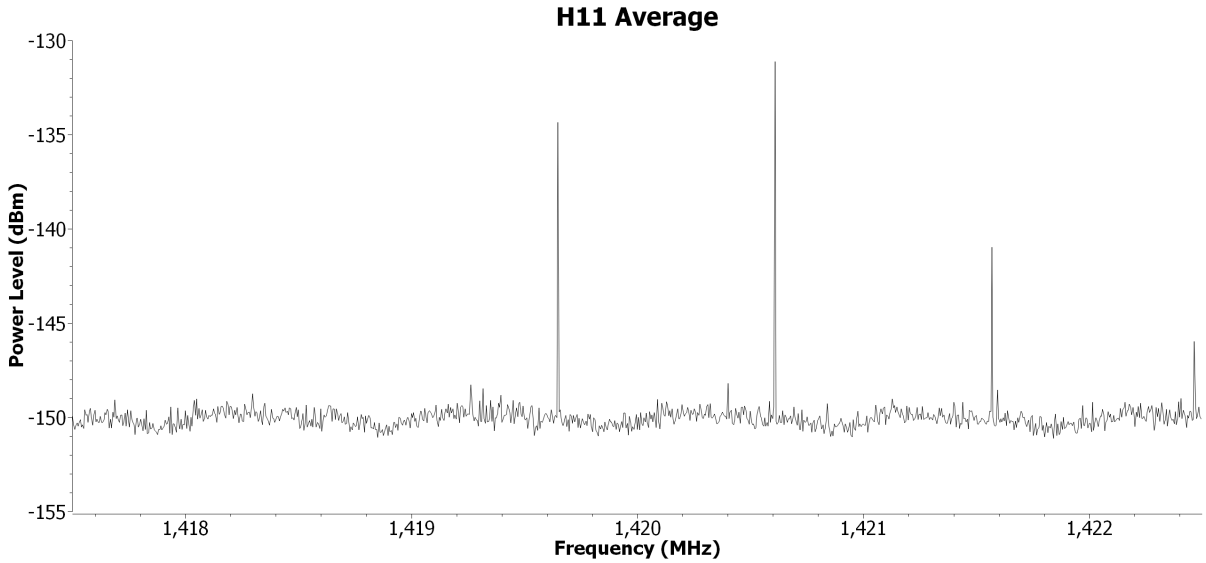

Figure 52: Averaged Spectra of H11

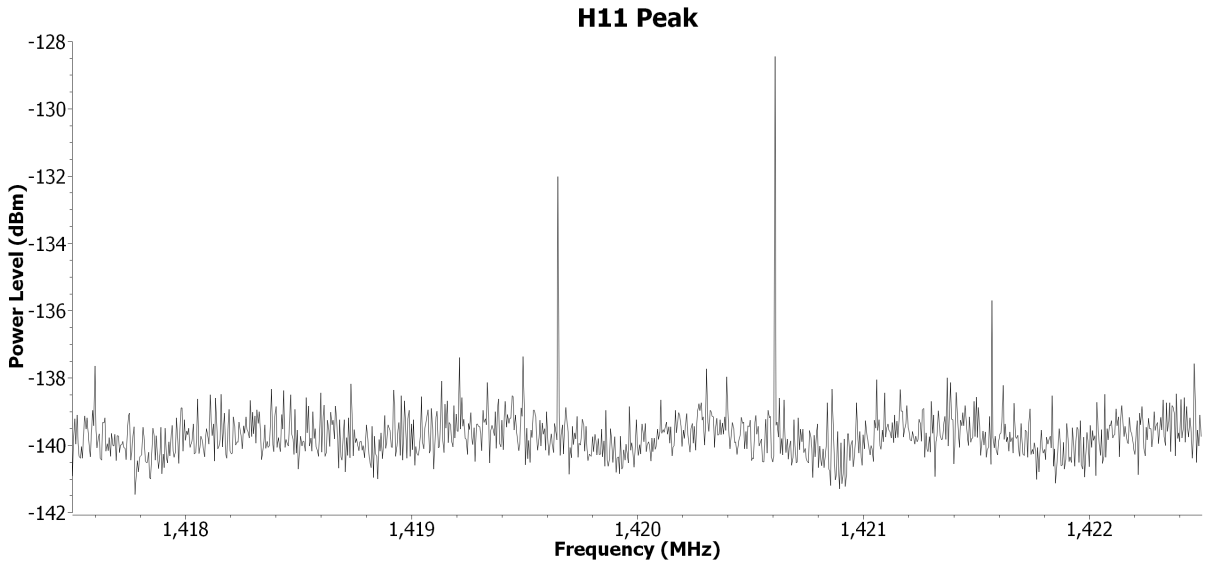

Figure 53: Peak Spectra of H11

In both, the two peaks shown in the comparison are shown, although with a much lower spread in the noise floor. The noise floor is also lower than the comparison, being around -140 dBm, as shown in Figure 54, which would be expected as the Alston site is outside the city, and so further away from any sources of interference that may cause the noise floor to raise. However, the two peaks that were shown in the comparison spectra, one at 1419.7 MHz, and the other at 1420.61 MHz also appear again, even when the furthest away from any buildings or devices on the site. This supports the theory

that either the interference is coming a part of the setup other than the laptop, such as the SDR itself, or a broadcast from a far away source, such as a satellite down link or AM/FM radio station.

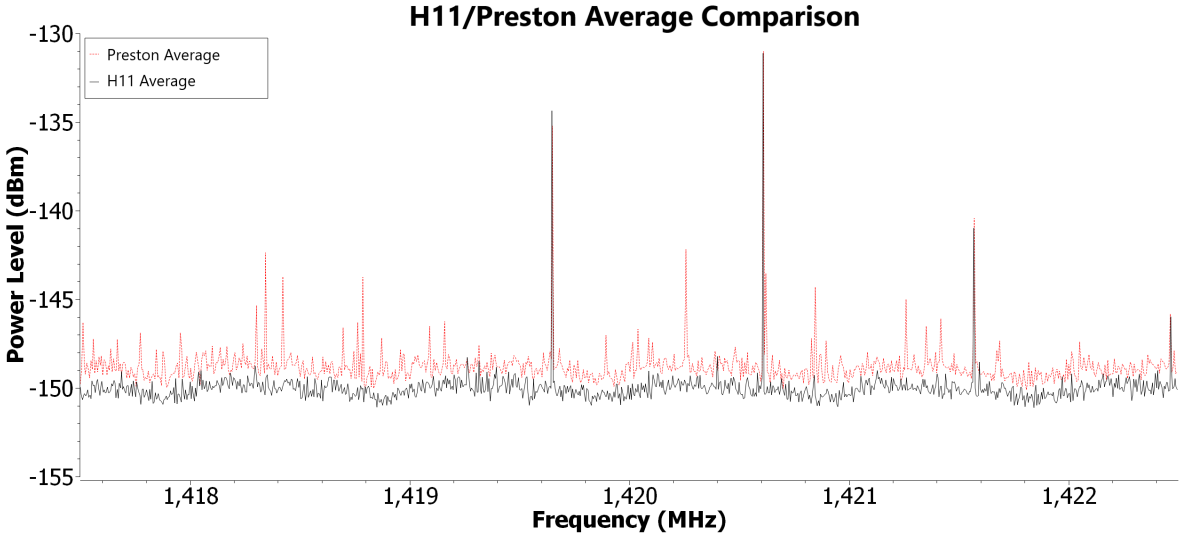

Figure 54: The H11 spectrum overlaid with the average comparison spectrum

7.2.2 Moses Holden Telescope (F5)

Moving to the point nearest to the MHT, F5, we again get the same peaks as before, as well as also a peak on the left side of the spectrum at 1418.3 MHz, only shown in the average spectrum (Figure 55. It is over the three σ value (1.5 dBm for this spectrum) above the noise floor, so it is most likely a signal and not just a noise issue from the SDR.

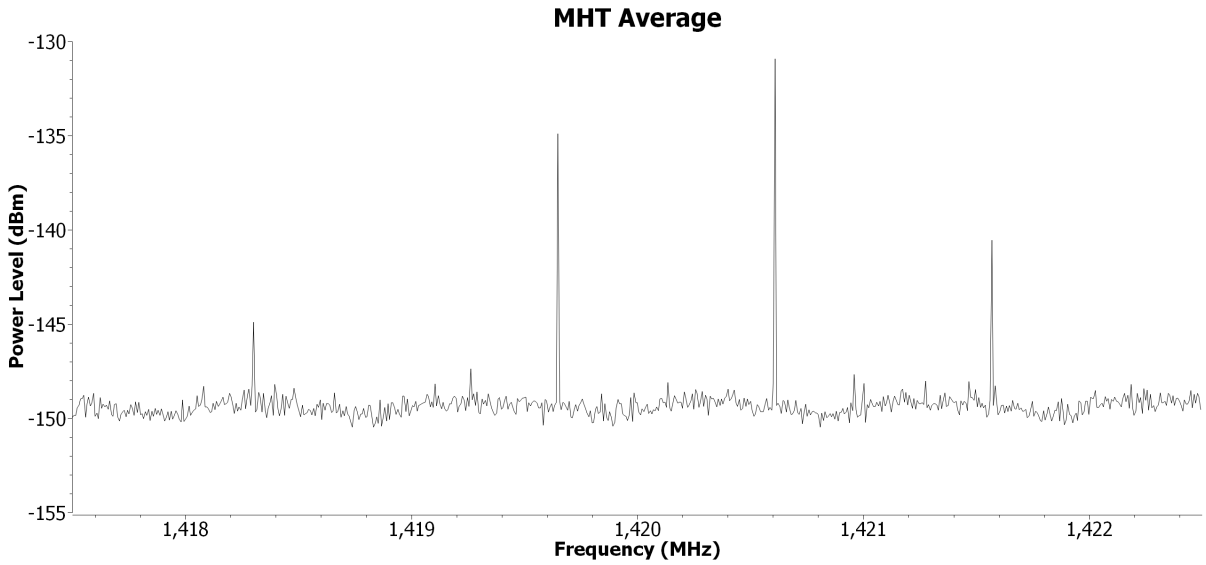

Figure 55: Averaged Spectra of F5

This is further supported by the peak spectrum in Figure 56, as the noise floor has raised enough that the peak is underneath the noise. This suggests that the signal does not fluctuate much in power, as otherwise it would raise above the noise floor and be visible in the peak spectrum.

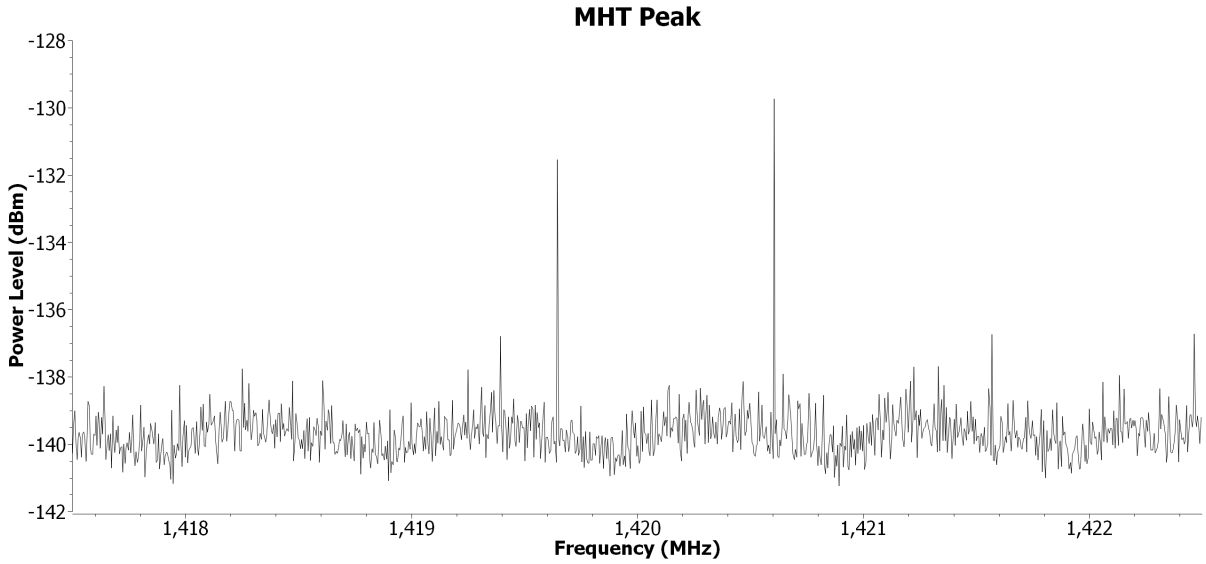

Figure 56: Peak Spectra of F5

This peak, however, does not appear in any other spectra across the site. This potentially means that it is coming from the MHT building. It is not coming from the

telescope itself, as it was turned off while the measurement was being taken. A possibility is that it could be from the power and data cables running to the building, which could also be causing the slight 1 MHz bumps across both spectra, that may be causing interference even when not in use.

7.2.3 Wilfred Hall Observatory (J5)

The average spectra shown in Figure 57 shows no new features compared to the previous spectrum, and still has the same peaks as previous spectra.

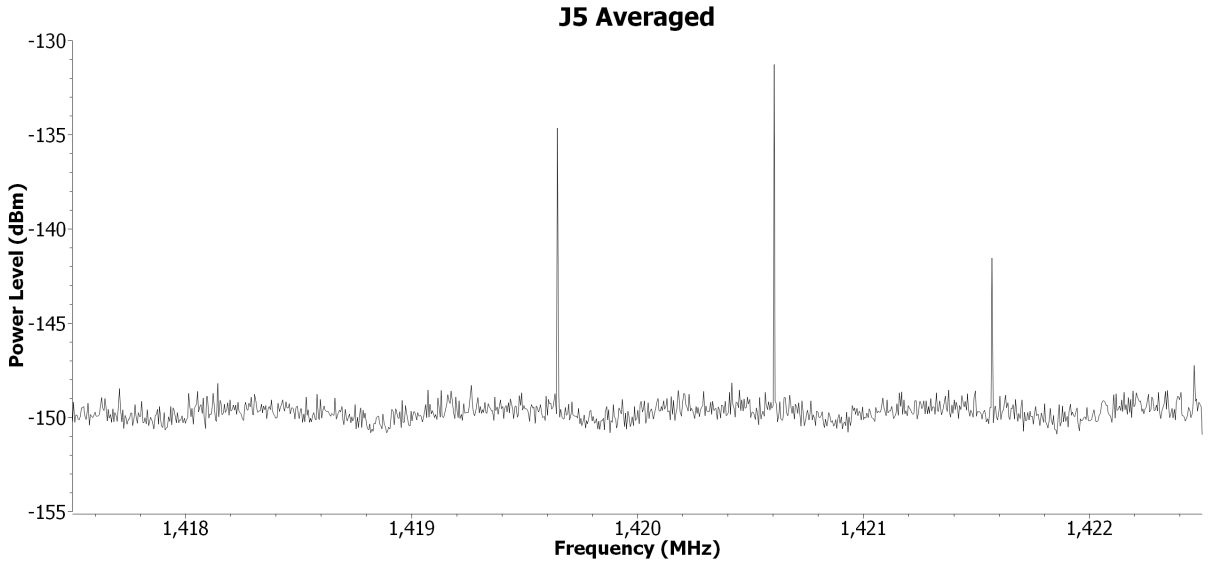

Figure 57: Averaged Spectrum of J5

However the peak spectra, Figure 58, shows a slight difference with the rightmost peak (at 1421.6 MHz) , where the peak is still showing above the noise, where it has not in other spectra. This indicates that the source of the peak potentially fluctuates, allowing the peak to rise above the noise in this particular spectra. It is also possible that the source of the peak is closer at this point.

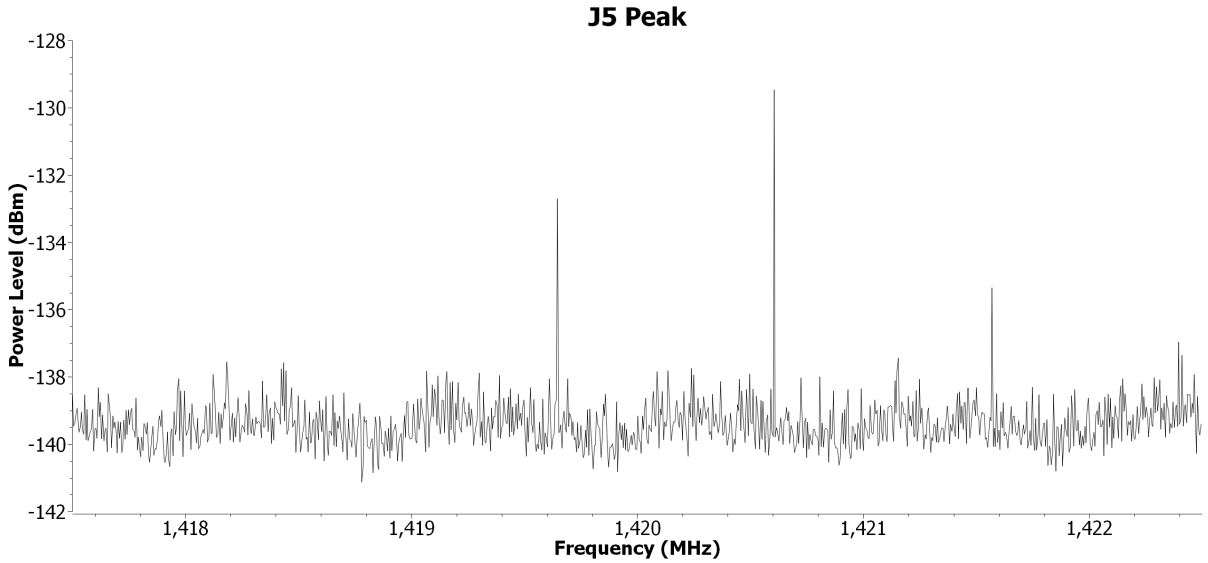

Figure 58: Peak Spectrum of J5

7.2.4 Planetarium (F1)

The point F1 shows some level of interference in both the average reading and peak reading, as shown in Figure 59 and Figure 60 respectively, as we would expect from being near the planetarium and from the comparison measurements that were taken inside the planetarium.

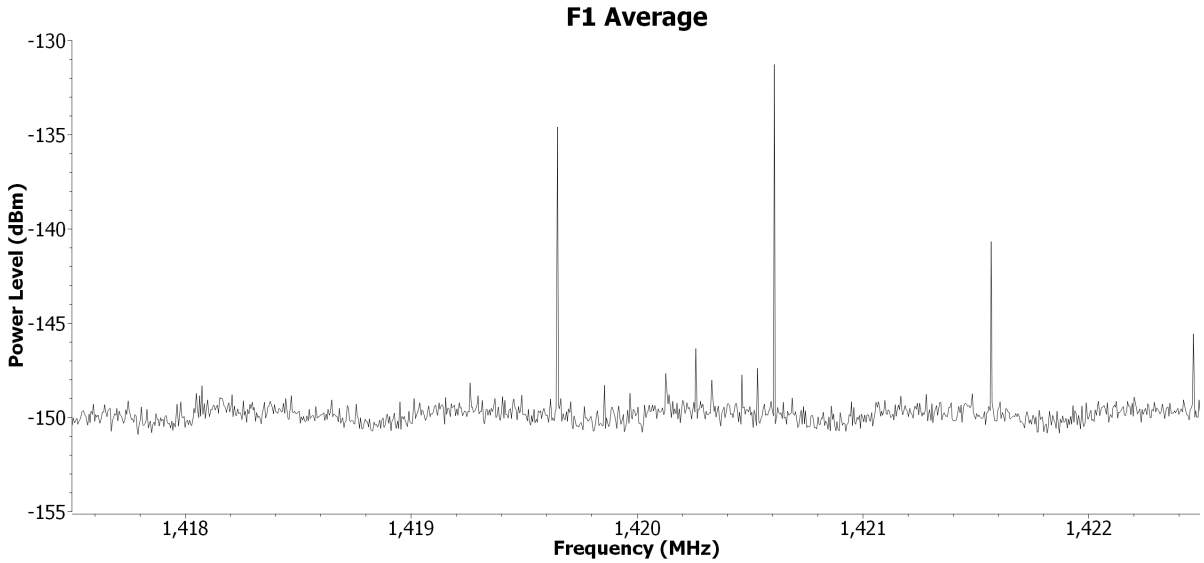

Figure 59: Averaged Spectra of F1

This effect is far more noticeable in the Peak spectrum, Figure 60, where the noise floor has more variation than most of the other peak spectra, as shown by the standard deviation being 0.8 dBm, with the only higher variation being F5 at 0.9 dBm. This shows that the signals from the server racks and other devices in the building do pass through the walls, as would be expected, but are still enough to cause a minor amount of interference, even with the strength of interference decreasing over the distance via the inverse square law.

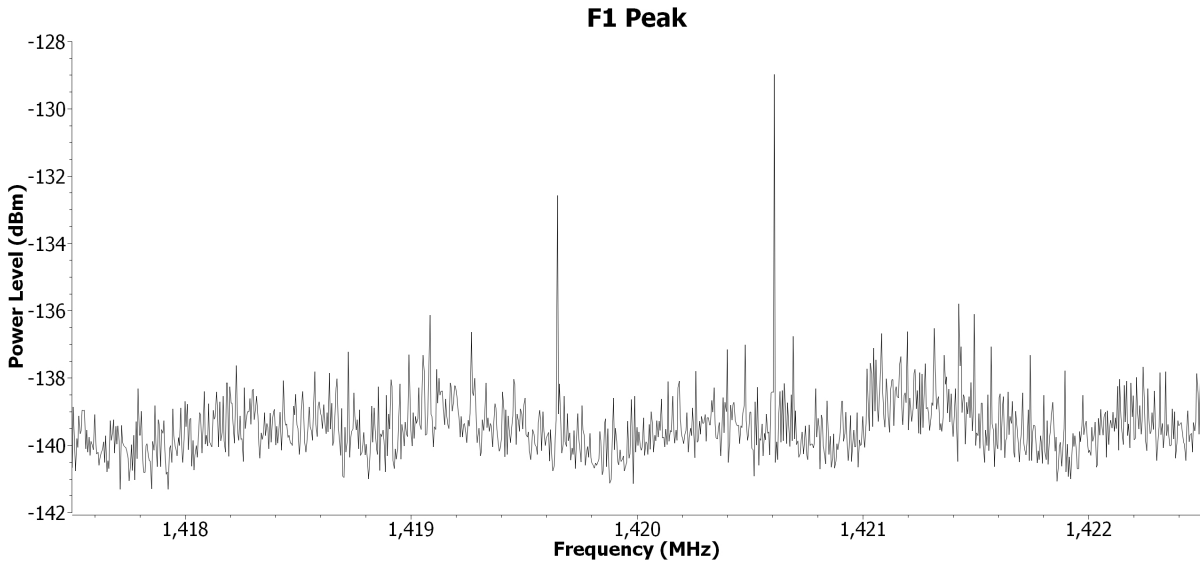

Figure 60: Peak Spectrum of F1

7.3 Wide Band Readings

7.3.1 Wide Band Survey at G2

To be able to see differences more clearly in the wide band readings, both the average and peak spectra were overlaid with the comparison readings taken in Preston, as shown in Figure 61 and Figure 62. With the average spectra, we can see that the noise floor is at its maximum 10 dBm above the comparison readings, such as at around 1260 MHz. This interference is most likely due to the planetarium, specifically the server racks that are on the side of the building that G2 is facing. This is expected, as the devices near the readings done in Preston would be a lot weaker and far less concentrated than the server racks present in the planetarium.

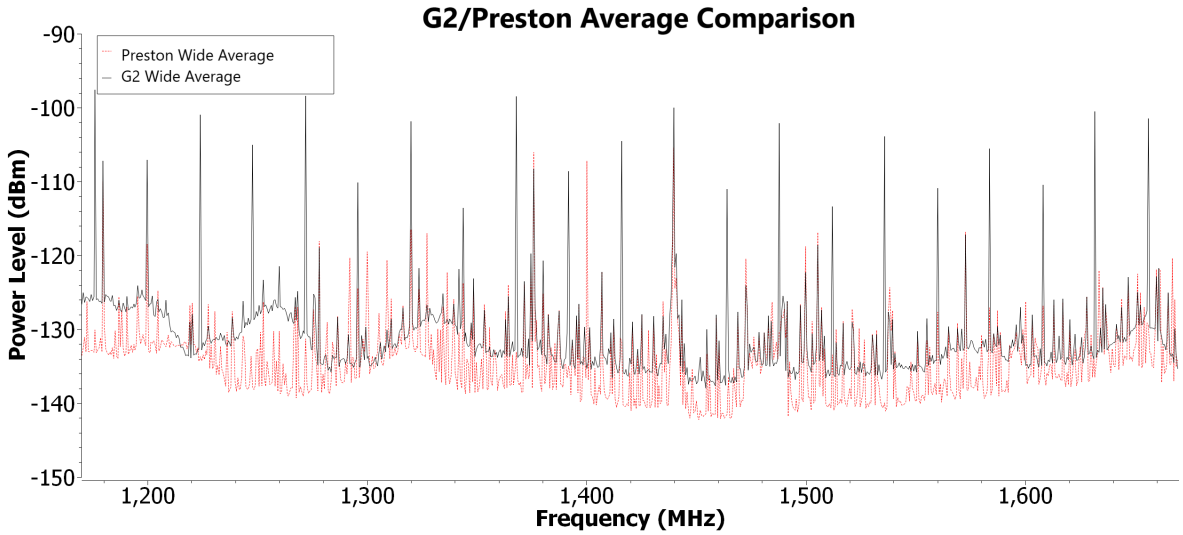

Figure 61: The Wide spectrum taken at G2, spanning from 1170 to 1670 MHz overlaid with the comparison wide spectrum, both taken in average mode

This difference in the noise floor level is also shown in the peak readings, as we would expect. Both of these spectra show that although the interference at the narrow 1420 MHz band seems to be minimal, looking at the wider spectra shows the potential issue of interference coming from the planetarium, with both an increase in the noise floor, and a lot more peaks being present with a far higher strength, with most being up to 20 dBm above the noise level, compared to the comparison where the peaks are mostly 10 dBm above the noise floor.

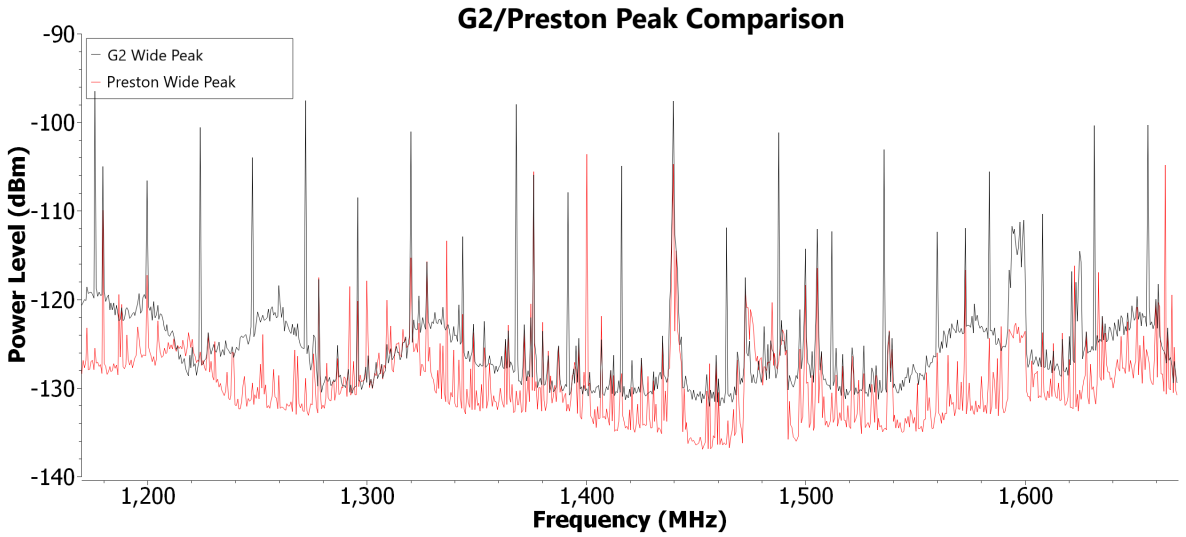

Figure 62: The Wide spectrum taken at G2, spanning from 1170 to 1670 MHz overlaid with the comparison wide spectrum, both taken in peak mode

7.3.2 Wide Band Survey at F9

Moving to the other potential point that the telescope could be built, F9, we see a lot less interference than with G2 when looking at the wide band readings, which is shown in both the average mode in Figure 63, and the peak mode in Figure 64. As expected, being further away from the server racks means that the noise floor is much closer to the comparison reading than at G2, and occasionally dips below the comparison reading, as would be expected with the Alston site being outside of Preston and far away from the city centre.

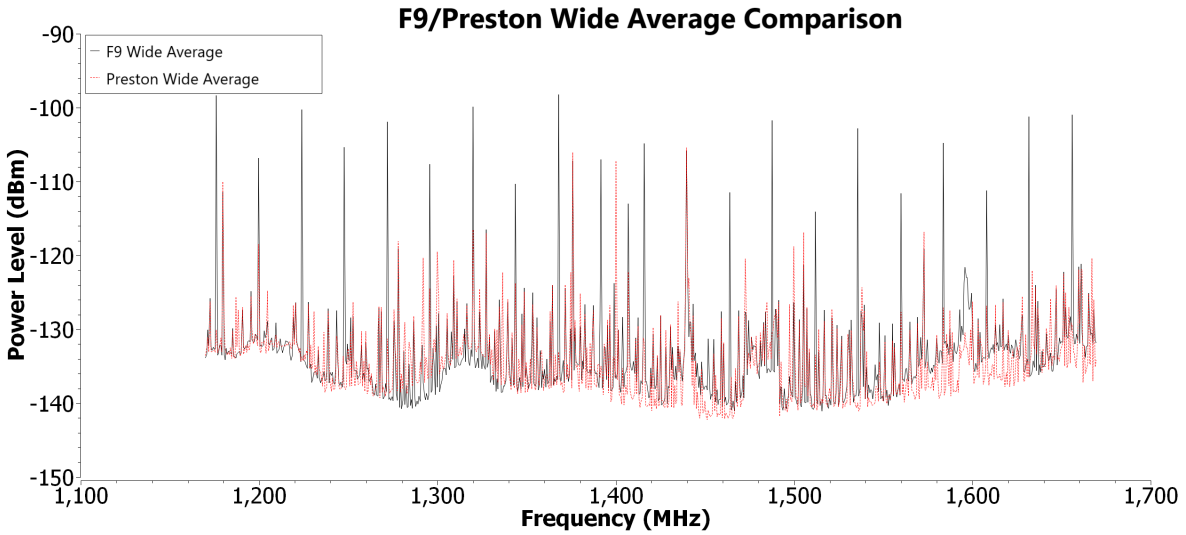

Figure 63: The Wide spectrum taken at F9, spanning from 1170 to 1670 MHz overlaid with the comparison wide spectrum, both taken in average mode

However there is a similarity with the readings at G2, with the tall peaks again, with most being 30 dBm over the noise floor. This puts both the peaks found at G2 and the

peaks at F9 at around -100 dBm. This indicates that the source for the taller peaks is not from the planetarium, and the server racks and other devices inside, but potentially the further away sources that may be causing the peaks in the narrow band reading, such as the AM/FM broadcasts, Radar etc. This also suggests that the source of these is closer to Alston than in Preston, if it a far away source. This could not be Winter Hill, as Alston is further away from the the transmitting mast than Preston is, however it could be potentially a source from Blackburn, as Alston is roughly halfway between the two.

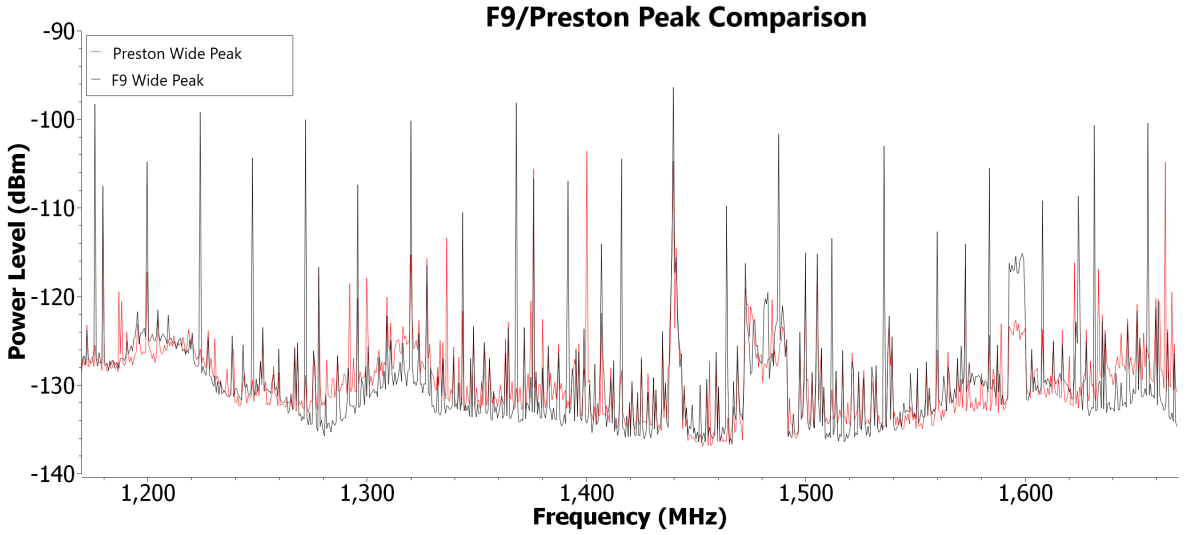

Figure 64: The Wide spectrum taken at F9, spanning from 1170 to 1670 MHz overlaid with the comparison wide spectrum, both taken in peak mode

7.4 Discussion

7.4.1 Tallest Peak-Potential Source

To be able to more easily tell whether there are any changes in the largest peak at 1420.61 MHz, or noise floor over the site more easily, the results were plotted going up/down the site map, going from West to East. To get the length of the full site, results from F and H were overlaid on the same graph. The results taken for this are shown in Figure 65. These were done for the largest peak in both average and peak mode, to see if there are any trends in the peak going across the site, and also compare it to the readings done in Preston, to help identify whether it is an external source, or from the SDR or other part of the setup itself. This was also done with the noise floor, to see if any broad band interference from the planetarium was causing a difference in the noise floor over the site.

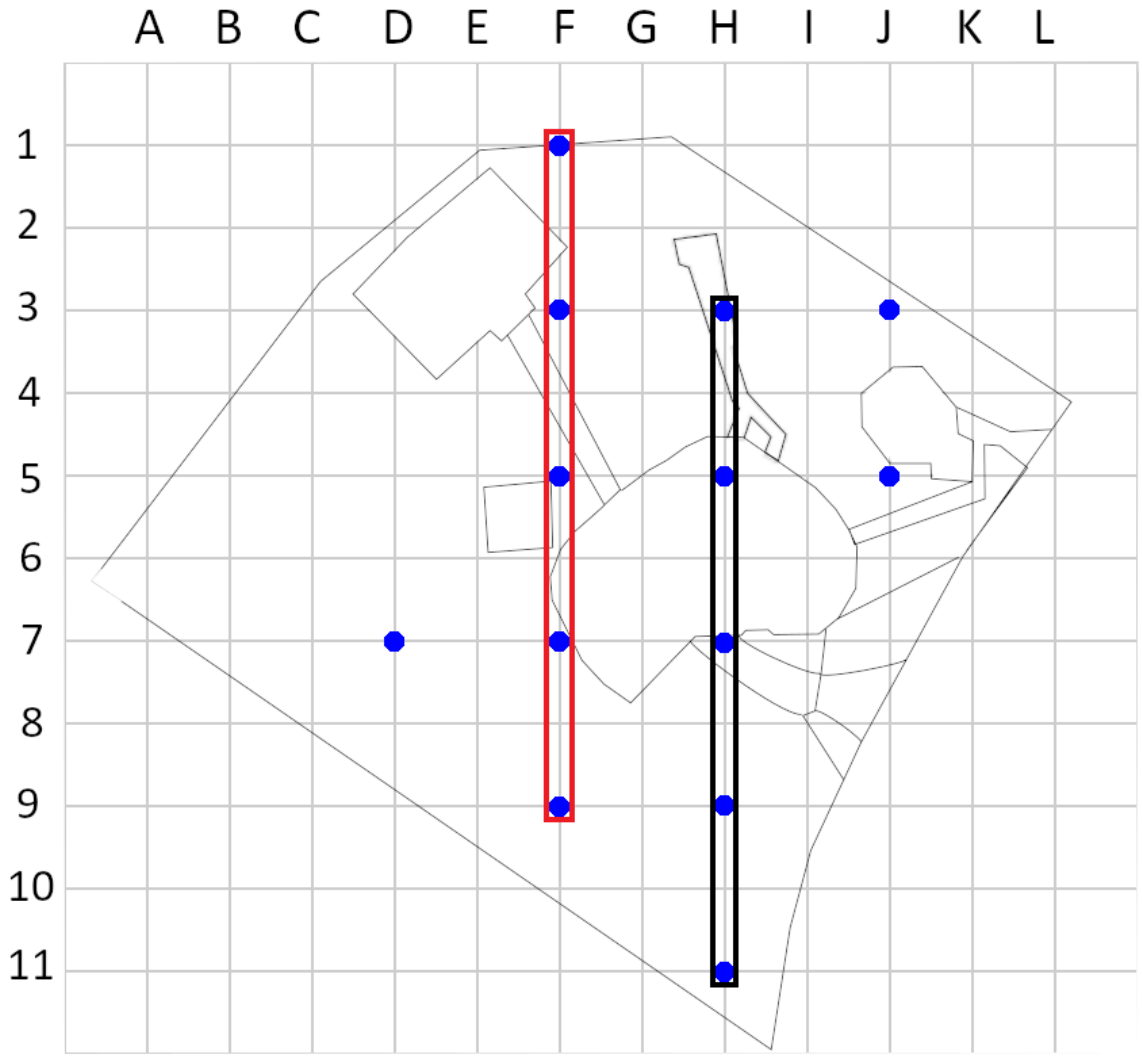

Figure 65: The results taken and graphed to see if there is any change in features over the site, with the respective colours corresponding to the colours on the following graphs

With the tallest peak in average mode, Figure 66, we can see that the value of the

tallest peak does not vary in any significant way, as shown by the error bars, as they all overlap with each other going across the site.

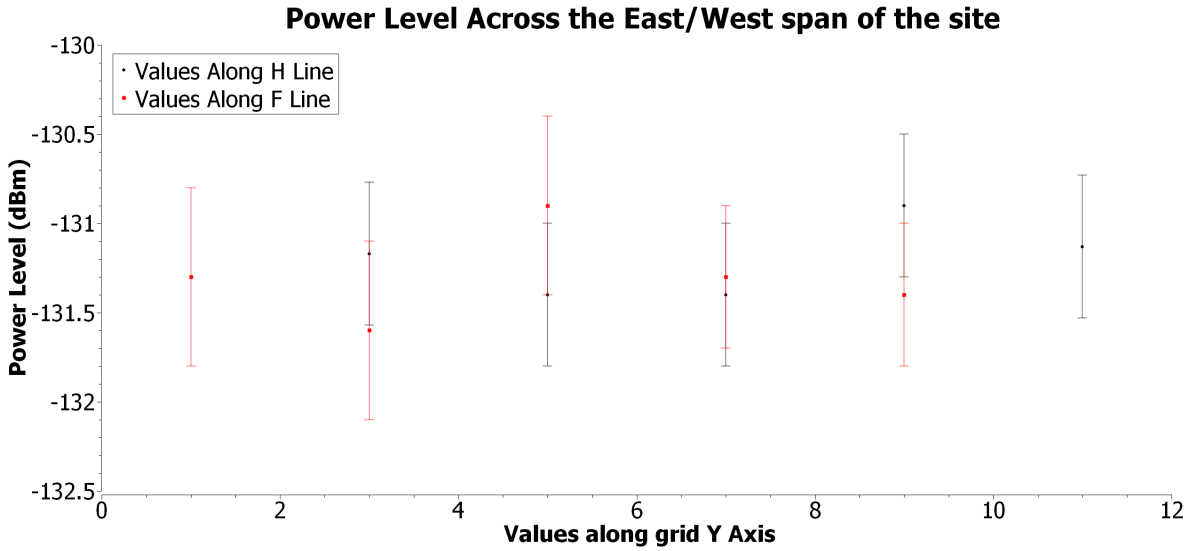

Figure 66: The power level of the tallest peak in average mode across the site

This is also shown in Figure 67, with the peak values. The fact that these values do not vary over site (within the error) and also that the readings in Preston also do not show any significant variance strongly supports the idea that these peaks that are shown come from the SDR itself, or some other part of the setup that is emitting. Therefore, we will exclude these peaks from this assessment of the site, pending further observations of the setup used, ideally with a directional antenna at the end of an extension cable, which would eliminate any interference from the setup and allow for further investigation into particular parts of the setup.

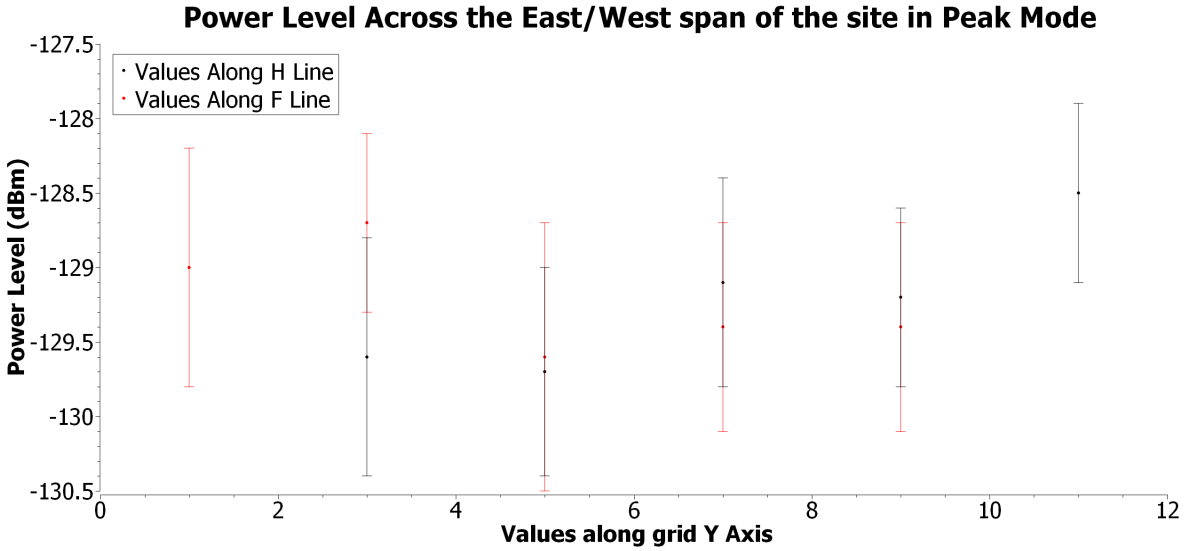

Figure 67: The power level of the tallest peak in peak mode across the site

7.4.2 Noise Floor

Next, we will look to see if there is any changes in the noise floor over the site. This is to identify if there are any broad band signals on the site that may be raising the noise floor, especially coming from the planetarium due to the results seen in both the wide and narrow band readings around it. If there are any broad band signals, we would expect a decrease in the noise floor going from East to West, away from the planetarium.

However, in both the average mode (Figure 68) and peak mode (Figure 69, we do not see a change in the overall noise floor across the site within the errors. This indicates that the planetarium does not appear to contribute to the noise floor in any significant way, at least when looking at a narrow band, as this does not correspond to what is shown in the wide band in Section 7.3.1, taken near the planetarium, which shows that in both the average and peak modes, the noise floor is raised above the readings taken in Preston, compared to the wide band readings taken on the opposite end of the site, which are closer to the comparison readings taken in Preston (Section 7.3.2).

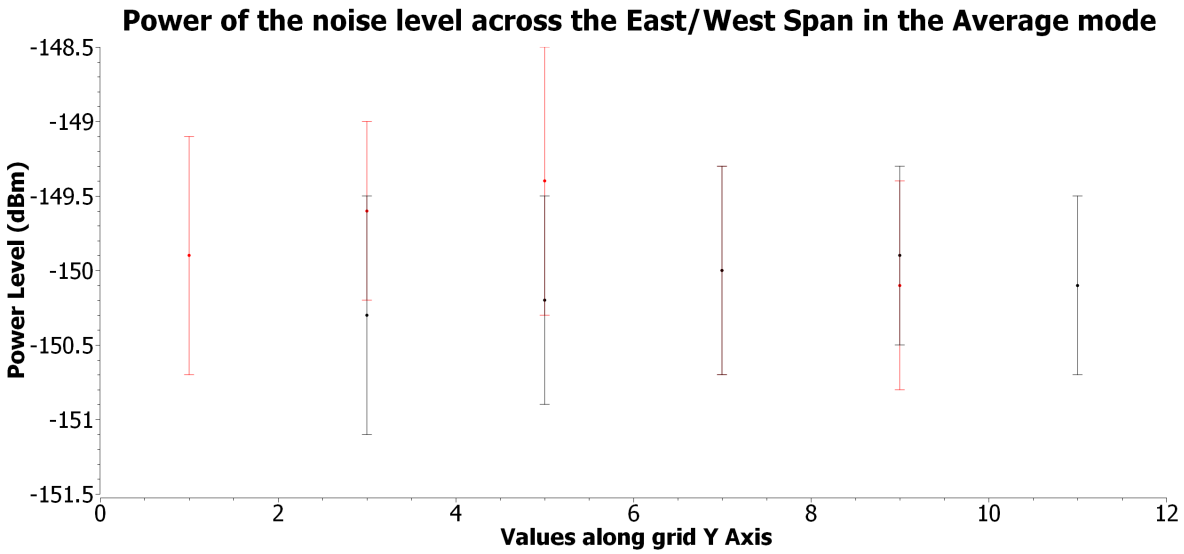

Figure 68: The power level of the noise in average mode across the site

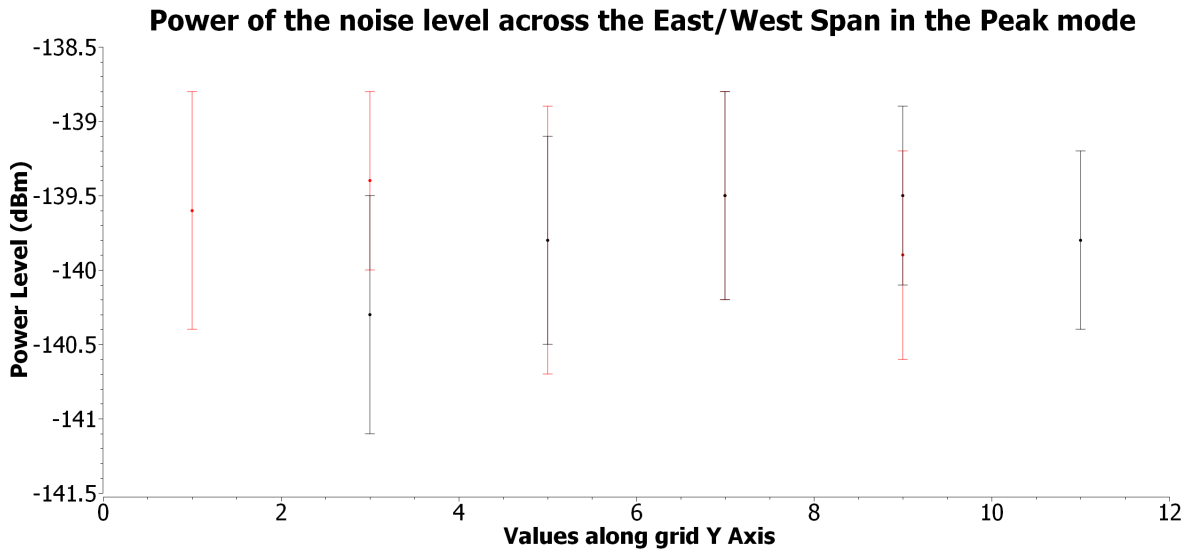

Figure 69: The power level of the noise in peak mode across the site

There is also a spectra that was recorded when doing the initial test, that was not seen in any of the other sets of data, unfortunately the csv file with the data was corrupted, so only a screenshot of the readings was made, Figure 70, where the peak spectra captured a sudden strong signal that raised the noise floor. As it was not seen in any other readings, this is potentially either an error with the software, or a very rare occurrence.

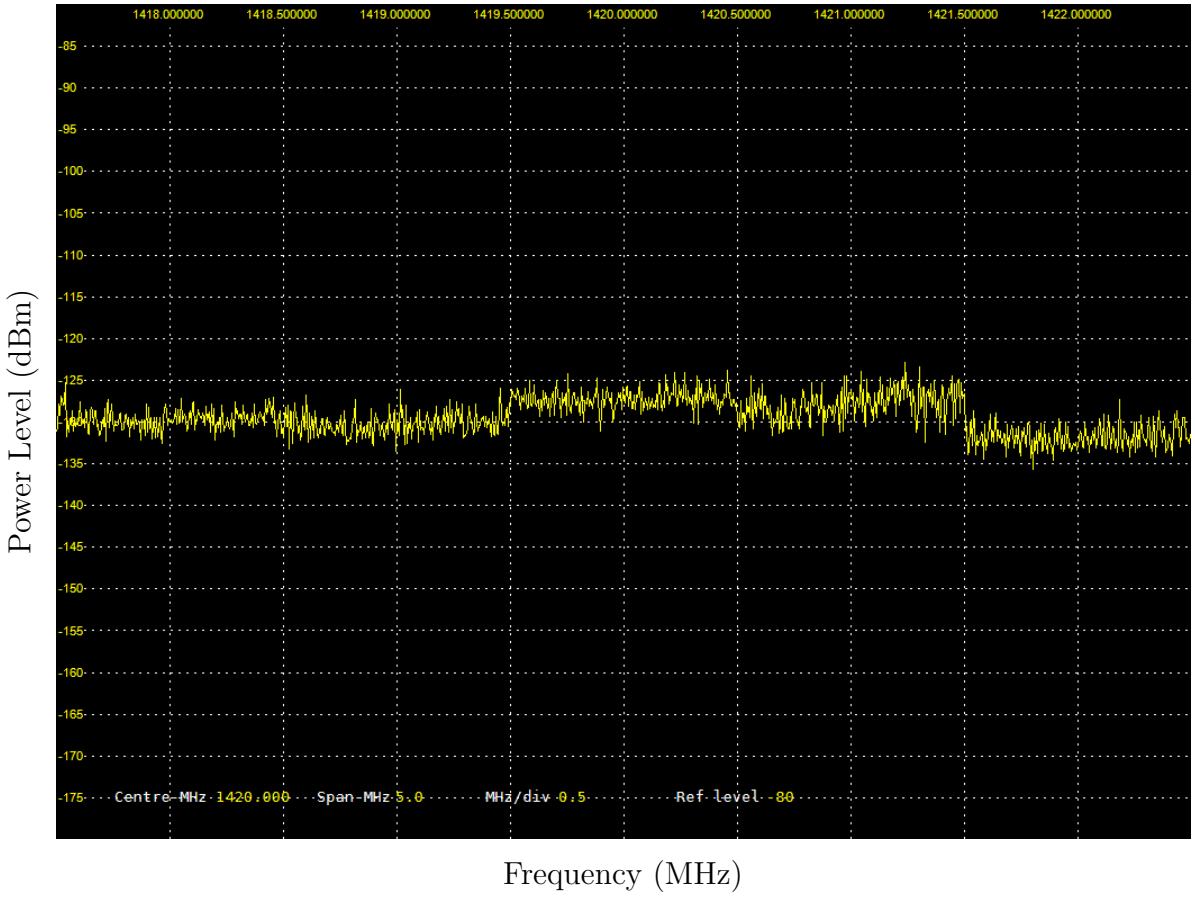

Figure 70: A peak spectrum captured when doing the initial testing on site (22/06/2021)

7.4.3 Comparison to other Surveys

Using the method described in Section 4, with equation 4.1, we can convert the results found into Spectral Flux Density, which can be used to compare the results found to the results found via the Thai Radio Telescope survey and SKA. As the data from the SKA presented in Section 4 was done in high sensitivity mode, the Peak mode from the Thai Radio Telescope Survey and the Peak readings from this survey will be compared as these are the methods across the surveys that are closest. To get a basic comparison, the $P(f)$ value with be the noise floor, which for a rough estimation will be considered to be -139 dBm, G_{LNA} will be considered 0, G_{ant} is -14.57 dBi, Δf_0 is 5 kHz and f is 1420 MHz. This gives a rough estimate of the Spectral Flux Density (SFD) of the noise floor over the site to be -195 dBW/m^2/Hz with the narrow band readings.

This is unexpected, as this puts the Spectral Flux Density at 1420 MHz far below the Thai Radio Telescope readings (where around 1420 MHz they find a SFD of around -130 dBW/m^2/Hz), giving a difference of around 70 dBW/m^2/Hz. This could potentially be due to a difference in the way the observations were taken, either with the Thai Radio survey or this survey at Alston, as the survey that was done at Alston was done with a far lower budget, and with far more limited time on the site due to Covid restrictions and weather issues. It could also be that the areas surveyed in the Thai survey were all done near to universities and other buildings, although if that was causing interference, we would expect a similar result from the survey done in Preston, but there is not an increase of that scale, only an increase of a few dBW/m^2/Hz in the wide readings and no statistical difference in the narrow band readings, as shown in Table 1.

When comparing the results from Preston and Alston to the SKA surveys however, we see what is expected, with the noise floor from our results being higher than the SKA, which we would expect due to the far more remote locations used for the SKA survey, with the noise floor from Preston and Alston being 20 dBW/m^2/Hz higher than the SKA site, showing that the results that were found are not necessarily completely unreasonable, however the vast difference to the Thai Radio Survey would ideally need to be followed up on with a future survey.

7.4.4 Noise floor Compared to Observational Signals

While the readings so far have been good to allow comparison to other surveys as well as looking for any particular sources of interference on the site, we can also see if a theoretical telescope, as described in section 3, would be able to detect a theoretical signal from an astronomical source. This source will be the same as described in section 2.5.1, from M31, with a signal strength of 0.24 Janskys. Converting to Watts gives a value of 6.42x10^{-17} (assuming an area of a dish with a diameter of 2.4m and at 1420 MHz), which converted to dBm gives a value of -132 dBm. Using the theoretical gain value for the planned telescope from section 3.1, at 2.85 dBi, with no LNA ($G_{LNA} = 0$), with a Δf_0 of 5 kHz. Using equation 4.1 from section 4, we can get a SFD estimate for a signal from the continuum emission M31 of -205 dBW/m^2/Hz if taken with the hypothetical telescope. This puts a potential reading at just below the noise floor found in the narrow band readings. Although this is not ideal, this does not mean the site is not suitable, as most observations, especially ones from distant faint objects such as M31, require an

integration over a period of time to be detected, so this sort of value is expected. This is also not taking into account the sensitivity of the receiver/feed-horn system, or LNA that may be fitted to the system. This means that objects such as M31 should be viewable on the site, providing the other parts of the system can compensate for the small difference. Even if they could not, closer, brighter objects such as the neutral hydrogen clouds in the Milky Way should be visible on the site over the noise floor.

7.4.5 Future Survey Plan

Due to the limited amount of data that was able to be collected, partially due to Covid, there is room for further investigation. The first priority would be investigating the devices used in the setup, especially the SDR, as it potentially has caused some false signals to show up on the spectrum. Ideally this would be done with a direction antenna placed at the end of an extension cable from the antenna port. This would allow the antenna to be aimed toward the SDR itself, and check any signals it may be emitting.

This directional antenna would also be useful for further surveys of the site. A plan similar to the SKA RFI surveys could be undertaken, where readings could be taken in different directions. Two separate measurements could be taken, one based off the Rural mode used in the SKA survey, which took integrations over 60 seconds, repeated 10 times for each direction. The second measurement would be based off the Max Hold mode, which would take short integrations, 0.1 seconds or shorter, with more repetitions, ideally 100 or more. This may allow for the identification of any weaker signals from outside the site that the small omnidirectional antenna may not have picked up.

Both of these measurements would ideally be repeated over a period of a week or two, at different points in the day, although this may require a remote motorised setup to properly do. If pending further surveys the telescope is built, these measurements should ideally be repeated even after the telescope is operational, as future issues either with new devices on the site, or satellite constellations would need to be identified as soon as possible to stop any interference with observations. The directional antenna could also be used to help identify any specific devices on the site that may be causing interference if any is being picked up, which would allow mitigation measures to be put in place if possible.

7.4.6 Placement of the Telescope

Overall, looking at the current data, the noise floor on the site appears to be low enough that a radio telescope can be built. The potential site further away (F9) appears to be ideal, as it has no interference from the planetarium, and in the wide band readings, has little to no increase in the noise floor. However, when looking at the terrain of the site, it has a slight slope to it, with the planetarium and dome path corner being on the high ground, and the MHT and the area surrounding it being on the lower ground. This could cause a potential issue, as if the telescope were to be built there, the telescope would only have to be slightly pointed towards the end of the site with the planetarium for it to be in the potential side lobes of the telescope, where the RFI from the planetarium, or from any devices such as mobiles phones or car electronics from visitors to the site could enter and disrupt observations. Not only that,

the raised ground also would block how low the telescope could view regardless of interference from any buildings or devices.

A potential alternative however that could potentially mitigate this issue however is placing the telescope on top of the planetarium roof, if planning permission allowed and a suitable way of mounting the telescope could be found. This would place the main source of interference of the site underneath the telescope, where any RFI would get bounced off of back side of the dish, and if RFI from the building is a problem, a mat of a material that would block signals at and around the 21 cm wavelength, such as chicken wire, could be placed on the roof to help block RFI. This would furthermore put the telescope at the highest point on the site, meaning it would have the largest amount of sky to observe at one time, without any other buildings in the way.

8 Conclusion

In conclusion the site was surveyed in a 13m grid, with peak and averaged narrow band readings taken at each point on the 29/07/2021, with further follow up wide band readings taken on 06/05/2022. These were done using a SDRPlay RSPdx receiver, and OMNILog 90200 antenna and the RSP Spectrum Analyser Software, with a laptop running the software.

It was found that the noise floor was better than expected, being around -195 dBW/m^2/Hz at 1420 MHz, which is significantly higher than the Thai Radio Telescope survey, which has a noise floor value of around -135 dBW/m^2/Hz at 1420 MHz which could potentially show an difference or issue with the survey setup. When compared to the SKA survey however, the results are as expected, with the SKA showing a noise floor around -220 dBW/m^2/Hz at 1420 MHz, suggesting that the results found are not necessarily incorrect.

There were a few features found in both the wide and narrow band readings, with the wide band readings potentially displaying features coming from sources such as mobile towers, radionavigation, and broadcasting. They also showed that the planetarium is a potential source of interference across the site, as the noise floor in the wide band readings was higher by around 10 dBW/m^2/Hz when compared to wide band reading done on the other side of the site. The narrow band readings at and around 1420 MHz showed a few features, specifically a few narrow peaks at 1419.65, 1420.61 and 1421.57, which due to the fact that they did not appear to be a trend in their strength over the site, and also appeared in the comparison readings taken in Preston, are most likely from the SDR receiver used, or another part of the system setup used. Therefore a further study using a directional antenna would be useful to identify the source of these peaks.

When comparing the noise floor with a theoretical observation of M31 taken by a telescope, the rough estimate gave a Spectral Flux Density close to the noise floor, which taking into account parts of the telescope that were not factored into the calculation, such as the antenna sensitivity and Low Noise Amplifier, would make the observation of objects such as M31, as well as other projects such as mapping the neutral hydrogen in the Milky Way possible with the noise conditions of the site.

For the placement of the telescope on the site, the planetarium building could limit the viewing angles of a telescope placed further away from the building, as it would be on lower ground, meaning if it were pointed towards the direction of the building, potential RFI could enter the side lobes of the telescope. Therefore a potential suggestion for the placement could be on the roof of the planetarium, where any interference would not be able to enter the telescope, and it would also be one of the highest points on the site, minimising any interference from other sources that may be on the site such as from visitors to the site that may have devices that could cause interference if any signals from them were to enter the dish.

It is also important to note that these results may change in the near future, due to planned satellite constellations such as Starlink, these constellations should not

transmit in protected bands, such as 1420 MHz, however there are other parts of the radio band that do not have protections, but are useful for astronomy, such as 1610.6-1613.8 MHz, used to observe OH molecules, but which may be impossible to detect due to planned constellations that are authorised to operate only above 1617.8 MHz, which could raise the noise floor making it impossible to detect the weaker signals. The amount of satellites also pose an issues, with a potentially for over 100 000 satellites in the future, it would mean that at any given time, there would be thousands of satellites above the horizon at any given time, and most likely be satellites passing in front of any observations being taken, potentially rendering them useless. This poses an issue for not just a radio telescope on the Alston site, but as a ground based observational method entirely[23].

[23]https://iau.org/static/publications/dqskies-book-29-12-20.pdf

References

[Anderson, 2003] Anderson, H. R. (2003). *Fixed Broadband Wireless System Design*. John Wiley and Sons, Incorporated, Hoboken.

[Ballard et al., 2008] Ballard, S., Harris, R., Lanz, L., Maruca, B., and noz, D. M. (2008). Haystack observatory project report. https://www.haystack.mit.edu/wp-content/uploads/2020/07/pubs_srt_haystack_FINAL_2_8.pdf.

[Boonstra and Millenaar, 2011] Boonstra, A. J. and Millenaar, R. P. (2011). Ska site spectrum monitoring, measurement program and data processing. Technical report.

[Burke et al., 2019] Burke, B. F., Graham-Smith, F., and Wilkinson, P. N. (2019). *An introduction to radio astronomy*. Cambridge University Press, Cambridge. Includes bibliographical references and index.; ID: alma991007193842503821.

[Collins et al., 2018] Collins, T., Getz, R., and Pu, D. (2018). *Software-Defined Radio for Engineers*. Artech House, Norwood.

[Condon and Ransom, 2016] Condon, J. J. and Ransom, S. M. (2016). *Essential Radio Astronomy*. Princeton University Press.

[Cram et al., 1980] Cram, T. R., Roberts, M. S., and Whitehurst, R. N. (1980). A complete, high-sensitivity 21-cm hydrogen line survey of m31. *Astronomy and Astrophysics Supplement Series*, 40:215–248.

[Dai et al., 2019] Dai, Y., Han, D., and Minn, H. (2019). Impacts of large-scale ngso satellites: Rfi and a new paradigm for satellite communications and radio astronomy systems. *IEEE Transactions on Communications*, 67(11):7840–7855.

[Frost, 2010] Frost, G. L. (2010). *Early FM radio : incremental technology in twentieth-century America*. Johns Hopkins University Press, Baltimore.

[Grant and Phillips, 1990] Grant, I. S. and Phillips, W. (1990). *Electromagnetism*. Wiley, Chichester, 2 edition. ID: alma991003626279703821.

[Gray and Mooley, 2017] Gray, R. H. and Mooley, K. (2017). A VLA search for radio signals from m31 and m33. *The Astronomical Journal*, 153(3):110.

[Halliday et al., 2014] Halliday, D., Walker, J., and Resnick, R. (2014). *Principles of physics*. Wiley, Hoboken, NJ. ID: alma991001537609703821.

[Horellou et al., 2015] Horellou, C., Johansson, D., and Varenius, E. (2015). Salsa project documentation:mapping the milky way. https://raw.githubusercontent.com/varenius/salsa/master/Lab_instructions/HI/English/SALSA HI_English.pdf.

[ITU-Radiocommunication-Assembly-RA.769-2, 2004] ITU-Radiocommunication-Assembly-RA.769-2 (2004). Recommendation ra.769-2. *ITU*, (E24357).

[ITU-Radiocommunication-Assembly-SM.329-10, 2003] ITU-Radiocommunication-Assembly-SM.329-10 (2003). Recommendation sm.329-10. *ITU*.

[Jaroenjittichai et al., 2017] Jaroenjittichai, P., Punyawarin, S., Singwong, D., Somboonpon, P., Prasert, N., Bandudej, K., Kempet, P., Leckngam, A., Poshyachinda, S., Soonthornthum, B., and Kramer, B. (2017). Radio frequency interference site survey for thai radio telescopes. *Journal of Physics: Conference Series*, 901:012062.

[Johnson, 2012] Johnson, D. (2012). *Haystack Small Radio Telescope: Hardware Installation Manual.* https://www.haystack.mit.edu/wp-content/uploads/2020/07/srt_SRT_Hardware_Manual.pdf.

[Johnson, 2013] Johnson, E. E. (2013). *Third-generation and wideband HF radio communications.* Mobile communications series. Artech House, Norwood, MA.

[Jondral, 2005] Jondral, F. K. (2005). Software-defined radio: basics and evolution to cognitive radio. *EURASIP Journal on Wireless Communications and Networking*, 2005(3):275–283.

[Klein et al., 2012] Klein, B., Hochgürtel, S., Krämer, I., Bell, A., Meyer, K., and Güsten, R. (2012). High-resolution wide-band fast fourier transform spectrometers. *Astronomy and astrophysics (Berlin)*, 542:L3.

[Klein et al., 2006] Klein, B., Philipp, S. D., Krämer, I., Kasemann, C., Güsten, R., and Menten, K. M. (2006). The apex digital fast fourier transform spectrometer. *Astronomy and astrophysics (Berlin)*, 454(2):L29–L32.

[Kumar and Western, 2021] Kumar, P. and Western, A. (2021). How can the fourier transform be used in radio astronomy to perform spectral analysis of pulsars. *Journal of student research (Houston, Tex.)*, 10(2).

[Millenaar, 2011] Millenaar, R. P. (2011). Overview of rfi at candidate ska core sites
. Technical report.

[Minoli, 2009] Minoli, D. (2009). Satellite systems engineering in an ipv6 environment. *SciTech Book News*, 33(2).

[Peng et al., 2004] Peng, B., Sun, J., Zhang, H., Piao, T., Li, J., Lei, L., Luo, T., Li, D., Zheng, Y., and NAN, R. (2004). Rfi test observations at a candidate ska site in china. *Experimental astronomy*, 17(1):423–430.

[Phuong et al., 2014] Phuong, N., Diep, P., Darriulat, P., Nhung, P., Anh, P., Pham Ngoc, D., Hoai, D., and Thao, N. (2014). The vatly radio telescope: Performance study. *Communications in Physics*, 24.

[Saje and Vidmar, 2017] Saje, T. and Vidmar, M. (2017). A compact radio telescope for the 21 cm neutral- hydrogen line. *Journal of Microelectronics, Electronic Components and Material*, 47(2):113–128.

[Santo and Uddin, 2013] Santo, T. R. and Uddin, S. A. (2013). Mapping the spiral structure of the milky way galaxy at 21cm wavelength using the salsa radio telescope of onsala space observatory. *International Journal of Astronomy.* https://vale.oso.chalmers.se/salsa/sites/default/files/10.5923.j.astronomy.20130203.03.pdf.

[Sobel'man et al., 1995] Sobel'man, I. I., Vainshtein, L. A., and Yukov, E. A. (1995). *Broadening of Spectral Lines*, pages 237–296. Springer Berlin Heidelberg, Berlin, Heidelberg.

[Spanakis-Misirlis et al., 2021] Spanakis-Misirlis, A., Eck, C. L. V., and Boven, E. (2021). Virgo: A versatile spectrometer for radio astronomy. *Journal of Open Source Software*, 6(62):3067.

[van Driel, 2009] van Driel, W. (2009). Radio quiet, please! – protecting radio astronomy from interference. *Proceedings of the International Astronomical Union*, 5(S260):457–464.

[Varenius, 2018] Varenius, E. (2018). *SALSA User Manual*. https://github.com/varenius/salsa/blob/main/User_manual/English/SALSA-USERMANUAL_English.pdf.

[Verschuur et al., 2012] Verschuur, G. L., Bouton, E., and Kellermann, K. I. (2012). *Galactic and Extragalactic Radio Astronomy*. Springer.

[Wagner et al., 1993] Wagner, V., Balda, J., Griffith, D., McEachern, A., Barnes, T., Hartmann, D., Phileggi, D., Emannuel, A., Horton, W., Reid, W., Ferraro, R., and Jewell, W. (1993). Effects of harmonics on equipment. *IEEE Transactions on Power Delivery*, 8(2):672–680.

[Ward-Thompson and Whitworth, 2011] Ward-Thompson, D. and Whitworth, A. P. (2011). *An introduction to star formation*. Cambridge University Press, Cambridge. ID: alma991000989179703821.

[Wilson et al., 2013] Wilson, T., Rohlfs, K., and Hüttemeister, S. (2013). *Tools of Radio Astronomy*. Springer, Berlin, Heidelberg, 6 edition. ID: cdi-askewsholts-vlebooks-9783642399503.